Faculty of Science and Engineering
School or Earth and Planetary Sciences

Mid Phanerozoic stromatolites in the Northern Perth Basin: Understanding their evolution and occurrence

Liam J. Olden

This thesis is presented for the Degree of
Masters by Research
of
Curtin University

2020

DECLARATION

To the best of my knowledge and belief this thesis contains no material previously published by any other person except where due acknowledgement has been made. This thesis contains no material which has been accepted for the award of any other degree or diploma in any university.

The author acknowledges that copyright of published works contained within this thesis resides with the copyright holder(s) of those works. I warrant that I have obtained, where necessary, permission from the copyright owners to use any third-party copyright material reproduced in the thesis (e.g. questionnaires, artwork, unpublished letters), or to use any of my own published work (e.g. journal articles) in which the copyright is held by another party (e.g. publisher, co-author).

	13/11/2020
Liam J. Olden	Date

ABSTRACT

Stromatolites in the northern Perth Basin, Western Australia have received relatively little attention despite their previous correlation with the End Permian Mass Extinction (EPME), as well as the Hovea member of the Kockatea Shale, a prominent source rock for petroleum systems in the region. This thesis is aimed at investigating the proposed relationship between the documented stromatolites and the EPME, looking at their spatial distribution, palaeodepositional setting and mechanisms of preservation. Geological mapping defines the stromatolites as part of a much more complex geological succession referred to as the northern Perth Basin Stromatolitic Sequence (PBS). The PBS has been found to extend much further than previously thought, expanding over 24 km, with three new significant outcrop locations discovered. The PBS is characterised by at least ten discrete stromatolitic morphological variants interfingered with coarse grained siliciclastic sediments. The nature of the siliciclastic sediments and the variability of stromatolite morphology is suggested to represent a restricted terrestrial palaeodepositional setting with fluvial influences. The revised palaeodepositional setting would not have been influenced by global marine anoxia following the EPME, and as such likely grew as a result of favourable environmental conditions rather than as a biotic rebound. The PBS has been found to have preserved alveolate – cell like – microstructures throughout the region. Following comparison with known biogenic and abiogenic microstructures the alveolate microstructures are suggested to be fossilised skeletal filamentous cyanobacterial sheaths. The preservation of the filamentous cyanobacterial sheaths is interpreted to be as a result of in-vivo/biogenic silicification, similar to what is observed in modern microbialites in siliceous springs and caldera lake settings. The mechanism for such early preservation of the filamentous cyanobacteria can be utilised as a marker for identifying similarly preserved cyanobacteria in preserved microbialites throughout geological time.

ACKNOWLEDGEMENTS

This thesis presents the research in the '*Mid Phanerozoic stromatolites in the Northern Perth Basin: Understanding their evolution and occurrence*' during my time in the School of Earth and Planetary Sciences, Curtin University. This research would not have been possible without the continual support and love from many people.

- ***My principal supervisor (first half of masters) Dr Jane Cunneen*** – The time and effort you put into helping me develop as a scientist during the first year of my masters was truly amazing. You pushed me to the limits and I am sincerely grateful for it, as I'm now a much better researcher than I was going into it. It was unfortunate you could not continue as a principal supervisor, but I know that you'll achieve boundless success as an independent consultant. I hope one day to work with you again.
- ***My principal supervisor (second half of masters) Dr Milo Barham*** – I thank you for being willing to 'take in' a supervisor-less masters student halfway through a project. Your support has been invaluable and has helped me develop as a sedimentologist. I would also like to thank you for your personal support during my research, it has really helped me cope with things and I have grown as a person from it.
- ***My associate supervisor Dr Hugo Olierook*** I would like to thank you for all the support you have given me throughout my project. It has been a privilege to be able to work and develop my research skills under your watchful eye. I'm especially thankful for general science conversations with a cup of tea in hand.
- ***My associate supervisor Greggory Smith*** – I would like to thank you for your support and advice during my research project.
- ***Collaborative researchers Dr Kathleen Grey, Arthur J. Mory, Dr Erica Suosaari, Dr Belinda Gohdel, Dr Denis Fourgese***– Your involvement throughout my research has inspired me and taught me valuable techniques which I can utilise through my continued work in the field of palaeontology.
- ***Dr Lucy Forman*** – Special thanks to Lucy who has been a massive supporter of my research and collaboration. As well as our lovely tea breaks and discussion, and being such a fabulous moral support.
- ***Sponsors*** – I would like to thank the Geological Society of Australia for grants provided that helped fund fieldwork. The

- ***Landowners*** – I would like to thank all the landowners from the Geraldton and Northampton Shires for their support with the project, allowing us to access their properties.
- ***My friends and family*** – The completion of this MRes would not have been possible without the support of my family, my parents Timothy and Jenni and my sister Tessa. The geology and palaeontology friends that I have made throughout my degree that has helped inspire me.
- ***My colleagues in UniPASS*** – I would like to especially thank Amada Smith and the rest of the UniPASS team as they have provided continued support to me throughout my studies as well in my personal life.

LIST OF PUBLICATIONS INCLUDED AS PART OF THE THESIS

This thesis compiles a collection of research papers that are currently under review at the time of writing this document. The objectives and relationship amongst the different papers are described in the introductory chapter. The final chapter summarizes the papers and places them into a wider context. All papers have a statement of co-authorships in Appendix A.

The research papers contained within this thesis are given below.

PAPER 1: Olden, L. J., Barham, M., Cunneen, J., Olierook, H. K. H., Suosaari, E., & Smith, G. (In Review). Microbialite forms and facies controls on stromatolite occurrences in the Perth Basin, Western Australia and their relationship to the End Permian Mass Extinction. *Australian Journal of Earth Sciences.*

PAPER 2: Olden, L. J., Barham, M., Olierook, H. K. H., Godel, B., Fougerouse, D., Cunneen, J., & Forman., L (In Review). The cell in the stone: exceptional preservation of cellular microstructures in Mid-Phanerozoic stromatolites from Western Australia *Geobiology*.

The formatting of each chapter within this thesis may appear to vary and may differ to the published form based on the requirements and formatting guidelines of each individual journal and this thesis. This hybrid thesis is a composite of scientific papers that have been submitted for peer review.

LIST OF CONFERENCE PRESENTATIONS RELEVANT TO THE THESIS

Several conference presentations where conducted during the time of the masters by research. The presentations are listed below:

CONFERENCE PRESENTATION A: Olden, L. J., Barham, M., Cunneen, J., Olierook, H. K. H., Suosaari, E., & Smith, G., 2018. Extent and Significance of Gondwanan stromatolites following the Permian-Triassic mass extinction. *GESSSWA*

- This presentation was at a student conference representing work from paper 1 (Chapter 2).

CONFERENCE PRESENTATION B: Olden, L. J., Barham, M., Cunneen, J., Olierook, H. K. H., Suosaari, E., & Smith, G., 2018. Are stromatolites in the northern Perth Basin following the End Permian Mass Extinction? *AESC*

- This presentation was at a national Australian conference representing work from paper 1 (Chapter 2).

CONFERENCE PRESENTATION C: Olden, L. J., 2018. Extent and significance of intra-continental Gondwanan stromatolites following the End Permian mass extinction? *Basins Symposium*

- This presentation was at a national Australian conference representing work from paper 1 (Chapter 2).

CONFERENCE PRESENTATION D: Olden, L. J., Barham, M., Cunneen, J., Olierook, H. K. H., Suosaari, E., & Smith, G., 2019. Are stromatolites in the northern Perth Basin following the End Permian Mass Extinction? *AEGC*

- This presentation was at a national Australian conference representing work from paper 1 (Chapter 2).

CONFERENCE PRESENTATION E: Olden, L. J., Barham, M., Cunneen, J., Olierook, H. K. H., Suosaari, E., & Smith, G., 2019. Mid Phanerozoic stromatolites in Western Australia: Implications for stromatolites as disaster biota. *Selwyn Symposium*

- This presentation was at a national Australian conference representing work from papers 1 & 2 (Chapter 2 & 3).

TABLE OF CONTENTS

FIGURE LIST

TABLE LIST

Chapter 1 INTRODUCTION

Microbialites are defined as organosedimentary deposits formed as a consequence of the trapping and binding of sediments, and/or mineral precipitation associated with microbial activity (Burne & Moore, 1987). Microbialites can be split into five main categories; stromatolites, thrombolites, dendrolites, leiolites (Riding, 2000, 2001, 2011) and microbially induced sedimentary structures (MISS's; Noffke, Gerdes, Klenke, & Krumbein, 2001; Fig 1.1). Microbialites have been used to further our scientific understanding of early Earth and the evolution of life, with the oldest confirmed stromatolite dated as 3.48 Ga (Djokic, Van Kranendonk, Campbell, Walter, & Ward, 2017). Microbialites dominated Earth's biosphere into the late Neoproterozoic when they experienced a substantial decline in diversity and distribution as a result of the evolution and proliferation of multicellular life in the Ediacaran and Cambrian.

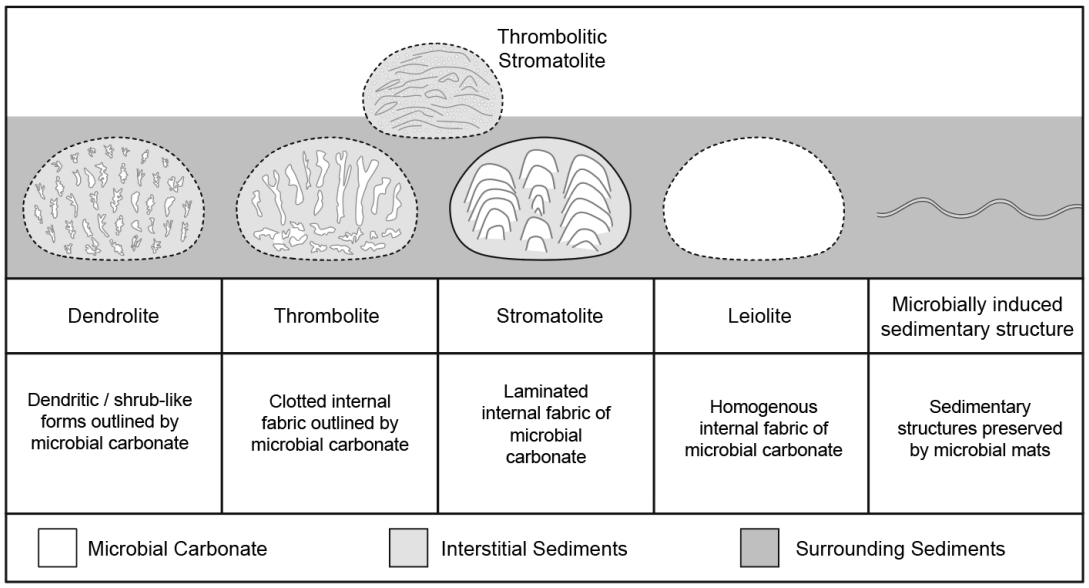

Fig. 1.1: Summary diagram demonstrating the five categories of microbialite. Adapted from Riding (2011).

The Phanerozoic microbialite rock record is marked by spikes in abundance and relative diversity, coinciding with periods of biotic crisis. The largest biotic crisis during the Phanerozoic was the End Permian Mass Extinction (EPME), with biodiversity losses of 80–96% (Chen & Benton, 2012; Schubert & Bottjer, 1992), driven by the eruption of the Siberian

Traps (Erwin, 1994; Hallam & Wignall, 1997; Harries, Kauffman, & Hansen, 1996; Keller, 2005). Stromatolites have been shown to be globally distributed following the EPME, with the largest populations in shallow marine equatorial settings now part of South China (Kershaw et al., 2012). The most distal (apparently related) stromatolitic occurrence recorded relative to the extinction mechanism is in Western Australia (Chen, Fraiser, & Bolton, 2012).

The West Australian stromatolitic occurrence, originally mapped in 1969 (Fig. 1.2), is considered lowermost Triassic (Smithian) in age based on ammonoid shell imprints identified in shales overlying the stromatolites (Chen et al., 2012). However, no dateable material has been sourced from within the stromatolitic unit. The stromatolites are described as growing atop of pebble conglomerates, representing a wave-cut platform along a Lower Triassic shoreline during a marine transgression (Chen et al., 2014). Based on the age and palaeo-depositional setting, the stromatolites have been tentatively correlated with the Hovea Member of the Kockatea Shale, a prominent source rock for the northern Perth Basin. The Hovea Member is considered to be latest Permian to Lower Triassic in age in the Hovea 3 core, which records the Permo-Triassic Boundary. Therefore, there is significant interest in the stratigraphic understanding of the stromatolitic unit and its spatial extent in the region.

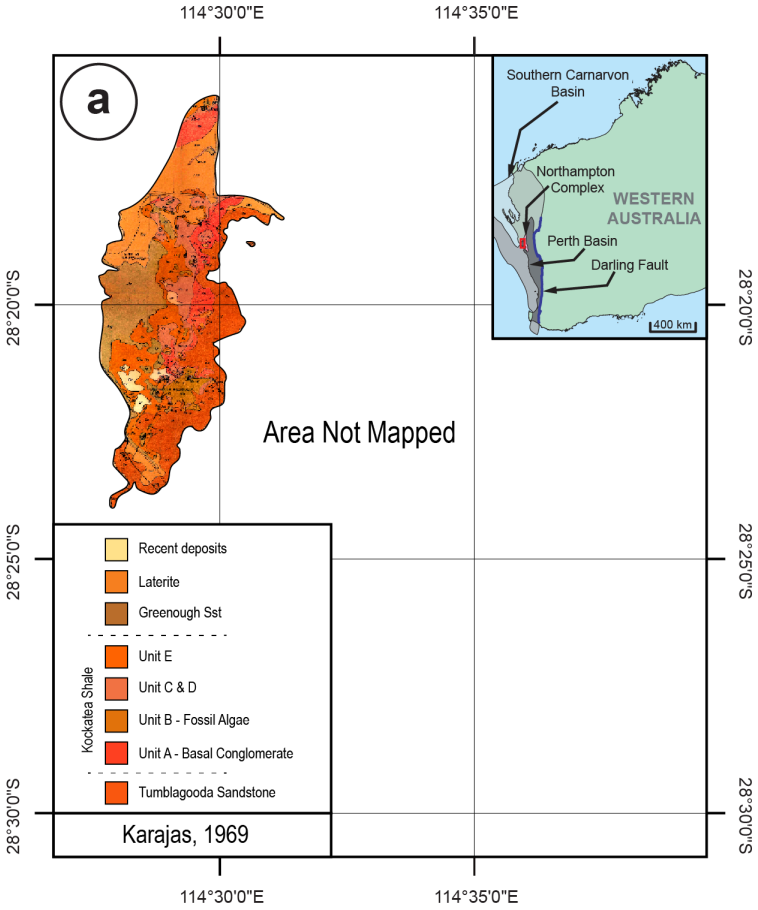
114°30'0"E
114°35'0"E
28°20'0"S
28°25'0"S
28°30'0"S
a
Area Not Mapped
Southern Carnarvon Basin
Northampton Complex
WESTERN AUSTRALIA
Perth Basin
Darling Fault
400 km
Recent deposits
Laterite
Greenough Sst
Kockatea Shale
Unit E
Unit C & D
Unit B - Fossil Algae
Unit A - Basal Conglomerate
Tumblagooda Sandstone
Karajas, 1969

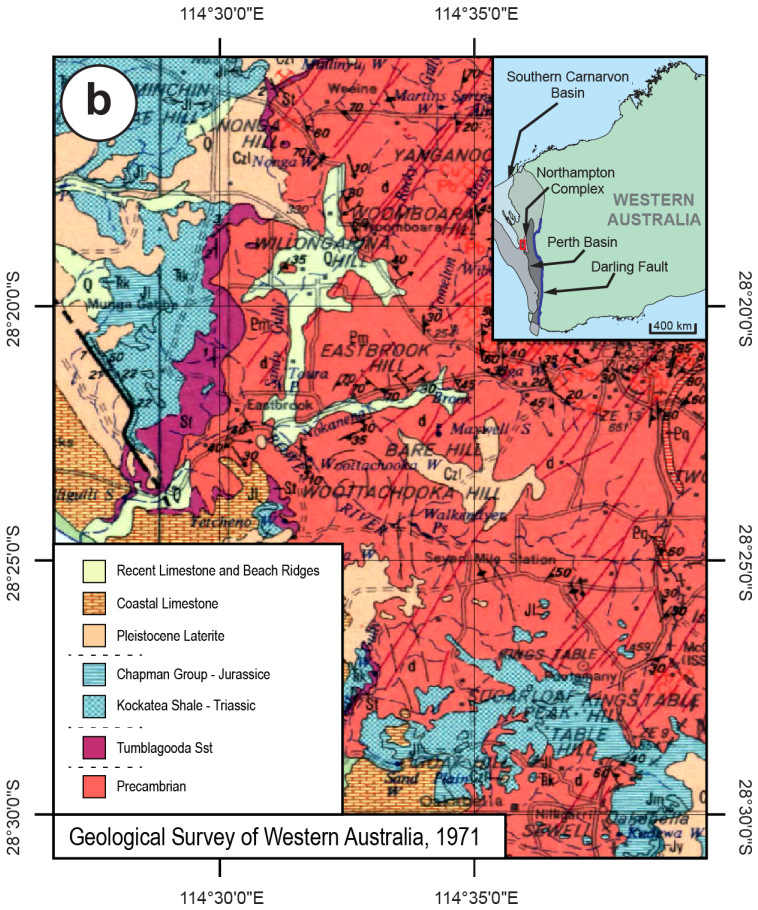
114°30'0"E
114°35'0"E
28°20'0"S
28°25'0"S
28°30'0"S
b
Southern Carnarvon Basin
Northampton Complex
WESTERN AUSTRALIA
Perth Basin
Darling Fault
400 km
Recent Limestone and Beach Ridges
Coastal Limestone
Pleistocene Laterite
Chapman Group - Jurassic
Kockatea Shale - Triassic
Tumblagooda Sst
Precambrian
Geological Survey of Western Australia, 1971

Fig. 1.2: Historical maps of the region. A) Adapted from Karajas, (1969) B) Adapted from Geological Survey of Western Australia (1971)

The identification of cellular structures within microbialites has played an important role in our understanding of early Earth. Cellular structures have been found as far back as 3.4 Ga (Wacey, 2010; Wacey, Kilburn, Saunders, Cliff, & Brasier, 2011), which are similar to those identified within living microbialites (Kremer, Kazmierczak, Łukomska-Kowalczyk, & Kempe, 2012; Wacey, Urosevic, Saunders, & George, 2018). Fluorescent imaging led Chen et al. (2014) to suggest that preserved bacterial filaments and calcified tube walls are present in the northern Perth Basin stromatolites, a significant finding for a purported Lower Triassic sequence. However, electron-dispersive X-ray spectrometry (EDS) mapping of the stromatolites showed little preservation of organic carbon and calcium (Chen et al., 2014), questioning the validity of the suggested preservation of original organic structures. Therefore, analysis of these alveolate microstructures is required to ascertain if the northern Perth Basin stromatolites do preserve cellular material. If present, assessing the mechanisms that govern the preservation of cellular material here can be important for identifying sequences prone to such preservation throughout geological time, as well as potentially improving our understanding of the evolution of life on Earth.

1 Aims & Objectives

The main aim of this thesis is to understand the evolution and occurrence of stromatolites in the northern Perth Basin of Western Australia, in order to constrain their relationship with the End Permian Mass Extinction and the validity of preserved filament sheaths. These aims are facilitated by several objectives. The chapters that satisfy these objectives are given in *parentheses*.

1. Characterise and determine the overall distribution of the stromatolitic succession *(chapter 2)*.
2. Establish a 3D palaeogeographic model of the setting that facilitated the growth of the stromatolitic succession *(chapter 2)*.
3. Review the purported association of the Perth Basin stromatolites with the End Permian Mass Extinction *(chapter 2)*.
4. Establish the origin of stromatolitic microstructures found in the Perth Basin stromatolites *(chapter 3)*.
5. Provide a mechanism for the preservation of stromatolitic microstructures found in the Perth Basin stromatolites *(chapter 3)*.

2 Thesis structure

A typical literature review has been omitted from this thesis, as each chapter (representing papers currently under review) includes its own background research incorporated into the text. The chapters are presented in a logical order to address the objectives of the research project. Co-authorship statements are present at the end of the thesis in Appendix A.

Chapter two, Microbialite forms and facies controls on stromatolite occurrences in the Perth Basin, Western Australia and their relationship to the end Permian mass extinction, of this thesis has been submitted to review in the *Australian Journal of Earth Sciences.*

This paper addresses the purported Smithian (lowest Triassic) age of the West Australian stromatolite occurrence, and subsequently its association with the End Permian Mass Extinction. Research herein found the stromatolites to outcrop over an area of 24 km^2. The stromatolites have ten morphological forms that alternate both spatially and vertically. The stromatolites are interfingered with coarse-grained clastic material and are interpreted to have formed within a fluvio-lacustrine depositional setting. The stromatolitic succession is bounded by a basal unconformity with the mid-Palaeozoic Tumblagooda Sandstone and is onlapped by white clays of the Smithian (Lowest Triassic) Kockatea Shale. As such the Northern Perth Basin stromatolitic sequence (PBS) is considered to be a discrete mappable unit. A revised palaeo-depositional setting of restricted aquatic settings influenced by cyclic periods of mass deposition of siliciclastic sediments. It is suggested that the PBS is unrelated to the End Permian Mass Extinction event, rather developed due to the presence of favourable environmental settings.

Chapter three, The cell in the stone: exceptional preservation of cellular microstructures in mid-Phanerozoic stromatolites from Western Australia, of this thesis has been submitted to review in *Geobiology.*

This paper addresses the origin of microstructures, originally identified by Chen et al. (2014), which are preserved within the stromatolitic succession. The microstructures have been found to be preserved, to differing degrees, both continuously across the outcrop area and vertically through the sequence. Microanalysis of the morphology and elemental distribution of structures suggest the microstructures are preserved skeletal filamentous cyanobacteria, conceivably being the first recorded occurrence of such continuous preservation of cellular structures within stromatolites during the Phanerozoic. Stacked mechanisms of preservation

are proposed, with the first being post-mortem silicification and/or biogenic silicification replacing cellular sheaths (following Kremer et al., 2012) and secondary ferruginisation replacing microbial carbonate and trichomes enhancing clarity. It is suggested that tiered methods of preservation could be used as markers to try and identify settings with high probabilities of exceptional cellular preservation.

REFERENCE LIST

Burne, R. V., & Moore, L. S. (1987). Microbialites: organosedimentary deposits of benthic microbial communities. *Palaios*, 241-254.

Chen, Z.-Q., & Benton, M. J. (2012). The timing and pattern of biotic recovery following the end-Permian mass extinction. *Nature Geoscience, 5*, 375. doi:10.1038/ngeo1475 https://www.nature.com/articles/ngeo1475#supplementary-information

Chen, Z.-Q., Fraiser, M. L., & Bolton, C. (2012). Early Triassic trace fossils from Gondwana Interior Sea: Implication for ecosystem recovery following the end-Permian mass extinction in south high-latitude region. *Gondwana Research, 22*(1), 238-255. doi:https://doi.org/10.1016/j.gr.2011.08.015

Chen, Z.-Q., Wang, Y., Kershaw, S., Luo, M., Yang, H., Zhao, L., . . . Zhang, L. (2014). Early Triassic stromatolites in a siliciclastic nearshore setting in northern Perth Basin, Western Australia: Geobiologic features and implications for post-extinction microbial proliferation. *Global and Planetary Change, 121*, 89-100. doi:https://doi.org/10.1016/j.gloplacha.2014.07.004

Djokic, T., Van Kranendonk, M. J., Campbell, K. A., Walter, M. R., & Ward, C. R. (2017). Earliest signs of life on land preserved in ca. 3.5 Ga hot spring deposits. *Nature communications, 8*, 15263.

Erwin, D. H. (1994). The Permo-Triassic extinction. *Nature, 367*(6460), 231.

Hallam, A., & Wignall, P. B. (1997). *Mass extinctions and their aftermath*: Oxford University Press, UK.

Harries, P. J., Kauffman, E. G., & Hansen, T. A. (1996). Models for biotic survival following mass extinction. *Geological Society, London, Special Publications, 102*(1), 41-60.

Keller, G. (2005). Impacts, volcanism and mass extinction: random coincidence or cause and effect? *Australian Journal of Earth Sciences, 52*(4-5), 725-757. doi:10.1080/08120090500170393

Kershaw, S., Crasquin, S., Li, Y., Collin, P. Y., Forel, M. B., Mu, X., . . . Guo, L. (2012). Microbialites and global environmental change across the Permian-Triassic boundary: a synthesis. *Geobiology., 10*(1), 25-47.

Kremer, B., Kazmierczak, J., Łukomska-Kowalczyk, M., & Kempe, S. (2012). Calcification and silicification: fossilization potential of cyanobacteria from stromatolites of Niuafo ‘ou's Caldera Lakes (Tonga) and implications for the early fossil record. *Astrobiology, 12*(6), 535-548.

Noffke, N., Gerdes, G., Klenke, T., & Krumbein, W. E. (2001). Microbially induced sedimentary structures: a new category within the classification of primary sedimentary structures. *Journal of Sedimentary Research, 71*(5), 649-656.

Riding, R. (2000). Microbial carbonates: the geological record of calcified bacterial–algal mats and biofilms. *Sedimentology, 47*, 179-214.

Riding, R. (2001). Calcified algae and bacteria. *Ecology of the Cambrian Radiation. Columbia University Press, New York*, 445-473.

Riding, R. (2011). Microbialites, stromatolites, and thrombolites. *Encyclopedia of geobiology*, 635-654.

Schubert, J. K., & Bottjer, D. J. (1992). Early Triassic stromatolites as post-mass extinction disaster forms. *Geology, 20*(10), 883-886.

Wacey, D. (2010). Stromatolites in the~ 3400 Ma Strelley Pool Formation, Western Australia: examining biogenicity from the macro-to the nano-scale. *Astrobiology, 10*(4), 381-395.

Wacey, D., Kilburn, M. R., Saunders, M., Cliff, J., & Brasier, M. D. (2011). Microfossils of sulphur-metabolizing cells in 3.4-billion-year-old rocks of Western Australia. *Nature Geoscience, 4*(10), 698.

Wacey, D., Urosevic, L., Saunders, M., & George, A. D. (2018). Mineralisation of filamentous cyanobacteria in Lake Thetis stromatolites, Western Australia. *Geobiology, 16*(2), 203-215.

Chapter 2 MICROBIALITE FORMS AND FACIES CONTROLS ON STROMATOLITE OCCURRENCES IN THE PERTH BASIN, WESTERN AUSTRALIA AND THEIR RELATIONSHIP TO THE END PERMIAN MASS EXTINCTION

Liam J. Olden[1,*], Milo Barham[1, 2], Jane Cunneen[1], Hugo K.H. Olierook[1, 2, 3], Erica Suosaari[4], Gregory Smith[1]

[1] School of Earth and Planetary Sciences, Curtin University, GPO Box U1987, Perth, WA 6845, Australia

[2] Centre for Exploration Targeting – Curtin node, Curtin University, GPO Box U1987, Perth, FWA 6845, Australia

[3] John de Laeter Centre, Curtin University, GPO Box U1987, Perth, WA 6845, Australia

[4] Department of Mineral Sciences, Smithsonian Institution, National Museum of Natural History, Washington DC, 20560, USA

This article is currently under peer review with the scientific journal '*Australian Journal of Earth Sciences'* as of *24th August 2020*.

ABSTRACT

Throughout geological history, biodiversity trends have been punctuated by sharp declines, coinciding with mass extinction events. Certain organisms – known as disaster forms – flourish during the extinction aftermath from a lack of ecological competition and predation. Microbialites (in particular stromatolites) are known to increase in environmental diversity following these biotic crises. However, it remains important to identify whether individual microbialite occurrences are a result of globally-driven competition reduction or favourable local conditions. Here, we reconsider stromatolites from the northern Perth Basin of Western Australia, previously reported as Smithian (late Olenekian) in age and part of a biotic rebound following the end-Permian mass extinction, and re-evaluate their palaeodepositional setting and age. Detailed mapping, macro- and meso-analysis of the Perth Basin locality has identified a well-preserved and diverse morphological assemblage of stromatolites that are intimately associated with a series of clastic sediments. Observations of the characteristics and relationships between the stromatolites and clastic sediments supports a restricted aquatic palaeodepositional environment with fluvial influences. In the Perth Basin, such depositional environments occurred most commonly during the Permian (Guadalupian to Lopingian). The robustness of previous age constraints interpreted from overlying strata (Kockatea Shale) are questioned by the identification of a depositional hiatus and on-lapping relationship of the Kockatea Shale on the stromatolitic sequence. Therefore, we suggest that the mid-Phanerozoic northern Perth Basin stromatolitic sequence (PBS) cannot be unequivocally associated with the end-Permian mass extinction, and thus, thrived due to favourable palaeodepositional settings. The mid-Phanerozoic northern Perth Basin stromatolites are not a unique case. A compilation of reported Permian and Triassic microbialite occurrences shows that stromatolites, although most common following the end-Permian mass extinction, also occur both before and after the extinction event in a range of environmental settings.

1 Introduction

Stromatolites – laminated structures formed via biogenic, microbial activity (Logan, Rezak, & Ginsburg, 1964) – record the first physical evidence of life on Earth, having dominated the Precambrian biosphere (Awramik, 1992; Awramik & Sprinkle, 1999; Djokic et al., 2017; Nutman, Bennett, Friend, Van Kranendonk, & Chivas, 2016; Suosaari et al., 2016). After the proliferation of more complex lifeforms in the Ediacaran (ca. 635 Ma) and in particular, the Cambrian (ca. 541 Ma), evidence of stromatolites and other microbialites in the rock record sharply decline (Awramik, 1992; Bosak, Knoll, & Petroff, 2013; Garrett, 1970; Schubert & Bottjer, 1992). The Phanerozoic stromatolitic record is punctuated by sharp, transient spikes in abundance directly following mass extinctions, which most authors have attributed to a reduction in predatory pressure and ecological competition (Chen & Benton, 2012; Kershaw et al., 2012; Schubert & Bottjer, 1992). While some workers consider Phanerozoic microbialites to represent disaster forms or anachronistic facies (Schubert & Bottjer, 1992), others consider microbialite occurrences to be independent of extinction events (Kershaw et al., 2009).

Throughout geological time there have been five recorded mass extinction events (Hallam & Wignall, 1997). The most catastrophic, the end-Permian mass extinction (EPME), occurred at ca. 252 Ma associated with the development of the large igneous province, the Siberian Traps (Burgess, Bowring, & Shen, 2014; Keller, 2005; Wignall, 2007). Microbialites are frequently reported following this ecological crisis (Adachi, Asada, Ezaki, & Liu, 2017; Ezaki, Liu, & Adachi, 2003; Fang, Chen, Kershaw, Li, & Luo, 2017a; Fang, Chen, Kershaw, Yang, & Luo, 2017b; Huang, Tong, & Fraiser, 2018; Kershaw et al., 2007; Lehrmann et al., 2003; Luo et al., 2016; Shen et al., 2012; Wu et al., 2017). The majority of stromatolite studies on this time period focused on carbonate ramp and shallow marine settings as these environments are particularly susceptible to extinction-related phenomena, thereby reducing ecological competition and promoting microbialite development. However, other depositional environments remain less well characterized.

In this study, the macro- and mesostructural features of stromatolites were mapped and characterized from outcrops in the northern Perth Basin, Western Australia that have been reported as Lower Triassic (Smithian) (Fig. 2.1). Few studies have been done on this relatively small site (6km^2) the main being Chen et al. (2014; Fig. 1.3), despite it being the southernmost recorded occurrence of stromatolites following the EPME. The palaeodepositional setting and

age of the Perth Basin stromatolites have been reviewed to evaluate whether they were associated with the EPME or if they formed temporally distinct from global extinction events.

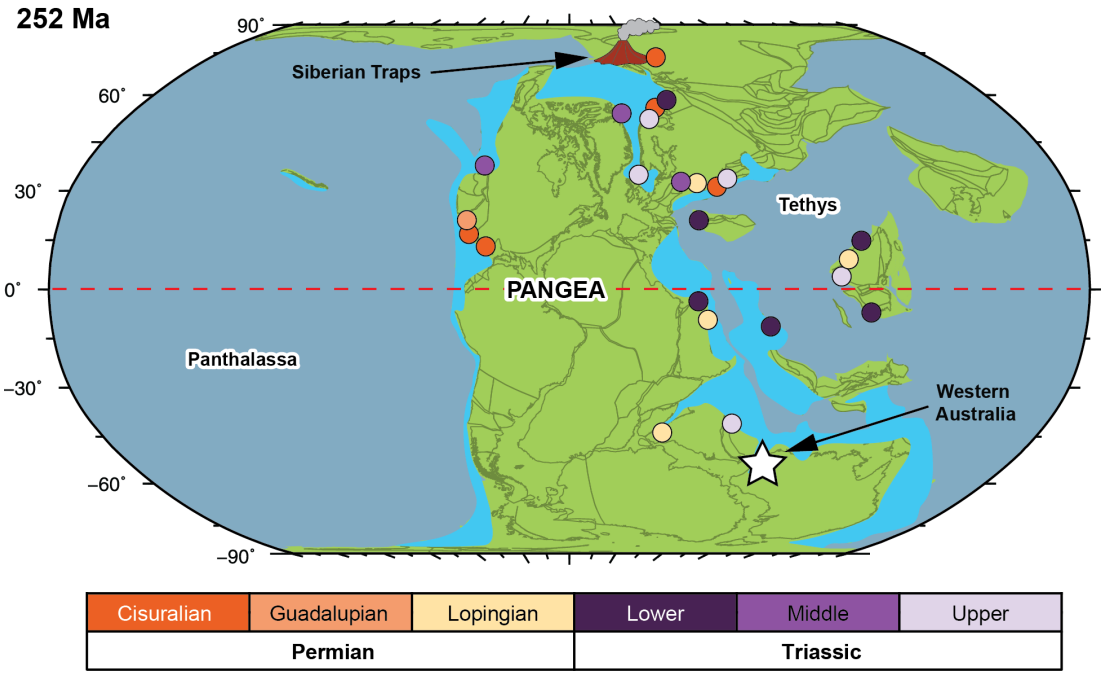

Fig. 2.1: Global distribution of stromatolites during the Lower Triassic (252 Ma) with respect to the Siberian Traps large igneous province (Courtillot, Jaupart, Manighetti, Tapponnier, & Besse, 1999). Tectonic projection based on Young et al. (2018) model. Stromatolite/microbialite occurrences (circles) coloured according to age; lower Permian (Chuvashov, 1983; Cross & Klosterman, 1981a, b; Freytet, Kerp, & Broutin, 1996; Kerp, Penati, Brambilla, Clement-Westerhof, & Van Bergen, 1996; Schäfer & Stapf, 1978; Shapiro & West, 1999; Szulc & Cwizewicz, 1989), mid-Permian (Newell, 1955), late Permian (Adachi et al., 2017; Angiolini, Checconi, Gaetani, & Rettori, 2010; Fang et al., 2017b; Freytet, Lebreton, & Paquette, 1992; Gaetani et al., 2009; Maurer, Martini, Rettori, Hillgärtner, & Cirilli, 2009; Peryt & Piatkowski, 1977; Taraz et al., 1981; Wescott, 1988; Wescott & Diggens, 1998; Wignall & Hallam, 1992), Lower Triassic (Adachi et al., 2017; Angiolini et al., 2007; 2001; Baud & Bernecker, 2010; Baud, Cirilli, & Marcoux, 1997; 2005; Chen et al., 2012; 2014; Escher & Watt, 1976; Ezaki et al., 2003; 2008; 2012; Fang et al., 2017a; Groves & Calner, 2004; Groves, Rettori, Payne, Boyce, & Altiner, 2007; Heydari, Hassandzadeh, & Wade, 2000; Hips & Haas, 2006; Insalaco et al., 2006; Kalkowsky, 1908; Kershaw et al., 2011; Kershaw et al., 2012; Kershaw, Guo, Swift, & Fan, 2002; Kershaw et al., 2007; Kershaw, Zhang, & Lan, 1999; Lehrmann, 1999; Lehrmann et al., 2003; Luo et al., 2016; Marenco, Griffin, Fraiser, & Clapham, 2012; Mary & Woods, 2008; Paul & Peryt, 2000; Perch-Nielsen, Bromley, Birkenmajer, & Aellen, 1972; Peryt, 1975; Pruss & Bottjer, 2004; Pruss, Bottjer, Corsetti, & Baud, 2006; Richoz, Baud, Krystyn, Twitchett, & Marcoux, 2005; Richoz et al., 2010; Sano & Nakashima, 1997; Taraz et al., 1981; Wang, Tong, Wang, & Zhou, 2005; Wignall & Twitchett, 2002; Yang et al., 2011), Middle Triassic (Buser, Ramovš, & Turnšek, 1982; Clemmensen, 1978; Clemmensen & Andreasen, 1977; Grasmück & Trümpy, 1969; Luo et al., 2014; Mary & Woods,

2008; Perch-Nielsen, Birkenmajer, Birkelund, & Aellen, 1974; Tałanda, Bajdek, Niedźwiedzki, & Sulej, 2017), Late Triassic (Arp, Bielert, Hoffmann, & Löffler, 2005; Baud et al., 2001; Gore, 1988; Hamilton, 1961; Mastandrea, Perri, Russo, Spadafora, & Tucker, 2006; Mayall & Wright, 1981; Perri, Mastandrea, Neri, & Russo, 2003; Perri & Tucker, 2007; Tałanda et al., 2017; Tucker, 1978; Wright & Mayall, 1981). The Western Australian occurrence discussed herein is marked by a white star.

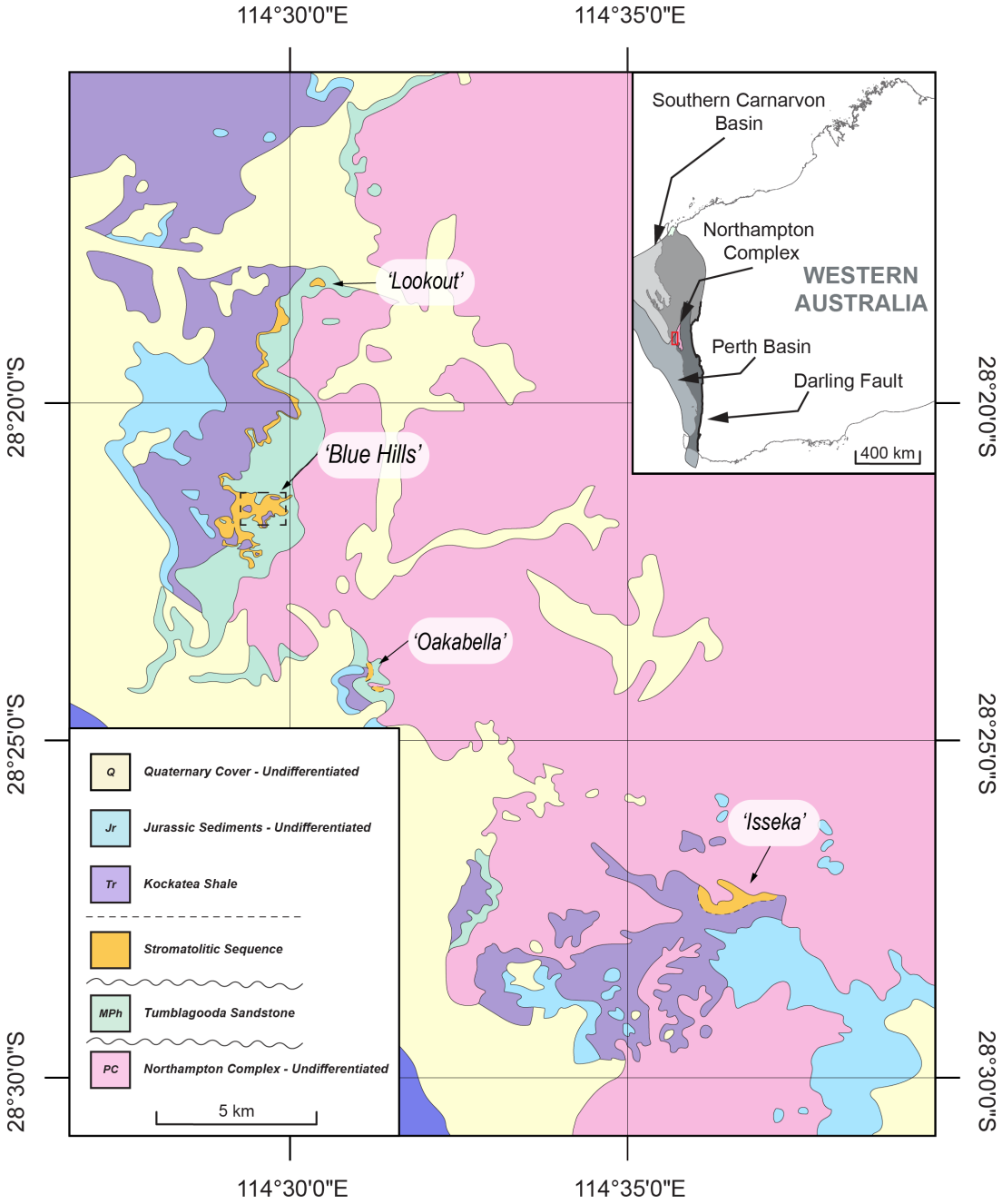

Fig. 2.2: Geological map of north-western Perth Basin. Inset: map of Western Australia with major components marked; red box indicates zoomed-in geological map. New stromatolite occurrences marked: 'Lookout', 'Oakabella' and 'Isseka', previous extent of Perth Basin stromatolites after Chen

et al. (2014) (dashed box). Ages of units given as; Q) Quaternary, Jr) Jurassic, Tr) Triassic, MPh) mid-Phanerozoic and PC) Precambrian. Map datum is WGS1984.

2 Geological Background

2.1 Tectono-stratigraphic overview of the Perth Basin

The northern Perth Basin developed from the Early Palaeozoic to the Mesozoic by several phases of rifting that led to separation between Greater India and Australia in the Early Cretaceous (Norvick, 2004). Deposition of the fluvial Tumblagooda Sandstone marks the earliest rifting phase (Fig. 2.3; Hocking, 1991; Mory & Iasky, 1996; Mory, Iasky, & Ghori, 2003; Thomas, 2014). From the mid-Carboniferous to Early Permian the Perth Basin formed part of the Eastern Gondwanan Interior Rift system (Norvick, 2004; Haig et al, 2015), where fluvio-glacial and fluvio-deltaic sediments were deposited in the Perth Basin, associated with the late Palaeozoic icehouse climate (Eyles, Mory, & Eyles, 2006; Mory, Redfern, & Martin, 2008). In the mid- to late Permian, dominantly fluvial and minor shallow marine deposition developed (Mory and Iasky, 1996). A major marine transgression during the latest Permian–Early Triassic deposited the Kockatea Shale (Fig. 2.3; Mory & Iasky, 1996). Subsidence continued through the Middle to Late Triassic, with another interval of extension occurring in the Early Jurassic (Gorter, Hearty, & Bond, 2004; Mory & Iasky, 1994; Norvick, 2004; Song & Cawood, 2000; Thomas, 2014). A period of tectonic quiescence during the Middle Jurassic was followed by rift-reactivation (Olierook et al., 2019a). This younger rift event continued into the Early Cretaceous, associated with the breakup of Australia and Greater India, around 137–136 Ma (Gibbons, Whittaker, & Müller, 2013; Olierook et al., 2016). The Perth Basin subsequently developed into a passive margin and has experienced relatively little tectonic activity since (Mory & Iasky, 1994; Norvick, 2004; Song & Cawood, 2000).

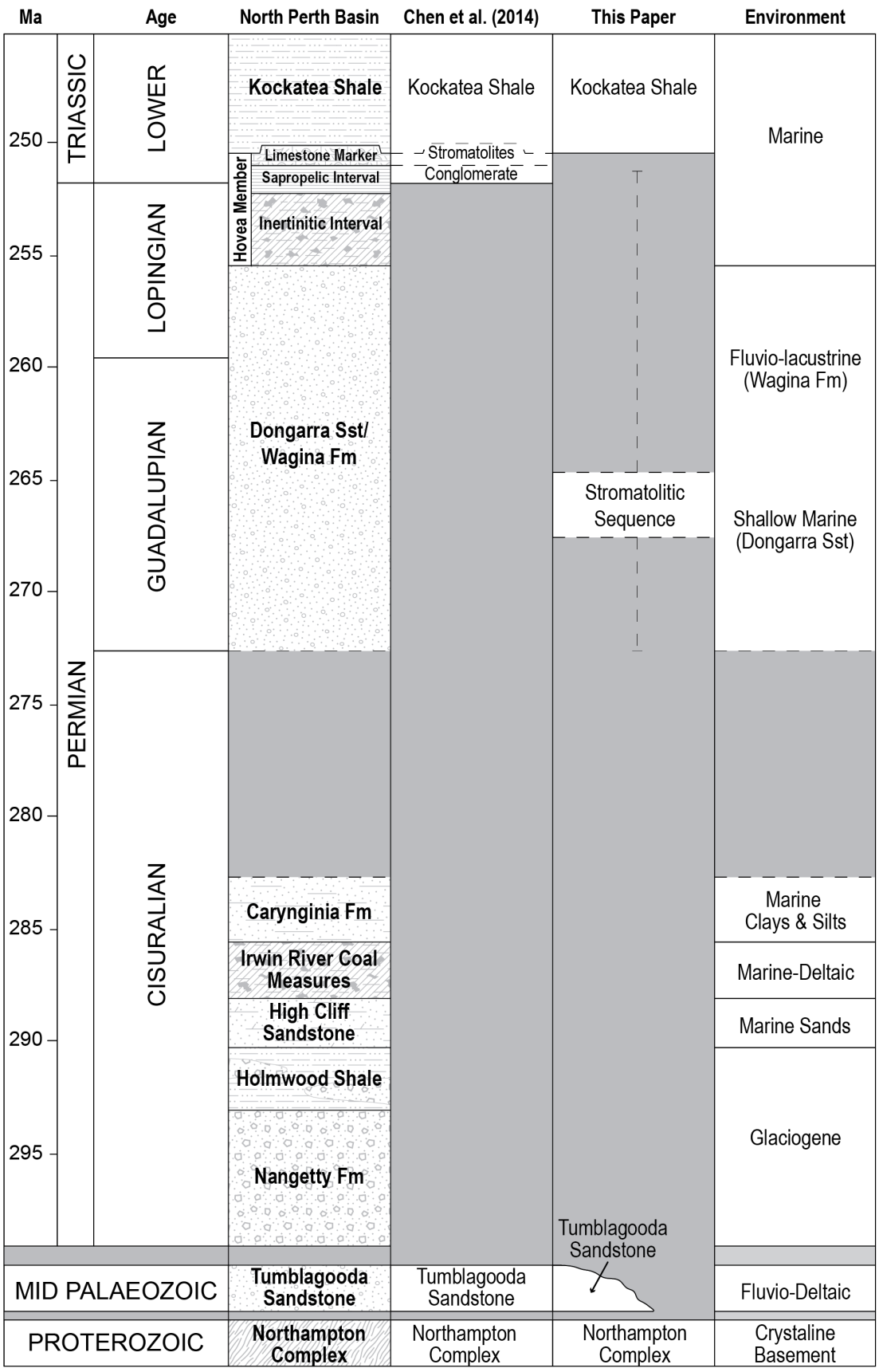
Ma
Age
North Perth Basin
Chen et al. (2014)
This Paper
Environment
250
255
260
265
270
275
280
285
290
295
TRIASSIC
PERMIAN
LOWER
LOPINGIAN
GUADALUPIAN
CISURALIAN
Kockatea Shale
Limestone Marker
Sapropelic Interval
Hovea Member
Inertinitic Interval
Dongarra Sst/
Wagina Fm
Carynginia Fm
Irwin River Coal
Measures
High Cliff
Sandstone
Holmwood Shale
Nangetty Fm
Tumblagooda
Sandstone
Northampton
Complex
Kockatea Shale
Stromatolites
Conglomerate
Tumblagooda
Sandstone
Northampton
Complex
Kockatea Shale
Stromatolitic
Sequence
Tumblagooda
Sandstone
Northampton
Complex
Marine
Fluvio-lacustrine
(Wagina Fm)
Shallow Marine
(Dongarra Sst)
Marine
Clays & Silts
Marine-Deltaic
Marine Sands
Glaciogene
Fluvio-Deltaic
Crystaline
Basement
MID PALAEOZOIC
PROTEROZOIC

Fig. 2.3: Composite Perth Basin stratigraphy after Thomas et al. (2004), Mory, Haig, Mcloughlin, and Hocking (2005), previous interpretation of 'Blue Hills' Chen et al. (2014) and a new interpretation of Perth Basin stromatolites (this paper).

2.2 Mid-Phanerozoic stromatolites in the Perth Basin, Western Australia

Mid-Phanerozoic stromatolites have been reported from a single small locality (~6 km^2; 'Blue Hills') in the northern Perth Basin, Western Australia, at 28°21'04.5"S and 114°37'51.6"E (Chen et al., 2014; Mory et al., 2005). The site is bound by the underlying Mid-Palaeozoic Tumblagooda Sandstone to the east and overlain by Triassic–Jurassic sedimentary successions to the south, west and north (Fig. 2.2). The stromatolites were assigned to the Smithian (Lower Triassic) based on interpreted conformity with the overlying Kockatea Shale containing biostratigraphically significant ammonoid trace fossils (Chen et al., 2014). Siltstone beds in the Kockatea Shale contain ichnofauna Arenicolites, Lockeia and Palaeophycus striatus, within a shallow marine setting (Chen et al., 2012).

The Blue Hills stromatolites have been tentatively correlated with a limestone marker that has been intersected in wells and drill core through the Kockatea Shale, which is a prominent source rock for the Perth Basin (Mory et al., 2005). In drill core, the limestone marker displays finely laminated fabrics associated with microbial influence and biogenic sedimentary structures (Luo et al., 2019; Thomas et al., 2004). Additionally, the limestone marker in places contains *Claraia* shells and has been dated recently using conodonts as late Dienerian to early Smithian (Metcalfe, Nicoll, & Willink, 2008).

3 Methods

3.1 Field mapping and sampling

Fieldwork was conducted ~420 km north of Perth, Western Australia, radiating out from the original site (Chen et al., 2014; and references therein). Satellite imagery was used to identify target areas along the boundary of the Northampton Complex or Tumblagooda Sandstone and the overlying Kockatea Shale (Fig. 2.2). Representative samples were collected from each locality, as well as images detailing relationships where sampling was not possible.

3.2 Sample imaging

Samples were cut and polished to expose cross-sectional profiles of stromatolites and associated strata. Selected thin section blocks were coated with clear epoxy and vacuum-sealed

to increase structural integrity. Blocks were mounted on glass slides and polished to a thickness of 30 μm. Thin sections were scanned on a Zeiss Axio Imager II optical microscope in both reflected and transmitted light at Curtin University.

4 Results

4.1 Microbialite forms

Regional mapping identified ten microbialite forms (Table 2.1; Fig. 2.4). Stromatolites were classified following techniques identified in Awramik (1992), Bosak et al. (2013), Cloud and Semikhatov (1969), Grey and Awramik (2020), Hofmann (1969), Hofmann (1976a), Preiss (1976), Walter (1977).

Form 1: stratiform (flatly layered) stromatolites grow directly on horizontal substrates, including older stromatolites. The microbialites occur as a generally thin continuous crust. Although the laminae are primarily stratiform, they can also be undulatory.

Form 2: stubby columnar microbialites encrust clasts, or grow on older stromatolites (form 1). The columns are mostly cylindrical but sometimes turbinate (columnar diameter increases upwards). The columns coalesce as they grow vertically. Walls of the columns are simple, enveloping the structure.

Form 3: slender columnar microbialites grow on older forms (forms 1 and 4). The columns are cylindrical and anastomosed. Branching occurs as alpha mode, with the branches maintaining the same diameter as the original column itself. Low degrees of divergence are present in the anastomosis, with branches parallel. Walls of the columns are patchy, with some sections having no wall and others developing simple enveloping walls.

Form 4: mini-branching (beta ± alpha) columnar microbialites grow on older forms (forms 1 to 3), and are branched (a single horizon simultaneously branches into two or more separate structures) at the transition into this form. The columns have an average diameter of ~3 mm, with typical 1 mm laminae amplitudes. Laminae are convex. The branching columns are erect and slender, with primarily beta branching (column splits into branches, with total diameter gradually increasing up structure) and minor alpha branching (columns split into branches but retain original diameters). The structure exhibits lateral branching styles.

Form 5: mini-branching (beta ± gamma) columnar microbialites grow on older forms (forms 1 and 6). The transition into this form is defined by furcatebranching. The columns have an

average diameter of ~5 mm, with the laminae having typical amplitudes of ~3 mm. The laminae are steeply convex. The branching columns are erect and slender, with primarily beta, and in some cases, gamma branching (columns split into branches that propagate laterally and then vertically, marking distinct boundaries between the original columns and the branches). The structure exhibits dichotomous branching. This microbialite form anastomoses in some thicker sections. Divergence of the branching structures depends heavily on the nature of the underlying/basal forms. Where the basal form is highly convex, the mini-branching columns have high degrees of divergence. As in stratiform basal forms, the subsequent branching mode is characteristic of low degrees of divergence.

Form 6: domal microbialites grow on older forms (forms 1 to 3), as well as directly onto the substrate. Domes have average diameters ranging between 10 and 30 cm. Composite domes (a coalesced structure comprising multiple individual structures) can reach up to 1 m in diameter. The domes are hemispherical and nodular.

Form 7: lobate columnar microbialites are sometimes polygonal, encrust stratiform forms (form 1) and underlying substrates. The columns have an average diameter of 1 cm and 2 mm laminae amplitudes. The columns are inclined.

Form 8: bulbous microbialites grow on older forms (forms 1, 4 and 7). The domes have a diameters of 1–2 cm with 1–2 mm amplitudes. The walls of the domes are predominantly simple, though in some cases complex. The domes are erect and coalesce into other microbialite forms (forms 1 and 5).

Form 9: teepee microbialites encrust cracks forming uplifted teepee-like structures. Laminae are undulatory, with a horizontal and gently convex-upwards profile. The laminae encrust cracks of other microbial material.

Form 10: mini-columnar stromatolites encrust older forms. They have diameters of 5–10 mm with laminae amplitudes of ~1 mm. Walls of the columns are simple, with the laminae gently to steeply convex. The columns are erect, uniform and stubby. The mini-columns coalesce together.

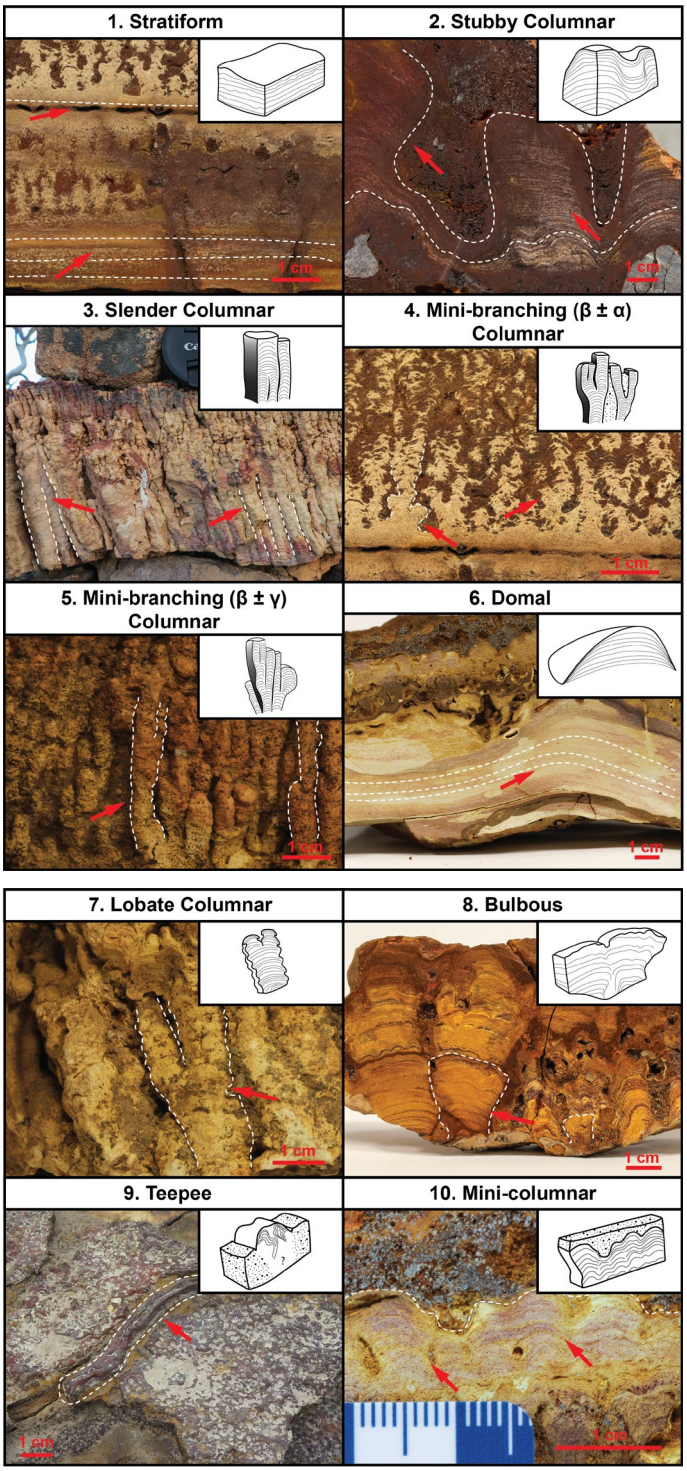

Fig. 2.4: Microbialite (stromatolite) forms: 1) stratiform, 2) stubby columnar, 3) slender columnar, 4) mini-branching (beta ± alpha) columnar, 5) mini-branching (beta ± gamma) columnar, 6) domal, 7) lobate columnar, 8) bulbous, 9) teepee, 10) mini-columnar. Red arrows point to the individual microbialite forms.

Table 2.1: Summary of microbialite forms as described in section 4.1 and Fig. 2.4

Form	Initiation	Spacing	Shape	Sub-shape	Height to width ratio	Variability of growth	Branching style	Branching mode	Angle of divergence	Laminae profile	Wall type	Diameter
1	directly onto substrate	continuous	stratiform/layered	-	-	-	-	-	-	stratiform/ undulatory	-	-
2	encrust clasts/older stromatolites	openly spaced	columnar	cylindrical/ turbinate	stubby	uniform, coalesce at top of structures	-	-	-	moderately convex	simple	3 cm
3	older stromatolites	openly-closely spaced	columnar	cylindrical	slender	uniform	anastomosed	alpha	low	moderately convex	patchy	2-3 cm
4	older stromatolites	closely spaced	mini-columnar	cylindrical	slender	uniform	furcate	alpha, minor beta	high	moderately convex	simple	3 mm
5	older stromatolites	closely spaced	mini-columnar	cylindrical	slender	uniform	furcate	beta, minor gamma	high	steeply convex	simple	5 mm
6	older stromatolites	closely spaced	domal	hemispherical	-	uniform	-	-	-	convex	-	10 – 30 cm
7	older stromatolites	closely spaced	columnar	cylindrical, lobate	slender	uniform	-	-	-	steeply convex	simple	1 cm
8	older stromatolites	closely spaced	domal	bulbous	-	uniform	-	-	-	steeply convex	-	1 – 2 cm
9	encrusting	continuous	-	-	-	horizontally, gently convex	-	-	-	undulatory	-	-
10	older stromatolites	closely spaced	mini-columnar	cylindrical	stubby	uniform, coalesce at top of structures	-	-	-	gently-steeply convex	simple	5-10 mm

4.2 Localities

Stromatolites sporadically crop out over a minimum mapped distance of ~24 km in a NW–SE trending belt (Fig. 2.2), significantly larger than originally reported. Mapping has identified three significant new stromatolite sites with similar lithologies to the Blue Hills locality: 'Lookout', 'Oakabella' and 'Isseka' (Fig. 2.2). The stratigraphic relationships of the different lithologies at each locality are summarised in Fig. 2.5.

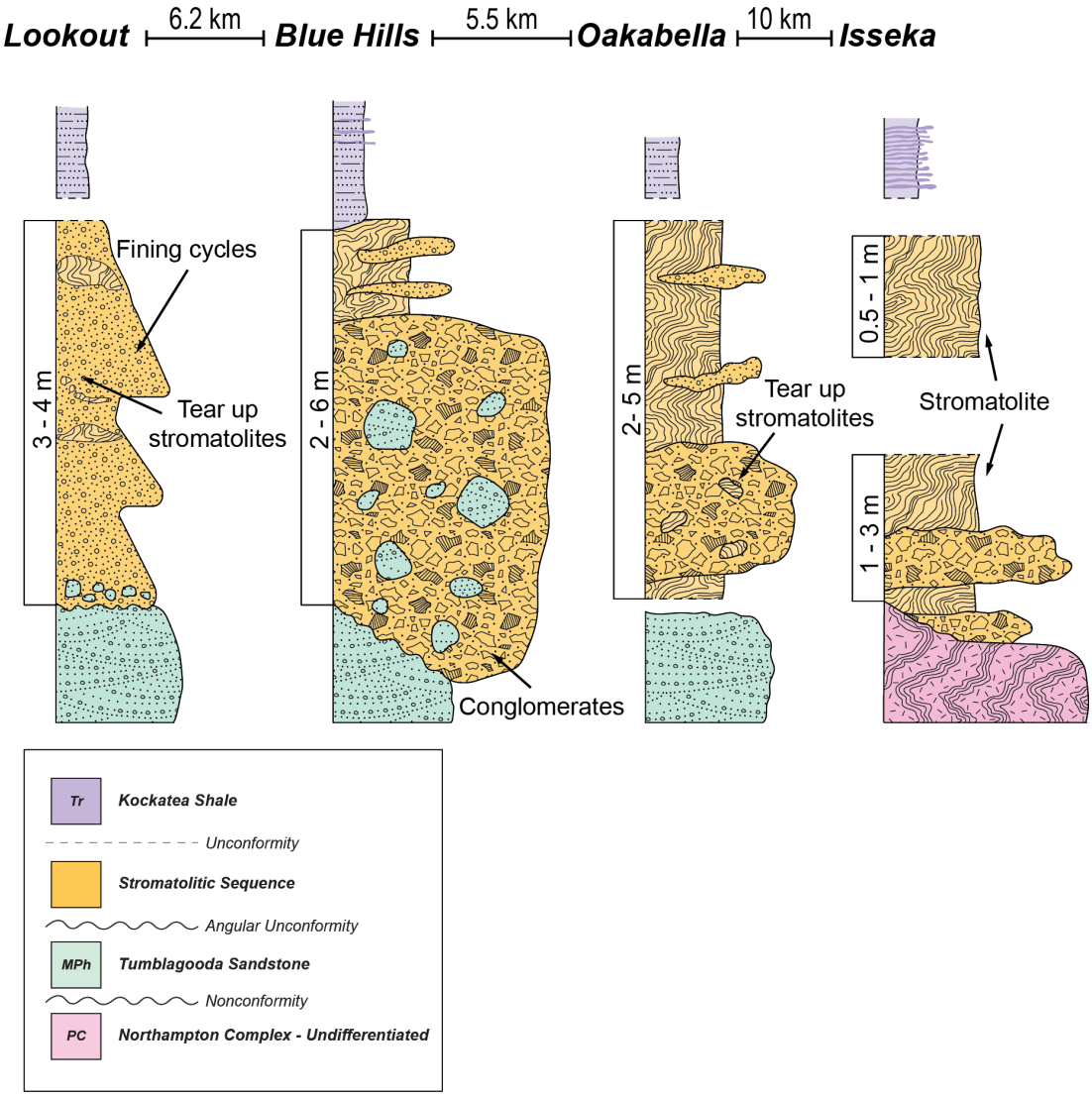

Fig. 2.5: Schematic lithological logs of the field localities, arranged approximately from the north on the left to south on the right. Logs are organised to demonstrated stratigraphic relationships between each locality.

The stromatolitic succession unconformably overlies the mid-Palaeozoic Tumblagooda Sandstone in some areas (Fig. 2.6), whereas elsewhere it rests nonconformably on the

Precambrian Northampton Complex. The upper constraints of this unit are defined by a difference in regional dips between the stromatolitic succession and the Kockatea Shale, with the shales onlapping at 5° onto the stromatolites at Blue Hills (Fig. 2.7). The stromatolitic succession is defined by interfingered and contemporaneous microbialites (stromatolites) and coarse-grained clastic sedimentary rocks. The succession has been heavily altered with silicification of original stromatolitic carbonates and later ferruginisation.

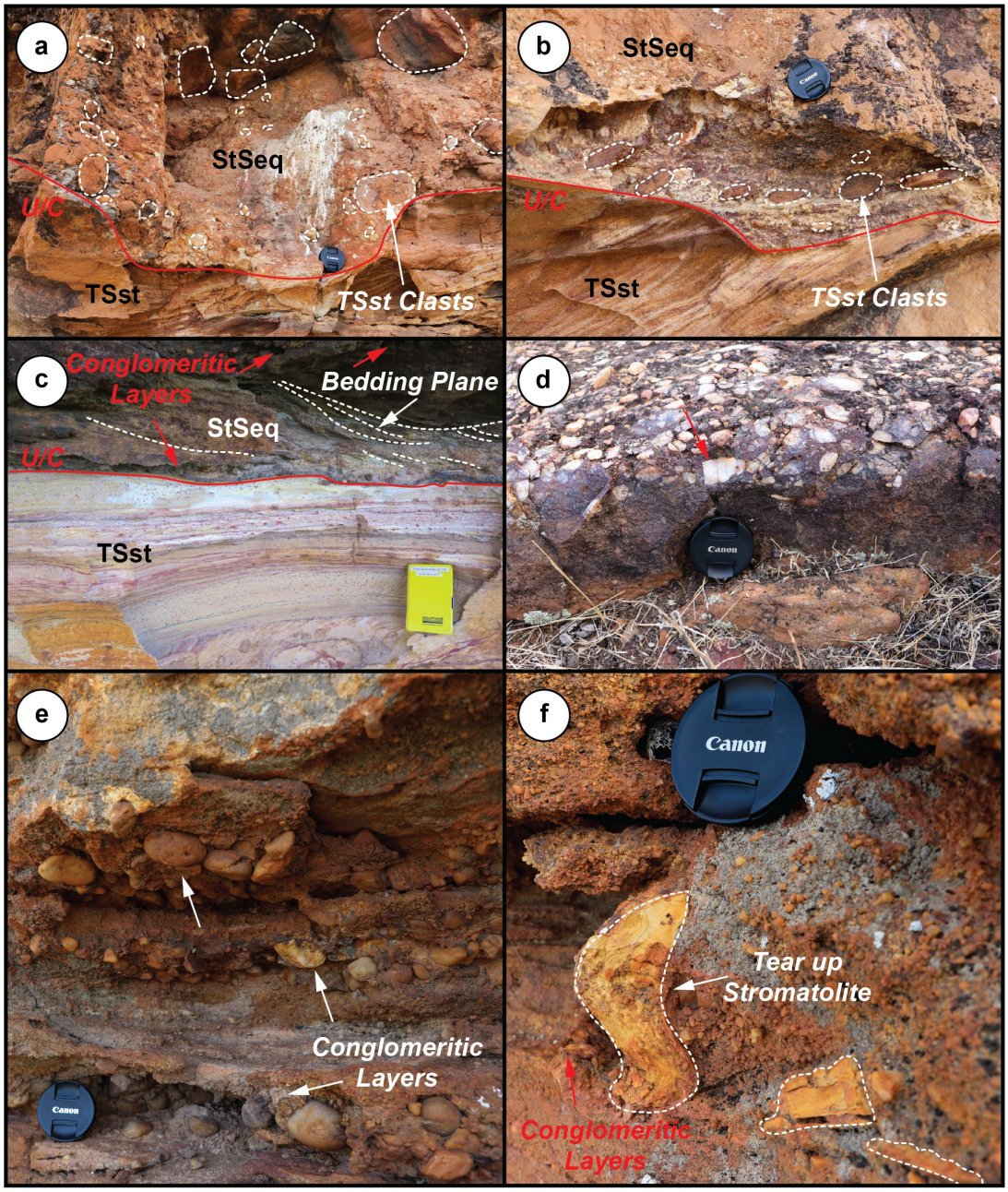

Fig. 2.6: Clastic material within the stromatolitic unit: a) incised 'channel' into the Tumblagooda Sandstone (Blue Hills), b) weakly imbricated clasts within the clastic sediments (Blue Hills), c) trough cross-bedding within clastic material unconformably overlying the Tumblagooda Sandstone (Blue Hills), d) conformable transition between sandstone and conglomerates (Lookout), e) alternating layers of sandstones and conglomerates within the stromatolitic sequence clastics (Blue Hills), f) stromatolitic rip-up clasts within clastic sediments (Lookout). StSeq = Stromatolitic sequence, TSst = Tumblagooda Sandstone. Red arrows point to small 'conglomeratic layers'.

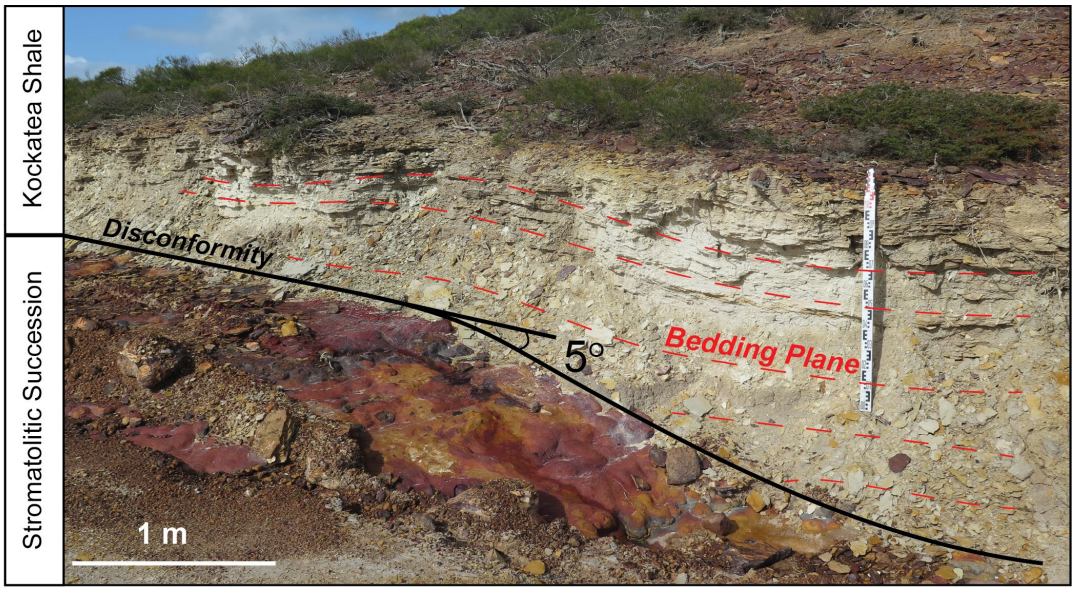

Fig. 2.7: Onlapping relationship of the Kockatea Shale on the stromatolitic succession. Red dashed lines represent bedding surfaces of the Kockatea Shale.

4.2.1 Blue Hills

The mid-Palaeozoic Tumblagooda Sandstone basement at Blue Hills is characterised by a matrix of medium-grained, high-sphericity, moderately-rounded quartz grains, which supports minor (10–12%) elliptical granules to pebbles of quartz. Relatively coarse-grained sediments are concentrated at the base of metre-scale trough cross-beds. The trough cross-bedding fines upwards with ripples on a 1–20 cm scale.

The clastic sedimentary rocks are primarily defined by cobble conglomerates and medium- to coarse-grained quartz sandstones. The clastic material forms lenses with both distinct and gradual transitions (Fig. 2.6c, d, e). In the thickest conglomerate section, there is isolated evidence of imbricated clasts, consistent with a tentative palaeocurrent suggested from cross-stratification towards 030° ($n = 6$; Fig. 2.6b).

The conglomerates have a coarse-grained matrix of quartz, which are highly spherical and sub-angular, making up ~45% of the unit, with a siliceous cement. The clasts comprise quartz (~25%) and lithic fragments (~10%). Lithic fragments range in size from 10 to 50 cm and are angular with moderate sphericity. The majority of lithic clasts are composed of the underlying Tumblagooda Sandstone, with the remainder representing metasedimentary rocks presumably from the Northampton Complex (Fig. 2.6a). The quartz clasts show bimodal sizes, with the larger quartz clasts moderately spherical and well rounded, appearing similar to clasts located in the underlying Tumblagooda Sandstone. The smaller quartz clasts have moderate sphericity

and are sub-angular. Conglomerates are interbedded with medium- and coarse-grained quartz sandstones (Fig. 2.6e). Clasts show high sphericity and are sub-rounded. Clasts are imbricated towards 030°, and bedding is ~10 cm thick (Fig. 2.6e).

Microbialites (stromatolites) are intimately related to the clastic sediments, with bioherms in lenses within and in places as rip-up clasts in the sediments (Fig. 2.6). At Blue Hills, an idealised succession of growth sees forms 1 (stratiform), 2 (stubby columnar) and 6 (domal) encrusting clasts of the conglomerate. Moving up section, these forms coalesce and then branch into form 4 (mini-branching [alpha ± beta] columnar). The branching mini-columns anastomose up sequence alternating with form 1 (stratiform). Changes in clastic material within the stromatolite interstitial spaces mark the transitions between forms. Teepee stromatolites (form 9) are found growing between cracks that cross-cut the lower growth horizon. At the same horizon, there are desiccated stromatolite mounds, with textures that resemble cross-sectioned garlic bulbs (Fig. 2.8g). The uppermost microbialite of the section changes across the locality, ending in either domes (form 6) or branching mini-columns (form 4).

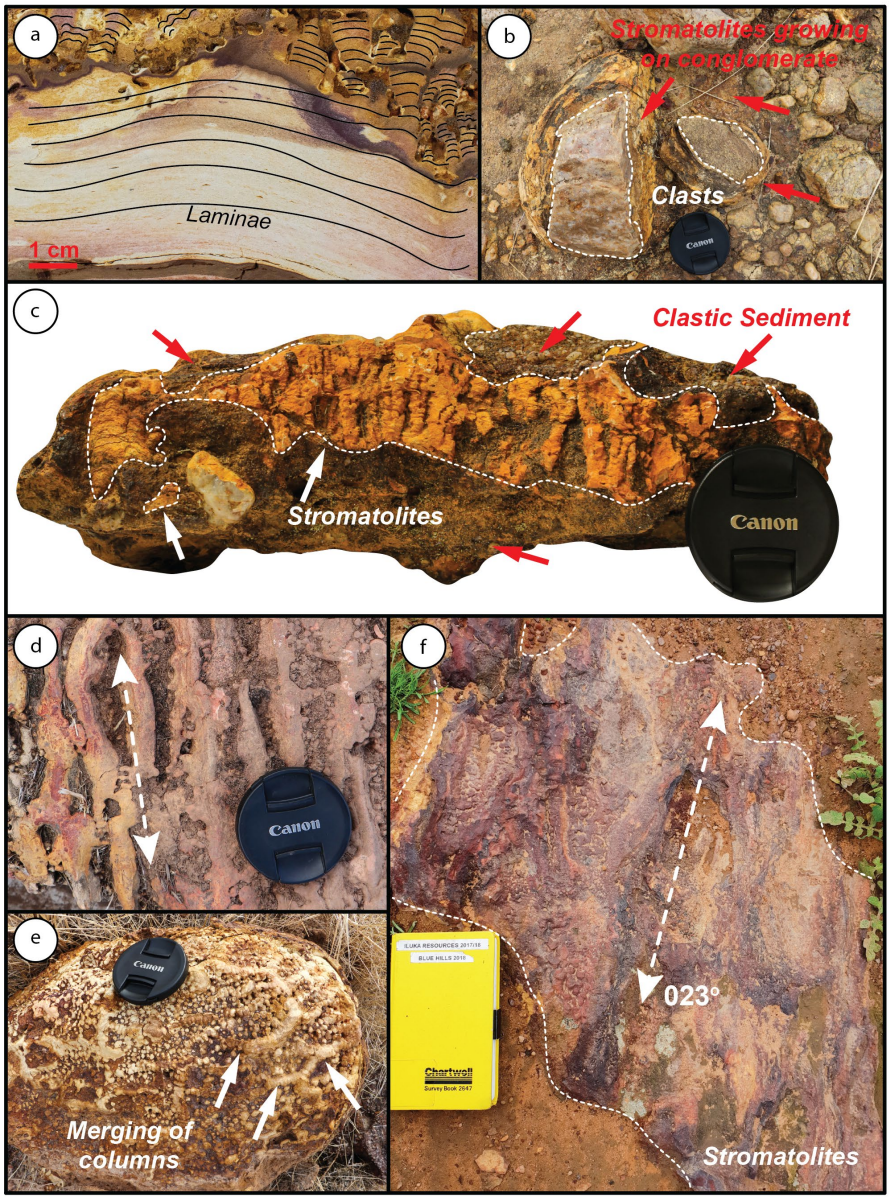
a
Laminae
1 cm
b
Stromatolites growing on conglomerate
Clasts
Canon
c
Clastic Sediment
Stromatolites
Canon
d
Canon
e
Canon
Merging of columns
f
023°
Stromatolites

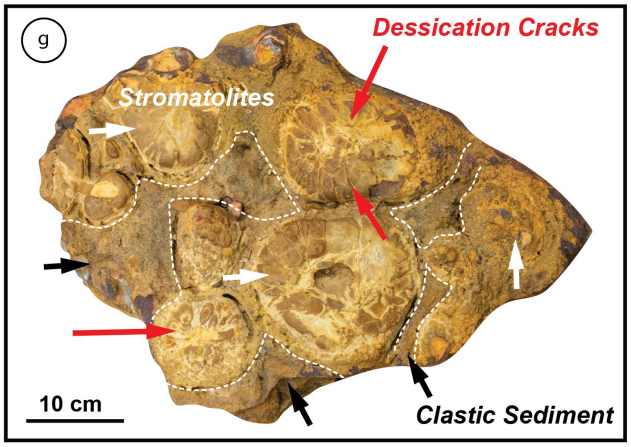
g
Dessication Cracks
Stromatolites
10 cm
Clastic Sediment

Fig. 2.8: Stromatolite macroscopic structures in outcrop: a) stromatolite domes and digitates occurring contemporaneously, b) stromatolites encrusting clasts, c) lens of stromatolite within clastic sediments, d) alignment and elongation of stromatolites formed from the coalescing of branching mini-columnar and columnar structures, e) coalescing stromatolites forming polygonal microbial growths, f) alignment of large stromatolite domes trending 023º on weathered outcrop surface, g) eroded stromatolite domes showing garlic garlic-like texture. StSeq = Stromatolitic sequence, TSst = Tumblagooda Sandstone.

The stromatolitic succession at Blue Hills is between 2-6 m in thickness, and onlapped by the Kockatea Shale (Fig. 2.7), the latter comprises alternating beds of finely laminated claystone and siltstone to fine-grained sandstone. Siltstone and fine-grained sandstone beds range in thickness from 1 to 6 cm and thicken up sequence. The frequency of siltstone and fine-grained sandstone increases from ~10 % at the base of the unit to ~60 % near the top. Soft white claystone beds, with thicknesses of ~2–10 cm decrease up sequence. Bioturbation increases vertically, occurring in >15 % of the siltstone beds of the sequence. The siltstone beds above the stromatolites preserve ichonofauna. Lower beds in the Kockatea Shale have microbial wrinkle structures. Heavily ferruginised siltstone and sandstone beds preserve trough cross-bedding occurring at dm scales with amplitudes at the cm-scale. Bedding surfaces of the siltstone layers have linguoid ripples.

4.2.2 Lookout

The mid-Palaeozoic Tumblagooda Sandstone, which unconformably overlies the Northampton Complex, defines the basement at Lookout (Fig. 2.5). The stromatolitic succession is 3-4m thick and composed of interfingered conglomerates, coarse-grained sandstones and stromatolites, unconformably overlies the Tumblagooda Sandstone. The stromatolites occur as forms 1 (stratiform), 2 (stubby columnar) and 4 (mini-branching (alpha ± beta) columnar). Thin lenses of the stromatolites occur within the clastic material. There are also thin veneers of form 1 (stratiform), which variably thicken laterally, that are more continuous through the clastic material; in some sections, these forms are ripped up and disturbed (Fig. 2.6f). Where the stromatolite veneers thicken, forms 2 (stubby columnar) and 4 (mini-branching (alpha ± beta) columnar) grow. To the south of the locality, clastic material in the stromatolitic sequence is trough cross-bedded (Fig. 2.6c). Shales ascribed to the Kockatea Shale overlie the stromatolitic succession; however, the contact is not preserved.

4.2.3 Oakabella

The mid-Palaeozoic Tumblagooda Sandstone defines the basement at Oakabella (Fig. 2.5). The stromatolitic succession is 2-5m thick and composed of interfingered conglomerates, coarse-grained sandstones and stromatolites, overlies the Tumblagooda Sandstone. However, the contact between the Tumblagooda Sandstone and the stromatolitic succession is not apparent in this locality (Fig. 2.2). The lower parts of the stromatolitic succession are composed of alternating conglomerates and coarse-grained sandstones. Within these clastic beds, there are rip-up clasts of microbialite forms 1 (stratiform) and 2 (stubby columnar). Up sequence of the rip-up clasts are microbialite forms 1 (stratiform), 3 (slender columnar), 6 (domal), 8 (bulbous) and 10 (mini-branching) that occur concurrently. The contact between the stromatolitic succession and the overlying Kockatea Shale is not evident at this locality (Fig. 2.2).

4.2.4 Isseka

The Precambrian Northampton Complex forms the basement at Isseka (Fig. 2.5) and is unconformably overlain by the stromatolitic succession which is here 1.5-4m in thickness. The lower part of this succession is comprised by poorly sorted, coarse-grained sands and conglomerates, which are interfingered with stromatolites. In some places, stromatolites (form 5, mini-branching [beta ± gamma] columnar) grow directly onto the Northampton Complex. The stromatolites encrust clasts of the clastic sediments (Fig. 2.8b). Stromatolite boulders are present, sourced near situ, with lobate columns coalescing into slender columns then branching into mini-branching (beta ± gamma) columnar stromatolites. Clasts of stromatolite forms are present within coarse-grained sandstone (Fig. 2.6f, Fig. 2.8c). The contact between the stromatolitic succession and the Kockatea Shale is not visible at this locality. Further south of Isseka, upper sandstones of the Kockatea Shale directly onlap the Northampton Complex.

5 Discussion

5.1 Palaeodepositional setting of the Mid-Phanerozoic stromatolites, Western Australia

The north Perth Basin stromatolites were previously interpreted to have grown within a wave-cut platform setting, where the conglomerates represent a basal lag and the overlying Kockatea Shale represent a regional transgression that flooded the sequence during the Lower Triassic (Chen et al., 2014). An alternative depositional setting is proposed of a restricted water body

with discrete fluvial influences. This is based on three primary observations: (i) the nature of clastic sediments and stromatolites, (ii) stromatolite macro- and mesostructures, and (iii) stratigraphic relationships.

5.1.1 Nature of clastic sediments and stromatolites

The interbedded sandstone and conglomerates of the stromatolitic succession vary significantly in thickness, typically lack consistant preferential imbrication of clasts, are poorly sorted and matrix supported (Fig. 2.6a, b and e), more characteristic of episodic mass-flow deposition (Gawthorpe & Leeder, 2000; Miall & Postma, 1997). Wave-cut platform conglomeratic lags are commonly clast-supported with strong continuous imbricated fabrics (Smith et al., 2018; 2011). Similarly, stromatolites growing in wave-cut platform settings are typically isolated to small rock pools, forming encrusting wrinkled/tussocky surfaces that bind storm deposits (Fig. 11a; Smith et al., 2018; 2011), distinct from those seen in the mid-Phanerozoic Perth Basin stromatolites (Fig. 11b).

Interfingering of the stromatolites with the clastic material indicates periods of quiescence, enabling stromatolite growth (Fig. 2.8b and c), with punctuated energetic events (mass flows?) disrupting and reworking stromatolite horizons (Fig. 2.6f). The intimate relationship between the clastic sediments and the stromatolites, and laterally variable nature of conglomeratic clast populations, could suggest multiple sedimentary inputs into the palaeo-depositional setting, features commonly associated with alluvial and fluvial systems (Miall & Postma, 1997).

The presence of clastic material atop the stromatolites appears to impede vertical growth, dependent on the thickness of the sediment. Where clastic material is thinnest (<1 mm), microbial colonies appear to have been able to migrate vertically and continue to grow (Fig. 2.9c). Where the clastic material is thicker (~>1 mm; Fig. 2.9c), growth of the microbial mat is impeded, likely due to a lack of sunlight and inability to photosynthesize (Buick, 1992).

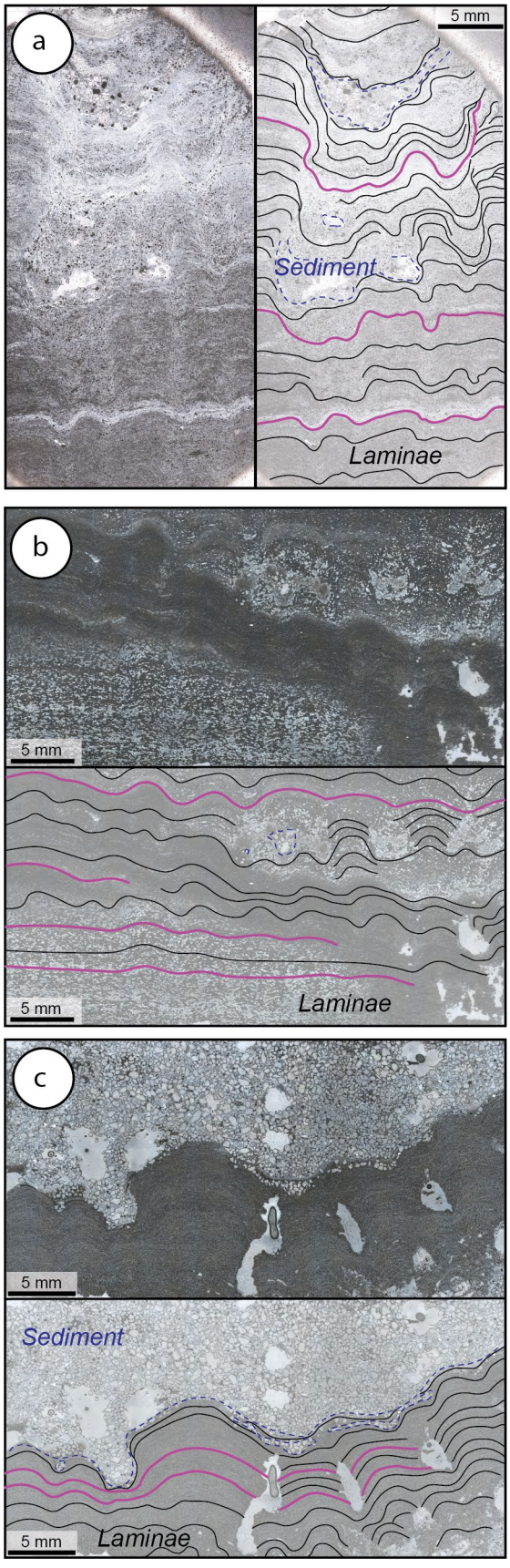
a
5 mm
Sediment
Laminae
b
5 mm
5 mm
Laminae
c
5 mm
Sediment
5 mm
Laminae

Fig. 2.9: Stromatolite microscopic structures in thin section and associated annotated interpretation with laminae (black) and laterally continuous laminae (purple): a) domal stromatolites transitioning into columnar structures, with undulating and laterally continuous laminae, b) smooth domal types transitioning laterally into digitates, with laterally continuous and undulating laminae, c) mini-columnar stromatolites merging together, growing around small sand lenses and arresting half-way up the thin section.

In fluvial environments (e.g., Benvenuti, 2003; Pollard, Steel, & Undersrud, 1982), conglomerates are typically locally derived, matrix-supported, and interfingered with claystone and/or carbonates (Arenas-Abad, Vázquez-Urbez, Pardo-Tirapu, & Sancho-Marcén, 2010). Stromatolites grew in these fluvial systems throughout the Phanerozoic, in: western Orkney during the Devonian (Fannin, 1969), Greenland during the Mid-Triassic (Clemmensen, 1978), California during the Pliocene (Link & Osborne, 1978; Link, Osborne, & Awramik, 1978), and Africa during the Cenozoic (Casanova, 1986, 1994). The nature of the Western Australian conglomerates described herein draws strong similarities to those seen in fluvial settings (Fig. 2.6 & 2.9; Arenas-Abad et al., 2010). Additionally, deposition of clastic material is cyclical in areas (see section 4.2), with measurable fining upwards sequences (Fig. 2.6e). This cyclic pattern is characteristic of discrete discharges observed in modern restricted water bodies (Link & Osborne, 1978). It is therefore likely that the stromatolitic succession formed in a palaeodepositional setting characterised by discrete fluvial and/or alluvial influences.

Alluvial fans form where streams, sourced from the hinterland, encounter a sudden decrease in slope, typically at the base of the upland region (Miall & Postma, 1997). Sediments are deposited rapidly as a consequence of the loss of energy and ‘fan’ out in a radial pattern. Typical characteristics of an alluvial fan include poorly-sorted coarse-grained sediments that are locally sourced (Blair & Mcpherson, 1994). Fans typically exhibit lateral fining textures. Main feeder channel sediments exhibit winnowing textures and imbrication of clasts. Reported occurrences of alluvial stromatolites commonly colonise the primary channel of the fan (Elmore, 1983). The stromatolitic succession exhibits negligible winnowing textures and has definite normal grading textures. Thus, a pure alluvial depositional environment is not consistent with observations for the Western Australian stromatolitic succession, although as mentioned above there may have been alluvial influences in the episodic deposition of the clastic sediments.

5.1.2 Stromatolite meso- and macrostructural evidence for palaeodepositional settings

Environmental conditions during the formation of the mid-Phanerozoic northern Perth Basin stromatolitic sequence (PBS) can be inferred from their meso- and macrostructures (e.g., Suosaari et al., 2019). Contemporaneous occurrences of different stromatolite morphologies occur with gradual lateral transitions across the field area (Fig. 2.8a). There are also distinguishable boundaries between different stromatolitic forms, moving up sequence (Fig. 2.4). These sudden vertical changes in morphologies with clastic material at the transitions are correlated with changes in environmental conditions resulting in a biotic response, following Horodyski (1977). Gradual, contemporaneous lateral transitions between morphologies are likely caused by biological influences (Golubic, 1976; Suosaari et al., 2019; Surdam & Wray, 1976). Alternating morphologies in the PBS in the northern Perth Basin, occurring laterally and vertically, suggest local environmental conditions varied significantly (Horodyski, 1977). Local environmental instability favours an isolated setting interpretation as open marine systems are typically buffered from local variations. Wave-cut platforms, although considered an open marine system at the exposed front, can form rock pools towards the back of the platform. Stromatolites in wave-cut platform rock pools commonly preserve storm deposits (Smith et al., 2011) whereas storm deposits trapped within laminae have not been found in PBS.

Environmental conditions also impact stromatolite structures, particularly those formed at higher energy and steeper gradients. Examples are sudden changes in stromatolite morphology, or the lineation/alignment of stromatolite structures with dominant currents. In contrast, stromatolites subject to low energy, coupled with low gradients, are more significantly influenced by biological factors. Examples being laterally contemporary stromatolite morphologies (Suosaari et al., 2019). The stromatolites described here infer and distal shoreline locations existed (*Fig. 2.10*).

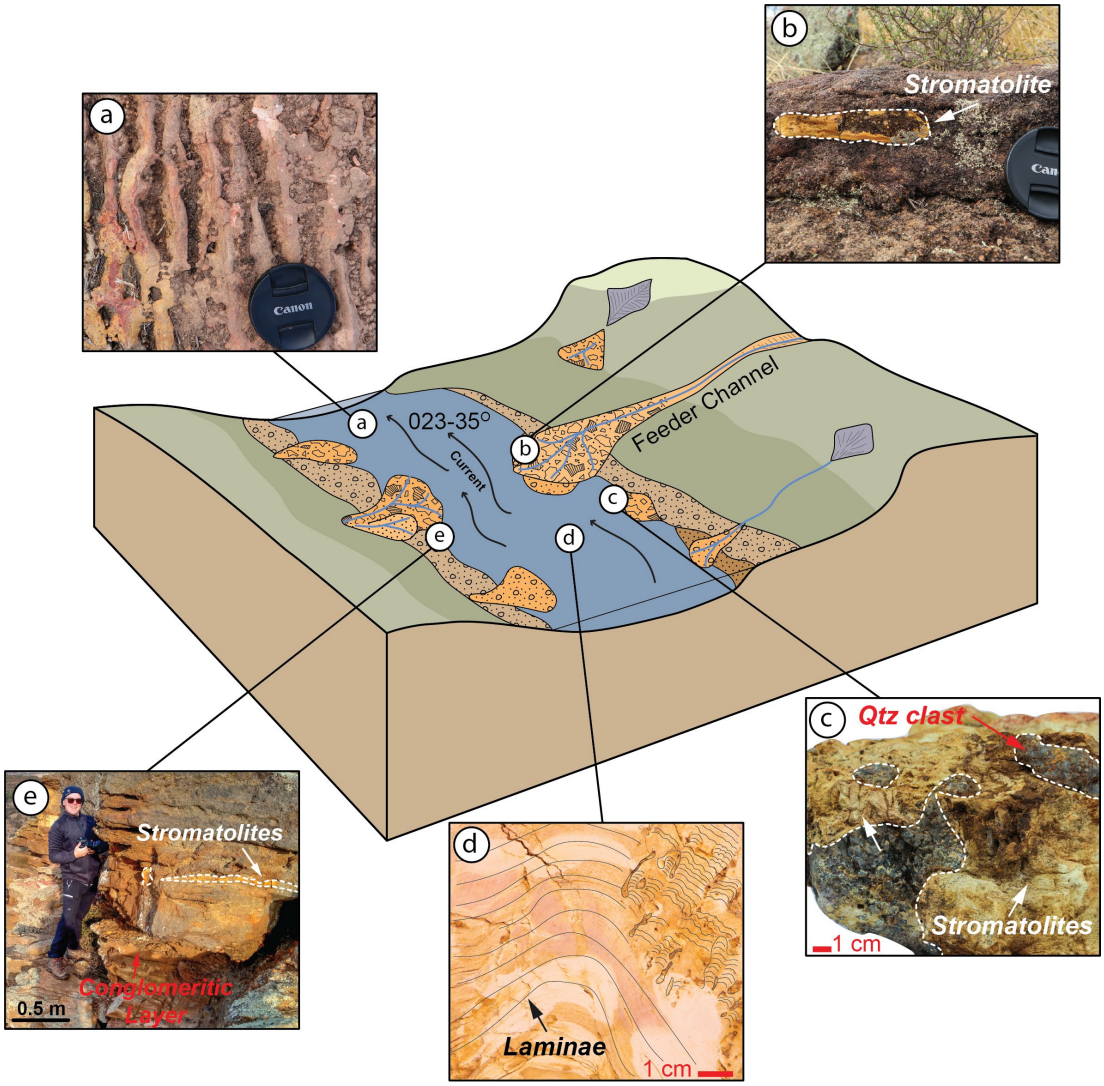

Fig. 2.10: A 3D palaeoenvironmental model of the northern Perth Basin during the development of the stromatolitic sequence, showing a restricted intracontinental setting with fluvial inputs. a) elongation of stromatolites aligning with the palaeocurrent (marked by arrows), b) stromatolite rip rip-up clasts in fluvial fans, c) stromatolites growing among quartz clasts (5 – 15cm, angular), d) laterally contemporaneous growth of differing stromatolite forms distal from environmental influences, e) local tearing of a stromatolitic horizon within coarse-grained clastic sediments.

Laterally continuous laminae, traceable across multiple stromatolite structures (Fig. 2.11b, c) are thought to reflect isolated environmental settings (Grey & Awramik, 2020; Monty, 1976). Examples of laterally continuous laminae include the lacustrine Eocene Green River Formation, western USA, (Fig. 2.11c) and *Asperia ashburtonia* from the Palaeoproterozoic Duck Creek Formation, Western Australia, interpreted to have developed in a lagoonal setting (Grey & Thorne, 1985). Stromatolites in open marine settings are not known to develop these laterally continuous laminae (Logan et al., 1964); instead, they display continuous

morphologies with little changes in visible structure (Walter, 1977). Hence, the presence of laterally continuous laminae in the PBS stromatolites suggests an isolated water body.

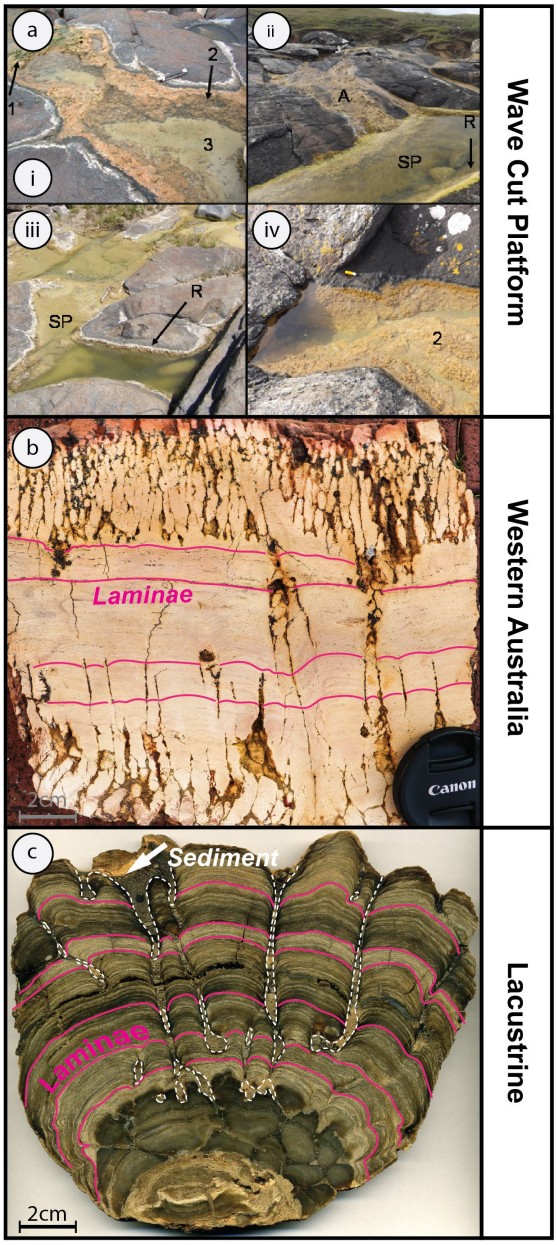

Fig. 2.11: Comparison between modern rock pool wave-cut platform and lacustrine stromatolites. a) Wave-cut platform stromatolites from i) Cape Morgan, South Africa, ii and iii) Luskentyre Bay, UK and iv) Mtentu, South Africa (Smith et al., 2018; 2011). Wave-cut platform rock pool stromatolites show pustular (1), laminar and columnar (2) and colloform (3) morphologies. SP = Stromatolite pool, A = stromatolite apron, R = stromatolite rim (R). b) Northern Perth Basin stromatolites (this study), showing laterally continuous laminae, similar to those in panel c. c) lacustrine stromatolites in the Eocene Green River Formation following Awramik and Buchheim (2015) and Surdam and Wray (1976).

The presence of tepee stromatolites (Fig. 2.4) and desiccated stromatolite domes (Fig. 2.8g) in the PBS indicates the unit was sub-aerially exposed prior to burial. Teepee stromatolites (Fig. 2.4) colonise walls of cracks, growing mini-dome structures into the created space and then vertically out of the structure (Von Der Borch, Bolton, & Warren, 1977). This is supported by the presence of desiccated stromatolitic domes, showing 'garlic-like' textures (Fig. 2.8g), similar to those exposed in modern day Shark Bay, Western Australia (Suosaari et al., 2016). These forms suggest that the PBS was subject to periods of 'drying' or water level change for extended periods.

5.1.3 Stratigraphic relationships

Unconformable relationships bounding the PBS prevent contextualisation of the sequence within the stratigraphic framework of adjacent successions. A major unconformity below the PBS suggests periods of erosion before deposition (Fig. 2.6a). Substantial periods of erosion with the episodic mass deposition of coarse-grained clastic sediments could promote a nascent isolated setting, similar to the modern East African Rift Valley (Casanova, 1986, 1994). The boundary between the PBS and the overlying Kockatea Shale is locally unconformable which demonstrates that they retained relief when drowned by the Kockatea Shale during the subsequent transgression as is typical of bioherms (Fig. 2.7).

5.2 Age of the Mid-Phanerozoic stromatolite occurrence, Western Australia

The age of the PBS is poorly constrained, as the sequence is typically too coarse-grained, diagenetically modified and exposed to oxidising conditions for geochemical analysis and preservation of age-diagnostic microfossils. Additionally, detrital zircon studies within the Perth Basin have demonstrated limited contemporaneous volcanic activity or incorporation of young zircons that provide meaningful maximum depositional ages to the sequences (Cawood & Nemchin, 2000; Markwitz et al., 2017; Olierook et al., 2019a). To constrain the age of the PBS, we evaluate its correlations with the under- and overlying stratigraphy, and place its deposition into a tectonic and stratigraphic framework of the Perth Basin.

The PBS was originally identified as late Smithian (Olenekian) based on ammonoid traces identified within the overlying Kockatea Shale (Chen et al., 2012; 2014). Subsequently, the PBS had been tentatively correlated with the limestone marker of the Hovea Member in the Kockatea Shale (Fig. 2.3), characterised in core by limestones rich in *Claraia* shells (Haig et al., 2015; Mory et al., 2005). The lack of *Claraia* shells in the PBS does not necessarily

preclude temporal equivalence with the limestone marker as the PBS could represent a laterally equivalent facies.

The overlying Kockatea Shale is assumed to have deposited relatively quickly, associated with a regional rapid marine transgression (Thomas & Barber, 2004). The implication is that there would be little temporal difference between the material deposited directly atop the PBS and the Olenekian part of the Kockatea Shale. An onlapping relationship between the Kockatea Shale and the PBS demonstrates a clear temporal gap, although the duration of this hiatus remains uncertain (Fig. 2.7). Conservatively, if the hiatus was minimal, the minimum age for the PBS is still Early Olenekian, based on fossil evidence in the overlying Kockatea Shale (Chen et al., 2012).

Constraining the maximum age is more problematic. The underlying Mid-Palaeozoic Tumblagooda Sandstone is loosely defined as late Silurian (Hocking, 1991; Trewin & Mcnamara, 1994), but lacks robust depositional age constraints due to a paucity of fossils (Trewin & Mcnamara, 1994) and non-diagnostic detrital zircon ages (Markwitz et al., 2017). The stromatolitic succession unconformably overlies the Tumblagooda Sandstone, meaning that the PBS must be no older than Silurian. However, bracketing the PBS between Silurian and Early Triassic is not particularly informative.

Across the Perth Basin, Devonian to Carboniferous sequences are rarely preserved due to a regional unconformity associated with late Carboniferous glaciation (Mory et al., 2008), but Devonian placoderms (*Turinia australiensis*) have been identified in sandstones from one drill core in the northern Perth Basin (Allen & Trinajstic, 2017). Given the paucity of Devonian to Carboniferous strata within the Perth Basin, we consider it unlikely that the PBS is of this age. From the late Carboniferous to earliest Triassic, the Perth Basin experienced periods of thermal sag and episodic rifting, with minimal exhumation until the breakup of Gondwana in the Early Cretaceous (Olierook et al., 2019a; 2019b; Song & Cawood, 2000). The upper Carboniferous and Cisuralian (early Permian) sequences in the Perth Basin are defined by glacial and fluvioglacial sedimentary rocks (Eyles et al., 2006; Playford, Cockbain, & Low, 1976). The PBS shows no direct evidence of a glacial influence. From the Guadalupian to Lopingian (mid to late Permian), the Perth Basin was characterised by marginal marine and fluvio-lacustrine settings (Norvick, 2004; Olierook, Timms, Wellmann, Corbel, & Wilkes, 2015; Thomas, 2014), which progressively developed into an intracontinental sea in the Early Triassic associated with a global rise in sea level (Erwin, 1994; Ross & Ross, 1987). The nearby area around the outcrops mapped here are devoid of the late Carboniferous to Guadalupian rift

sequences. The Guadalupian to Lopingian (mid-late Permian) postrift sequences occur far to the south and are also not known from this area, though it is possible the PBS could have developed in an isolated setting as proposed (*Fig.* 2.10). Hence, the PBS could be Guadalupian to Lopingian although they may still be Induan, and although unlikely, it is possible that they are significantly older (Fig. 2.3). Until more definitive age constraints are obtained it should not be assumed that PBS is representative of the end-Permian mass extinction recovery (e.g., Chen et al., 2014). Instead they may simply be indicators of environmental conditions more favourable to stromatolite development, that is, a facies indicator.

5.3 Global Permo–Triassic microbialite record

A compilation of microbialite (ignoring microbially induced sedimentary structures) occurrences (*n = 77*) reveal microbialite growth throughout the Permian and Triassic in a large variety of environments, from continental to open marine settings (Fig. 2.12). Overall, there is an increase in palaeoenvironmental diversity of microbialites into open marine settings during the Lower Triassic compared to other Permian–Triassic intervals (Fig. 2.12). The increase in environmental distribution is likely a result of a significant reduction in predation and ecological competition that would otherwise make many of these environments unfavourable to microbialite development (Schubert & Bottjer, 1992). Disregarding the distal open marine environments during this time frame (Hungary and Japan), microbialitic environments were relatively consistent throughout the Permian and the later Triassic. Therefore, the major control on microbialite growth during the Phanerozoic is favourable environmental conditions rather than periods of biotic crises (e.g., Arp et al., 2005; Benvenuti, 2003; Kerp et al., 1996; Schäfer & Stapf, 1978).

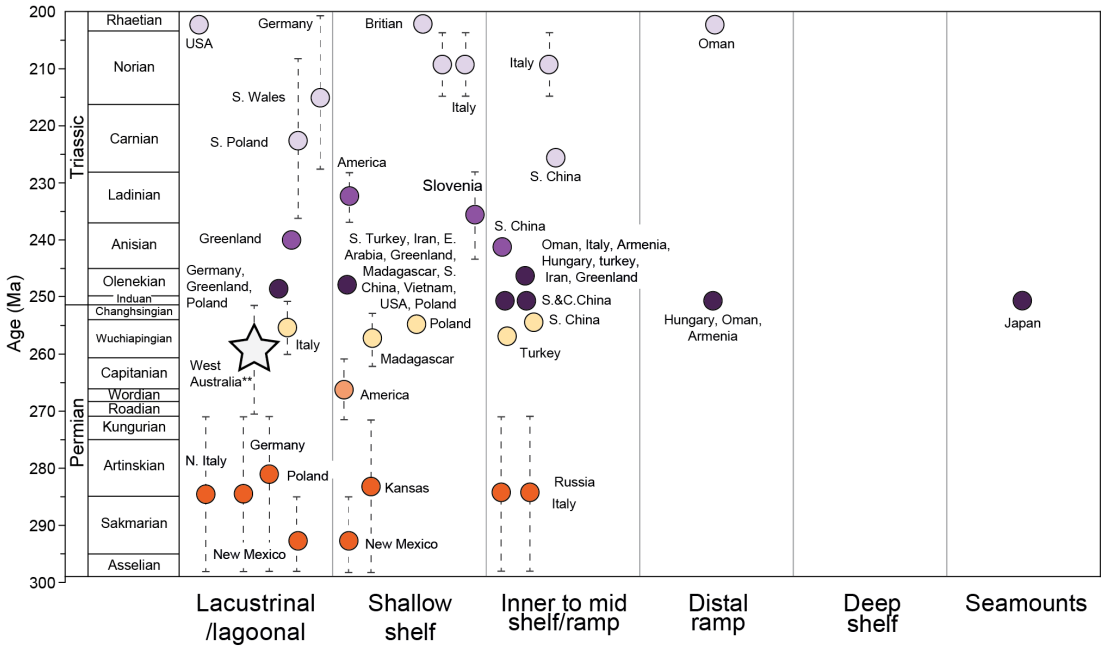

Fig. 2.12: Compilation (number of studies = 77) of temporal ranges of stromatolites from the Lower Permian to the Upper Triassic shown with their corresponding palaeodepositional setting. References: Lower Permian (Chuvashov, 1983; Cross & Klosterman, 1981a, b; Freytet et al., 1996; Kerp et al., 1996; Schäfer & Stapf, 1978; Shapiro & West, 1999; Szulc & Cwizewicz, 1989), Middle Permian - (Newell, 1955), Upper Permian (Adachi et al., 2017; Angiolini et al., 2010; Fang et al., 2017b; Freytet et al., 1992; Gaetani et al., 2009; Maurer et al., 2009; Peryt & Piatkowski, 1977; Taraz et al., 1981; Wescott, 1988; Wescott & Diggens, 1998; Wignall & Hallam, 1992), Early Triassic (Adachi et al., 2017; Angiolini et al., 2007; Baud et al., 2001; Baud & Bernecker, 2010; Baud et al., 1997; Baud et al., 2005; Chen et al., 2012; Chen et al., 2014; Escher & Watt, 1976; Ezaki et al., 2003; Ezaki et al., 2008; Ezaki et al., 2012; Fang et al., 2017a; Groves & Calner, 2004; Groves et al., 2007; Heydari et al., 2000; Hips & Haas, 2006; Insalaco et al., 2006; Kalkowsky, 1908; Kershaw et al., 2011; Kershaw et al., 2012; Kershaw et al., 2002; Kershaw et al., 2007; Kershaw et al., 1999; Lehrmann, 1999; Lehrmann et al., 2003; Luo et al., 2016; Marenco et al., 2012; Mary & Woods, 2008; Paul & Peryt, 2000; Perch-Nielsen et al., 1972; Peryt, 1975; Pruss & Bottjer, 2004; Pruss et al., 2006; Richoz et al., 2005; Richoz et al., 2010; Sano & Nakashima, 1997; Taraz et al., 1981; Wang et al., 2005; Wignall & Twitchett, 2002; Yang et al., 2011), Middle Triassic (Buser et al., 1982; Clemmensen, 1978; Clemmensen & Andreasen, 1977; Grasmück & Trümpy, 1969; Luo et al., 2014; Mary & Woods, 2008; Perch-Nielsen et al., 1974; Tałanda et al., 2017), Upper Triassic (Arp et al., 2005; Baud et al., 2001; Gore, 1988; Hamilton, 1961; Mastandrea et al., 2006; Mayall & Wright, 1981; Perri et al., 2003; Perri & Tucker, 2007; Tałanda et al., 2017; Tucker, 1978; Wright & Mayall, 1981). The full data table may be found in the Supplementary Table A.

Our case study in the northern Perth Basin is a pertinent example of how suitable local environmental conditions are the dominant control for growth and do not necessitate

association with global biotic recoveries as has been interpreted in the past (Chen et al., 2014). Our work reveals that the PBS could have formed during the Guadalupian to Lopingian and possibly Induan, supporting arguments presented by Kershaw et al. (2009) that disaster forms/anachronistic facies are not necessarily suitable concepts when discussing extinction aftermaths.

6 Conclusions

Three new localities of mid-Phanerozoic northern Perth Basin stromatolitic succession (PBS) have been identified, with discontinuous outcrops over 24 km. Stromatolites with interfingered clastic material are identified as a separate unit to the Smithian Kockatea Shale. Ten distinct morphological forms of stromatolite are identified and described in detail. The stromatolites are intimately related with clastic sediments, growing during and between episodic high-energy depositional events. The lithological nature of the clastic sediments combined with meso- and macrostructural features of stromatolites and the stratigraphic relationships with other defined units suggest the PBS likely formed in a restricted water body with fluvial influences.

The PBS is unlikely to be contemporaneous with the Lower Triassic Hovea Member of Kockatea Shale but probably formed during the Guadalupian to Lopingian (Permian). Thus, the PBS was not likely associated with the end-Permian mass extinction as had previously been interpreted. Comparing the PBS with other global microbialites from the Permian–Triassic interval shows that, during the Phanerozoic, stromatolites are present in a wide variety of settings, with proliferation into greater open marine settings following ecological crises. These results show, when studying sections containing microbialites at or near extinction intervals, it is important to assess whether growth is a direct result of biotic crises or simply local harsh/restrictive environmental palaeodepositional settings.

Acknowledgements

We would like to acknowledge the following: The Smithsonian National Museum of Natural History for preparation of thin sections; special mention to Kath Grey, for support and advice on the classification of stromatolites and redefining the palaeo-environment; reviewers and editors comments; fieldwork was completed via funding from the School of Earth and Planetary Sciences, Curtin University and the Geological Society of Australia, Western Australia Division, and the support of an Australian Government Research Training Program

(RTP) Scholarship to L.J.O. This manuscript benefited from earlier comments by anonymous reviewers and the editorial handling of I. Montanez.

REFERENCES

Adachi, N., Asada, Y., Ezaki, Y., & Liu, J. (2017). Stromatolites near the Permian–Triassic boundary in Chongyang, Hubei Province, South China: A geobiological window into palaeo-oceanic fluctuations following the end-Permian extinction. *Palaeogeography, Palaeoclimatology, Palaeoecology, 475*, 55-69. https://doi.org/https://doi.org/10.1016/j.palaeo.2017.01.030

Allen, H., & Trinajstic, K. (2017). *An Early Devonian fish fauna from an unnamed sandstone in petroleum exploration well Wendy 1, northern Perth Basin*.

Angiolini, L., Carabelli, L., Nicora, A., Crasquin-Soleau, S., Marcoux, J., & Rettori, R. (2007). Brachiopods and other fossils from the Permo–Triassic boundary beds of the Antalya Nappes (SW Taurus, Turkey). *Geobios, 40*(6), 715-729.

Angiolini, L., Checconi, A., Gaetani, M., & Rettori, R. (2010). The latest Permian mass extinction in the Alborz Mountains (north Iran). *Geological Journal, 45*(2-3), 216-229.

Arenas-Abad, C., Vázquez-Urbez, M., Pardo-Tirapu, G., & Sancho-Marcén, C. (2010). Fluvial and associated carbonate deposits. *Developments in Sedimentology, 61*, 133-175.

Arp, G., Bielert, F., Hoffmann, V.-E., & Löffler, T. (2005). Palaeoenvironmental significance of lacustrine stromatolites of the Arnstadt Formation ("Steinmergelkeuper", Upper Triassic, N-Germany). *Facies, 51*(1-4), 419-441.

Awramik, S. M. (1992). The history and significance of stromatolites. In *Early Organic Evolution* (pp. 435-449). Springer.

Awramik, S. M., & Buchheim, H. P. (2015). Giant stromatolites of the Eocene Green River Formation (Colorado, USA). *Geology, 43*(8), 691-694.

Awramik, S. M., & Sprinkle, J. (1999). Proterozoic stromatolites: the first marine evolutionary biota. *Historical Biology, 13*(4), 241-253.

Baud, A., Béchennec, F., Krystyn, L., Le Métour, J., Marcoux, J., Maury, R., & Richoz, S. (2001, 2001). Permo-Triassic Deposits: from the Platform to the Basin and Seamounts. Conference on the Geology of Oman, Field guidebook, Excursion A01.

Baud, A., & Bernecker, M. (2010, 2010). The Permian-Triassic transition in the Oman mountains.IGCP,

Baud, A., Cirilli, S., & Marcoux, J. (1997). Biotic response to mass extinction: the lowermost Triassic microbialites. *Facies, 36*, 238-242.

Baud, A., Richoz, S., & Marcoux, J. (2005). Calcimicrobial cap rocks from the basal Triassic units: western Taurus occurrences (SW Turkey). *Comptes Rendus Palevol, 4*(6-7), 569-582.

Benvenuti, M. (2003). Facies analysis and tectonic significance of lacustrine fan-deltaic successions in the Pliocene–Pleistocene Mugello Basin, Central Italy. *Sedimentary Geology, 157*(3-4), 197-234.

Blair, T. C., & McPherson, J. G. (1994). Alluvial fan processes and forms. In *Geomorphology of desert environments* (pp. 354-402). Springer.

Bosak, T., Knoll, A. H., & Petroff, A. P. (2013). The meaning of stromatolites. *Annual Review of Earth and Planetary Sciences, 41*, 21-44.

Buick, R. (1992). The antiquity of oxygenic photosynthesis: evidence from stromatolites in sulphate-deficient Archaean lakes. *Science, 255*(5040), 74-77.

Burgess, S. D., Bowring, S., & Shen, S.-z. (2014). High-precision timeline for Earth's most severe extinction. *Proceedings of the National Academy of Sciences, 111*(9), 3316-3321.

Buser, S., Ramovš, A., & Turnšek, D. (1982). Triassic reefs in Slovenia. *Facies, 6*(1), 15-23.

Casanova, J. (1986). East African rift stromatolites. *Geological Society, London, Special Publications, 25*(1), 201-210.

Casanova, J. (1994). Stromatolites from the East African Rift: a synopsis. In *Phanerozoic stromatolites II* (pp. 193-226). Springer.

Cawood, P. A., & Nemchin, A. A. (2000). Provenance record of a rift basin: U/Pb ages of detrital zircons from the Perth Basin, Western Australia. *Sedimentary Geology, 134*(3-4), 209-234.

Chen, Z.-Q., & Benton, M. J. (2012). The timing and pattern of biotic recovery following the end-Permian mass extinction [Review Article]. *Nature Geoscience, 5*, 375. https://doi.org/10.1038/ngeo1475

https://www.nature.com/articles/ngeo1475#supplementary-information

Chen, Z.-Q., Fraiser, M. L., & Bolton, C. (2012). Early Triassic trace fossils from Gondwana Interior Sea: Implication for ecosystem recovery following the end-Permian mass extinction in south high-latitude region. *Gondwana Research, 22*(1), 238-255. https://doi.org/https://doi.org/10.1016/j.gr.2011.08.015

Chen, Z.-Q., Wang, Y., Kershaw, S., Luo, M., Yang, H., Zhao, L., Feng, Y., Chen, J., Yang, L., & Zhang, L. (2014). Early Triassic stromatolites in a siliciclastic nearshore setting in northern Perth Basin, Western Australia: Geobiologic features and implications for post-extinction microbial proliferation. *Global and Planetary Change, 121*, 89-100. https://doi.org/https://doi.org/10.1016/j.gloplacha.2014.07.004

Chuvashov, B. I. (1983). Permian reefs of the Urals. *Facies, 8*(1), 191.

Clemmensen, L. B. (1978). Lacustrine facies and stromatolites from the Middle Triassic of East Greenland. *Journal of Sedimentary Research, 48*(4), 1111-1127.

Clemmensen, L. B., & Andreasen, F. (1977). Sedimentological observations in middle and late Triassic rocks, Jameson Land Basin, central East Greenland. In *Rapp. Grønlands Geol. Unders* (pp. 106-110).

Cloud, P. E., & Semikhatov, M. A. (1969). Proterozoic stromatolite zonation. *American Journal of Science, 267*(9), 1017-1061.

Courtillot, V., Jaupart, C., Manighetti, I., Tapponnier, P., & Besse, J. (1999). On causal links between flood basalts and continental breakup. *Earth and Planetary Science Letters, 166*(3), 177-195. https://doi.org/https://doi.org/10.1016/S0012-821X(98)00282-9

Cross, T. A., & Klosterman, M. J. (1981a). Autecology and development of a stromatolitic-bound phylloid algal bioherm, Laborcita Formation (Lower Permian), Sacramento Mountains, New Mexico, USA. In *Phanerozoic Stromatolites* (pp. 45-59). Springer.

Cross, T. A., & Klosterman, M. J. (1981b). Primary submarine cements and neomorphic spar in a stromatolitic-bound phylloid algal bioherm, Laborcita Formation (Wolfcampian),

Sacramento Mountains, New Mexico, USA. In *Phanerozoic stromatolites* (pp. 60-73). Springer.

Djokic, T., Van Kranendonk, M. J., Campbell, K. A., Walter, M. R., & Ward, C. R. (2017). Earliest signs of life on land preserved in ca. 3.5 Ga hot spring deposits. *Nature communications, 8*, 15263.

Elmore, R. D. (1983). Precambrian non-marine stromatolites in alluvial fan deposits, the Copper Harbor Conglomerate, upper Michigan. *Sedimentology, 30*(6), 829-842.

Erwin, D. H. (1994). The Permo-Triassic extinction. *Nature, 367*(6460), 231.

Escher, A., & Watt, W. S. (1976). *Geology of Greenland*. Geological Survey of Greenland.

Eyles, N., Mory, A. J., & Eyles, C. H. (2006). 50-Million-year-long record of glacial to postglacial marine environments preserved in a Carboniferous–Lower Permian graben, Northern Perth Basin, Western Australia. *Journal of Sedimentary Research, 76*(3), 618-632.

Ezaki, Y., Liu, J., & Adachi, N. (2003). Earliest Triassic microbialite micro-to megastructures in the Huaying area of Sichuan Province, South China: implications for the nature of oceanic conditions after the end-Permian extinction. *Palaios, 18*(4-5), 388-402.

Ezaki, Y., Liu, J., Nagano, T., & Adachi, N. (2008). Geobiological aspects of the earliest Triassic microbialites along the southern periphery of the tropical Yangtze Platform: initiation and cessation of a microbial regime. *Palaios, 23*(6), 356-369.

Ezaki, Y., Liu, J. B., & Adachi, N. (2012). Lower Triassic stromatolites in Luodian County, Guizhou Province, South China: evidence for the protracted devastation of the marine environments. *Geobiology., 10*(1), 48-59.

Fang, Y., Chen, Z.-Q., Kershaw, S., Li, Y., & Luo, M. (2017). An Early Triassic (Smithian) stromatolite associated with giant ooid banks from Lichuan (Hubei Province), South China: Environment and controls on its formation. *Palaeogeography, Palaeoclimatology, Palaeoecology, 486*, 108-122. https://doi.org/https://doi.org/10.1016/j.palaeo.2017.02.006

Fang, Y., Chen, Z.-Q., Kershaw, S., Yang, H., & Luo, M. (2017). Permian–Triassic boundary microbialites at Zuodeng Section, Guangxi Province, South China: Geobiology and

palaeoceanographic implications. *Global and Planetary Change, 152*, 115-128. https://doi.org/https://doi.org/10.1016/j.gloplacha.2017.02.011

Fannin, N. G. T. (1969). Stromatolites from the middle Old Red Sandstone of western Orkney. *Geological Magazine, 106*(1), 77-88.

Freytet, P., Kerp, H., & Broutin, J. (1996). Permian freshwater stromatolites associated with the conifer shoots Cassinisia orobica Kerp et al.—a very peculiar type of fossilization. *Review of Palaeobotany and Palynology, 91*(1-4), 85-105.

Freytet, P., Lebreton, M.-L., & Paquette, Y. (1992). The carbonates of the Permian lakes of North Massif Central, France. *Carbonates and Evaporites, 7*(2), 122.

Gaetani, M., Angiolini, L., Ueno, K., Nicora, A., Stephenson, M. H., Sciunnach, D., Rettori, R., Price, G. D., & Sabouri, J. (2009). Pennsylvanian–Early Triassic stratigraphy in the Alborz Mountains (Iran). *Geological Society, London, Special Publications, 312*(1), 79-128.

Garrett, P. (1970). Phanerozoic stromatolites: noncompetitive ecologic restriction by grazing and burrowing animals. *Science, 169*(3941), 171-173.

Gawthorpe, R. L., & Leeder, M. R. (2000). Tectono-sedimentary evolution of active extensional basins. *Basin Research, 12*(3-4), 195-218.

Gibbons, A. D., Whittaker, J. M., & Müller, R. D. (2013). The breakup of East Gondwana: Assimilating constraints from Cretaceous ocean basins around India into a best-fit tectonic model. *Journal of geophysical research: solid earth, 118*(3), 808-822.

Golubic, S. (1976). .2 Taxonomy of Extant Stromatolite-Building Cyanophytes. In *Developments in Sedimentology* (Vol. 20, pp. 127-140). Elsevier.

Gore, P. J. W. (1988). Paleoecology and sedimentology of a Late Triassic lake, Culpeper basin, Virginia, USA. *Palaeogeography, palaeoclimatology, palaeoecology, 62*(1-4), 593-608.

Gorter, J. D., Hearty, D. J., & Bond, A. J. (2004). Jurassic petroleum systems in the Houtman Sub-Basin, northwestern offshore Perth Basin, Western Australia: A frontier petroleum province on the doorstep? *The APPEA Journals*, 13-58. https://doi.org/https://doi.org/10.1071/AJ03001

Grasmück, K., & Trümpy, R. (1969). Triassic stratigraphy and general geology of the country around Fleming Fjord (East Greenland). *Meddelelser om Grønland, 168*(2), 3-76.

Grey, K., & Awramik, S. M. (2020). *Handbook for the study and description of microbialites*. Geological Survey of Western Australia.

Groves, J. R., & Calner, M. (2004, 2004). Lower Triassic oolites in Tethys: a sedimentologic response to the end-Permian mass extinction.

Groves, J. R., Rettori, R., Payne, J. L., Boyce, M. D., & Altiner, D. (2007). End-Permian mass extinction of lagenide foraminifers in the southern Alps (northern Italy). *Journal of Paleontology, 81*(3), 415-434.

Haig, D. W., Martin, S. K., Mory, A. J., McLoughlin, S., Backhouse, J., Berrell, R. W., Kear, B. P., Hall, R., Foster, C. B., Shi, G. R., & Bevan, J. C. (2015). Early Triassic (early Olenekian) life in the interior of East Gondwana: mixed marine–terrestrial biota from the Kockatea Shale, Western Australia. *Palaeogeography, Palaeoclimatology, Palaeoecology, 417*, 511-533. https://doi.org/https://doi.org/10.1016/j.palaeo.2014.10.015

Hallam, A., & Wignall, P. B. (1997). *Mass extinctions and their aftermath*. Oxford [England] ; New York : Oxford University Press.

Hamilton, D. (1961). Algal growths in the Rhaetic Cotham Marble of southern England. *Palaeontology, 4*(3), 324-333.

Heydari, E., Hassandzadeh, J., & Wade, W. J. (2000). Geochemistry of central Tethyan upper Permian and lower Triassic strata, Abadeh region, Iran. *Sedimentary Geology, 137*(1-2), 85-99.

Hips, K., & Haas, J. (2006). Calcimicrobial stromatolites at the Permian–Triassic boundary in a western Tethyan section, Bükk Mountains, Hungary. *Sedimentary Geology, 185*(3-4), 239-253.

Hocking, R. M. (1991). *The Silurian Tumblagooda Sandstone, Western Australia* (Vol. 27). Geological Survey of Western Australia.

Hofmann, H. J. (1969). *Stromatolites from the Proterozoic Animikie and Sibley Groups, Ontario* (Vol. 68). Department of Energy, Mines and Resources.

Hofmann, H. J. (1976). .2 Graphic Representation of Fossil Stromatoids; New Method with Improved Precision. In *Developments in Sedimentology* (Vol. 20, pp. 15-20). Elsevier.

Horodyski, R. J. (1977). Environmental influences on columnar stromatolite branching patterns: examples from the Middle Proterozoic Belt Supergroup, Glacier National Park, Montana. *Journal of Paleontology*, 661-671.

Huang, Y., Tong, J., & Fraiser, M. L. (2018). A Griesbachian (Early Triassic) Mollusc Fauna from the Sidazhai Section, Southwest China, with Paleoecological Insights on the Proliferation of Genus Claraia (Bivalvia). *Journal of Earth Science, 29*(4), 794-805.

Insalaco, E., Virgone, A., Courme, B., Gaillot, J., Kamali, M., Moallemi, A., Lotfpour, M., & Monibi, S. (2006). Upper Dalan Member and Kangan Formation between the Zagros Mountains and offshore Fars, Iran: depositional system, biostratigraphy and stratigraphic architecture. *GeoArabia, 11*(2), 75-176.

Kalkowsky, E. (1908). Oolith und Stromatolith im norddeutschen Buntsandstein. *Zeitschrift der deutschen geologischen Gesellschaft*, 68-125.

Keller, G. (2005). Impacts, volcanism and mass extinction: random coincidence or cause and effect? *Australian Journal of Earth Sciences, 52*(4-5), 725-757. https://doi.org/10.1080/08120090500170393

Kerp, H., Penati, F., Brambilla, G., Clement-Westerhof, J. A., & van Bergen, P. F. (1996). Aspects of Permian palaeobotany and palynology. XVI. Three-dimensionally preserved stromatolite-incrusted conifers from the Permian of the western Orobic Alps (northern Italy). *Review of Palaeobotany and Palynology, 91*(1-4), 63-84.

Kershaw, S., Crasquin, S., Collin, P.-Y., Li, Y., Feng, Q., & Forel, M. B. (2009). Microbialites as disaster forms in anachronistic facies following the end-Permian mass extinction: a discussion. *Australian Journal of Earth Sciences, 56*(6), 809-813.

Kershaw, S., Crasquin, S., Forel, M. B., Randon, C., Collin, P. Y., Kosun, E., Richoz, S., & Baud, A. (2011). Earliest Triassic microbialites in Çürük Dag, southern Turkey: composition, sequences and controls on formation. *Sedimentology, 58*(3), 739-755.

Kershaw, S., Crasquin, S., Li, Y., Collin, P. Y., Forel, M. B., Mu, X., Baud, A., Wang, Y., Xie, S., Maurer, F., & Guo, L. (2012). Microbialites and global environmental change across the Permian-Triassic boundary: a synthesis. *Geobiology., 10*(1), 25-47.

Kershaw, S., Guo, L., Swift, A., & Fan, J. (2002). ? Microbialites in the Permian-Triassic boundary interval in central China: Structure, age and distribution. *Facies, 47*(1), 83-89.

Kershaw, S., Li, Y., Crasquin-Soleau, S., Feng, Q., Mu, X., Collin, P.-Y., Reynolds, A., & Guo, L. (2007). Earliest Triassic microbialites in the South China block and other areas: controls on their growth and distribution. *Facies, 53*(3), 409-425.

Kershaw, S., Zhang, T., & Lan, G. (1999). A? microbialite carbonate crust at the Permian–Triassic boundary in South China, and its palaeoenvironmental significance. *Palaeogeography, Palaeoclimatology, Palaeoecology, 146*(1-4), 1-18.

Lehrmann, D. J. (1999). Early Triassic calcimicrobial mounds and biostromes of the Nanpanjiang basin, south China. *Geology, 27*(4), 359-362.

Lehrmann, D. J., Payne, J. L., Felix, S. V., Dillett, P. M., Wang, H., Yu, Y., & Wei, J. (2003). Permian–Triassic boundary sections from shallow-marine carbonate platforms of the Nanpanjiang Basin, South China: implications for oceanic conditions associated with the end-Permian extinction and its aftermath. *Palaios, 18*(2), 138-152.

Link, M. H., & Osborne, R. H. (1978). Lacustrine facies in the Pliocene Ridge Basin Group: Ridge Basin, California. *Modern and Ancient Lake Sediments, Spec. Publ, 2*, 169-187.

Link, M. H., Osborne, R. H., & Awramik, S. M. (1978). Lacustrine stromatolites and associated sediments of the Pliocene ridge Route Formation, Ridge Basin, California. *Journal of Sedimentary Research, 48*(1), 143-157.

Logan, B. W., Rezak, R., & Ginsburg, R. N. (1964). Classification and Environmental Significance of Algal Stromatolites. *The Journal of Geology, 72*(1), 68-83. https://doi.org/10.1086/626965

Luo, M., Chen, Z.-Q., Shi, G. R., Fang, Y., Song, H., Jia, Z., Huang, Y., & Yang, H. (2016). Upper Lower Triassic stromatolite from Anhui, South China: Geobiologic features and paleoenvironmental implications. *Palaeogeography, Palaeoclimatology, Palaeoecology, 452*, 40-54. https://doi.org/https://doi.org/10.1016/j.palaeo.2016.04.008

Luo, M., Chen, Z.-Q., Shi, G. R., Feng, X., Yang, H., Fang, Y., & Li, Y. (2019). Microbially induced sedimentary structures (MISSs) from the Lower Triassic Kockatea

Formation, northern Perth Basin, Western Australia: Palaeoenvironmental implications. *Palaeogeography, Palaeoclimatology, Palaeoecology, 519*, 236-247.

Luo, M., Chen, Z.-Q., Zhao, L., Kershaw, S., Huang, J., Wu, L., Yang, H., Fang, Y., Huang, Y., Zhang, Q., Hu, S., Zhou, C., Wen, W., & Jia, Z. (2014). Early Middle Triassic stromatolites from the Luoping area, Yunnan Province, Southwest China: Geobiologic features and environmental implications. *Palaeogeography, Palaeoclimatology, Palaeoecology, 412*, 124-140. https://doi.org/https://doi.org/10.1016/j.palaeo.2014.07.028

Marenco, P. J., Griffin, J. M., Fraiser, M. L., & Clapham, M. E. (2012). Paleoecology and geochemistry of Early Triassic (Spathian) microbial mounds and implications for anoxia following the end-Permian mass extinction. *Geology, 40*(8), 715-718.

Markwitz, V., Kirkland, C. L., Wyrwoll, K. H., Hancock, E. A., Evans, N. J., & Lu, Y. (2017). Variations in zircon provenance constrain age and geometry of an Early Paleozoic rift in the Pinjarra Orogen, East Gondwana. *Tectonics, 36*(11), 2477-2496.

Mary, M., & Woods, A. D. (2008). Stromatolites of the Lower Triassic Union Wash Formation, CA: evidence for continued post-extinction environmental stress in western North America through the Spathian. *Palaeogeography, Palaeoclimatology, Palaeoecology, 261*(1-2), 78-86.

Mastandrea, A., Perri, E., Russo, F., Spadafora, A., & Tucker, M. (2006). Microbial primary dolomite from a Norian carbonate platform: northern Calabria, southern Italy. *Sedimentology, 53*(3), 465-480.

Maurer, F., Martini, R., Rettori, R., Hillgärtner, H., & Cirilli, S. (2009). The geology of Khuff outcrop analogues in the Musandam Peninsula, United Arab Emirates and Oman. *GeoArabia, 14*(3), 125-158.

Mayall, M. J., & Wright, V. P. (1981). Algal tuft structures in stromatolites from the Upper Triassic of south-west England. *Palaeontology, 24*(3), 655-660.

Metcalfe, I., Nicoll, R. S., & Willink, R. J. (2008). Conodonts from the Permian–Triassic transition in Australia and position of the Permian–Triassic boundary. *Australian Journal of Earth Sciences, 55*(3), 365-377. https://doi.org/10.1080/08120090701769480

Miall, A. D., & Postma, G. (1997). The Geology of Fluvial Deposits, Sedimentary Facies, Basin Analysis and Petroleum Geology. *Sedimentary Geology, 110*(1), 149.

Monty, C. L. V. (1976). .1 The Origin and Development of Cryptalgal Fabrics. In *Developments in sedimentology* (Vol. 20, pp. 193-249). Elsevier.

Mory, A., & Iasky, R. (1994). *Structural evolution of the onshore northern Perth Basin, Western Australia*.

Mory, A. J., Haig, D. W., McLoughlin, S., & Hocking, R. M. (2005). Geology of the Northern Perth Basin, Western Australia - A Field Guide. *Geological Society of Western Australia Record, 2005/09*, 1-58.

Mory, A. J., & Iasky, R. P. (1996). Stratigraphic and structure of the onshore Northern Perth Basin, Western Australia. *46*, 1-101.

Mory, A. J., Iasky, R. P., & Ghori, K. A. R. (2003). A summary of the geological evolution and petroleum potential of the Southern Carnarvon Basin, Western Australia. *Geological Survey of Western Australia Report, 86*, 1-26.

Mory, A. J., Redfern, J., & Martin, J. R. (2008). A review of Permian–Carboniferous glacial deposits in Western Australia. *Geological Society of America Special Papers, 441*, 29-40.

Newell, N. D. (1955). Depositional fabric in Permian reef limestones. *The Journal of Geology, 63*(4), 301-309.

Norvick, M. S. (2004). Tectonic and Stratigraphic History of the Perth Basin. Record 2004/16. *Geoscience Australia Record, 2004/16*, 1-18.

Nutman, A. P., Bennett, V. C., Friend, C. R. L., Van Kranendonk, M. J., & Chivas, A. R. (2016). Rapid emergence of life shown by discovery of 3,700-million-year-old microbial structures. *Nature, 537*(7621), 535.

Olierook, H. K. H., Barham, M., Fitzsimons, I. C. W., Timms, N. E., Jiang, Q., Evans, N. J., & McDonald, B. J. (2019). Tectonic controls on sediment provenance evolution in rift basins: Detrital zircon U–Pb and Hf isotope analysis from the Perth Basin, Western Australia. *Gondwana Research, 66*, 126-142.

Olierook, H. K. H., Jiang, Q., Jourdan, F., & Chiaradia, M. (2019). Greater Kerguelen large igneous province reveals no role for Kerguelen mantle plume in the continental breakup of eastern Gondwana. *Earth and Planetary Science Letters, 511*, 244-255.

Olierook, H. K. H., Jourdan, F., Merle, R. E., Timms, N. E., Kusznir, N., & Muhling, J. R. (2016). Bunbury Basalt: Gondwana breakup products or earliest vestiges of the Kerguelen mantle plume? *Earth and Planetary Science Letters, 440*, 20-32. https://doi.org/https://doi.org/10.1016/j.epsl.2016.02.008

Olierook, H. K. H., Timms, N. E., Wellmann, J. F., Corbel, S., & Wilkes, P. G. (2015). 3D structural and stratigraphic model of the Perth Basin, Western Australia: Implications for sub-basin evolution. *Australian Journal of Earth Sciences, 62*(4), 447-467.

Paul, J., & Peryt, T. M. (2000). Kalkowsky's stromatolites revisited (Lower Triassic Buntsandstein, Harz Mountains, Germany). *Palaeogeography, Palaeoclimatology, Palaeoecology, 161*(3-4), 435-458.

Perch-Nielsen, K., Birkenmajer, K., Birkelund, T., & Aellen, M. (1974). Revision of Triassic stratigraphy of the Scoresby Land an d Jameson Land region, east Greenland. *Meddelelser om Gronland*.

Perch-Nielsen, K., Bromley, R. G., Birkenmajer, K., & Aellen, M. (1972). Field observations in Palaeozoic and Mesozoic sediments of Scoresby Land and northern Jameson Land. *Danmarks Og Grønlands Geologiske Undersøgelse, Rapport*(48), 39-59.

Perri, E., Mastandrea, A., Neri, C., & Russo, F. (2003). A micrite-dominated Norian carbonate platform from Northern Calabria (Southern Italy). *Facies, 49*(1), 101-118.

Perri, E., & Tucker, M. (2007). Bacterial fossils and microbial dolomite in Triassic stromatolites. *Geology, 35*(3), 207-210.

Peryt, T. M. (1975). Significance of stromatolites for the environmental interpretation of the Buntsandstein (Lower Triassic) rocks. *Geologische Rundschau, 64*(1), 143-158.

Peryt, T. M., & Piatkowski, T. S. (1977). Stromatolites from the Zechstein Limestone (Upper Permian) of Poland. In *Fossil Algae* (pp. 124-135). Springer.

Playford, P. E., Cockbain, A. E., & Low, G. H. (1976). Geology of the Perth Basin Western Australia. *Geological Survey of Western Australia Bulletin, 124*.

Pollard, J. E., Steel, R. J., & Undersrud, E. (1982). Facies sequences and trace fossils in lacustrine/fan delta deposits, Hornelen Basin (M. Devonian), western Norway. *Sedimentary Geology, 32*(1-2), 63-87.

Preiss, W. V. (1976). .1 Basic Field and Laboratory Methods for the Study of Stromatolites. In *Developments in Sedimentology* (Vol. 20, pp. 5-13). Elsevier.

Pruss, S. B., & Bottjer, D. J. (2004). Late Early Triassic microbial reefs of the western United States: a description and model for their deposition in the aftermath of the end-Permian mass extinction. *Palaeogeography, Palaeoclimatology, Palaeoecology, 211*(1-2), 127-137.

Pruss, S. B., Bottjer, D. J., Corsetti, F. A., & Baud, A. (2006). A global marine sedimentary response to the end-Permian mass extinction: examples from southern Turkey and the western United States. *Earth-science reviews, 78*(3-4), 193-206.

Richoz, S., Baud, A., Krystyn, L., Twitchett, R., & Marcoux, J. (2005). Permo-Triassic deposits of the Oman Mountains: from basin and slope to the shallow platform.

Richoz, S., Krystyn, L., Baud, A., Brandner, R., Horacek, M., & Mohtat-Aghai, P. (2010). Permian–Triassic boundary interval in the Middle East (Iran and N. Oman): Progressive environmental change from detailed carbonate carbon isotope marine curve and sedimentary evolution. *Journal of Asian Earth Sciences, 39*(4), 236-253.

Ross, C. A., & Ross, J. R. P. (1987). Late Paleozoic sea levels and depositional sequences. *Cushman Foundation for Foraminiferal Research*, 137.

Sano, H., & Nakashima, K. (1997). Lowermost Triassic (Griesbachian) microbial bindstone-cementstone facies, southwest Japan. *Facies, 36*(1), 1-24.

Schäfer, A., & Stapf, K. R. G. (1978). Permian Saar-Nahe Basin and recent Lake Constance (Germany): two environments of lacustrine algal carbonates. *Modern and ancient lake sediments*, 83-107.

Schubert, J. K., & Bottjer, D. J. (1992). Early Triassic stromatolites as post-mass extinction disaster forms. *Geology, 20*(10), 883-886. https://doi.org/10.1130/0091-7613(1992)020<0883:ETSAPM>2.3.CO;2

Shapiro, R. S., & West, R. R. (1999). Late Paleozoic stromatolites: new insights from the Lower Permian of Kansas. *Lethaia, 32*(2), 131-139.

Shen, J., Algeo, T. J., Zhou, L., Feng, Q., Yu, J., & Ellwood, B. (2012). Volcanic perturbations of the marine environment in South China preceding the latest Permian mass extinction and their biotic effects. *Geobiology., 10*(1), 82-103.

Smith, A., Cooper, A., Misra, S., Bharuth, V., Guastella, L., & Botes, R. (2018). The extant shore platform stromatolite (SPS) facies association: a glimpse into the Archean? *Biogeosciences, 15*(7), 2189-2203.

Smith, A. M., Andrews, J. E., Uken, R., Thackeray, Z., Perissinotto, R., Leuci, R., & Marca-Bell, A. (2011). Rock pool tufa stromatolites on a modern South African wave-cut platform: partial analogues for Archaean stromatolites? *Terra Nova, 23*(6), 375-381.

Song, T., & Cawood, P. A. (2000). Structural styles in the Perth Basin associated with the Mesozoic break-up of Greater India and Australia. *Tectonophysics, 317*(1), 55 - 72. https://doi.org/https://doi.org/10.1016/S0040-1951(99)00273-5

Suosaari, E. P., Reid, R. P., Oehlert, A. M., Playford, P. E., Steffensen, C. K., Andres, M. S., Suosaari, G. V., Milano, G. R., & Eberli, G. P. (2019). Stromatolite Provinces of Hamelin Pool: Physiographic Controls On Stromatolites and Associated Lithofacies. *Journal of Sedimentary Research, 89*(3), 207-226.

Suosaari, E. P., Reid, R. P., Playford, P. E., Foster, J. S., Stolz, J. F., Casaburi, G., Hagan, P. D., Chirayath, V., Macintyre, I. G., Planavsky, N. J., & Eberli, G. P. (2016). New multi-scale perspectives on the stromatolites of Shark Bay, Western Australia [Article]. *Scientific Reports, 6*, 20557. https://doi.org/10.1038/srep20557

https://www.nature.com/articles/srep20557#supplementary-information

Surdam, R. C., & Wray, J. L. (1976). .3 Lacustrine Stromatolites, Eocene Green River Formation, Wyoming. In *Developments in Sedimentology* (Vol. 20, pp. 535-541). Elsevier.

Szulc, J., & Cwizewicz, M. (1989). The Lower Permian freshwater carbonates of the Slawkow graben, southern Poland: Sedimentary facies context and stable isotope study. *Palaeogeography, Palaeoclimatology, Palaeoecology, 70*(1-3), 107-120.

Tałanda, M., Bajdek, P., Niedźwiedzki, G., & Sulej, T. (2017). Upper Triassic freshwater oncoids from Silesia (southern Poland) and their microfossil biota. *Neues Jahrbuch für Geologie und Paläontologie-Abhandlungen, 284*(1), 43-56.

Taraz, H., Golshani, F., Nakazawa, K., Shimizu, D., Bando, Y., Ishii, K.-i., Murata, M., Okimura, Y., Sakagami, S., & Nakamura, K. (1981). The Permian and the Lower Triassic systems in Abadeh region, central Iran.

Thomas, B. M., & Barber, C. J. (2004). A re-evaluation of the hydrocarbon habitat of the Northern Perth Basin. *The APPEA Journals, 44*(1), 59-92. https://doi.org/https://doi.org/10.1071/AJ03002

Thomas, B. M., Willink, R. J., Grice, K., Twitchett, R. J., Purcell, R. R., Archbold, N. W., George, A. D., Tye, S., Alexander, R., Foster, C. B., & Barber, C. J. (2004). Unique marine Permian-Triassic boundary section from Western Australia. *Australian journal of earth sciences, 51*(3), 423-430.

Thomas, C. M. (2014). The Tectonic Framework of the Perth Basin: Current understanding. *14*, 1-36.

Trewin, N. H., & McNamara, K. J. (1994). Arthropods invade the land: trace fossils and palaeoenvironments of the Tumblagooda Sandstone (? late Silurian) of Kalbarri, Western Australia. *Earth and Environmental Science Transactions of The Royal Society of Edinburgh, 85*(3), 177-210.

Tucker, M. E. (1978). Triassic Lacustrine Sediments from South Wales: Shore-Zone, Evaporites and Carbonates. *Modern and ancient lake sediments*, 205-224.

Von der Borch, C. C., Bolton, B., & Warren, J. K. (1977). Environmental setting and microstructure of subfossil lithified stromatolites associated with evaporites, Marion Lake, South Australia. *Sedimentology, 24*(5), 693-708.

Walter, M. R. (1977). Interpreting stromatolites: these fossils can tell us much about past organisms and environments if we can learn to decode their message. *American Scientist, 65*(5), 563-571.

Wang, Y., Tong, J., Wang, J., & Zhou, X. (2005). Calcimicrobialite after end-Permian mass extinction in South China and its palaeoenvironmental significance. *Chinese Science Bulletin, 50*(7), 665-671.

Wescott, W. A. (1988). A late Permian fan-delta system in the southern Morondava Basin, Madagascar. *Fan deltas: sedimentology and tectonic settings. Blackie, London*, 226-238.

Wescott, W. A., & Diggens, J. N. (1998). Depositional history and stratigraphical evolution of the Sakamena Group (Middle Karoo Supergroup) in the southern Morondava Basin, Madagascar. *Journal of African Earth Sciences, 27*(3-4), 461-479.

Wignall, P. B. (2007). The End-Permian mass extinction–how bad did it get? *Geobiology, 5*(4), 303-309.

Wignall, P. B., & Hallam, A. (1992). Anoxia as a cause of the Permian/Triassic mass extinction: facies evidence from northern Italy and the western United States. *Palaeogeography, Palaeoclimatology, Palaeoecology, 93*(1-2), 21-46.

Wignall, P. B., & Twitchett, R. J. (2002). Permian–Triassic sedimentology of Jameson Land, East Greenland: incised submarine channels in an anoxic basin. *Journal of the Geological Society, 159*(6), 691-703. https://doi.org/10.1144/0016-764900-120

Wright, V. P., & Mayall, M. (1981). Organism-sediment interactions in stromatolites: an example from the Upper Triassic of South West Britain. In *Phanerozoic Stromatolites* (pp. 74-84). Springer.

Wu, S., Chen, Z.-Q., Fang, Y., Pei, Y., Yang, H., & Ogg, J. (2017). A Permian-Triassic boundary microbialite deposit from the eastern Yangtze Platform (Jiangxi Province, South China): Geobiologic features, ecosystem composition and redox conditions. *Palaeogeography, Palaeoclimatology, Palaeoecology, 486*, 58-73. https://doi.org/https://doi.org/10.1016/j.palaeo.2017.05.015

Yang, H., Chen, Z. Q., Wang, Y., Tong, J., Song, H., & Chen, J. (2011). Composition and structure of microbialite ecosystems following the end-Permian mass extinction in South China. *Palaeogeography, Palaeoclimatology, Palaeoecology, 308*(1), 111-128. https://doi.org/https://doi.org/10.1016/j.palaeo.2010.05.029

Young, A., Flament, N., Maloney, K., Williams, S., Matthews, K., Zahirovic, S., & Müller, R. D. (2018). Global kinematics of tectonic plates and subduction zones since the late Paleozoic Era. *Geoscience Frontiers*.

SUPPLEMENTARY MATERIAL

XXX

Chapter 3 THE CELL IN THE STONE: EXCEPTIONAL PRESERVATION OF CELLULAR MICROSTRUCTURES IN MID-PHANEROZOIC STROMATOLITES FROM WESTERN AUSTRALIA

Liam J. Olden[1,*], Milo Barham[1,2], Hugo K.H. Olierook[1,2,3], Belinda Godel[4], Denis Fougerouse[1], Jane Cunneen[1,5], Lucy Forman[1,6,7]

[1]School of Earth and Planetary Sciences, Curtin University, GPO Box U1987, Perth, WA 6845, Australia

[2]Centre for Exploration Targeting – Curtin node, Curtin University, GPO Box U1987, Perth, WA 6845, Australia

[3]John de Laeter Centre, Curtin University, GPO Box U1987, Perth, WA 6845, Australia

[4]CSIRO Mineral Resources, Australian Resources Research Centre, Kensington, WA 6151, Australia

[5]Basin Scope Consulting Pty. Ltd., Perth, WA, Australia

[6]Space Science & Technology Centre, School of Earth & Planetary Sciences, Curtin University, GPO Box U1987, Perth, WA 6845, Australia

[7]Department of Earth and Planetary Sciences, Western Australian Museum, Locked Bag 49 Welshpool DC, Western Australia 6986

This article is currently under peer review with the scientific journal '*Geobiology*' as of 7*th October 2020*.

ABSTRACT

Stromatolites, laminated structures formed via grain capture or biogenic precipitation, represent the most conclusive evidence for microbial activity in the fossil record and are critical for understanding the early evolution of life. However, preservation of the microbial life that formed stromatolites is rare within the fossil record. Mid-Phanerozoic stromatolites from the northern Perth Basin, Western Australia, exhibit exceptional preservation of alveolate —cell-like— microstructures. These alveolate microstructures are 10 to 14 μm in internal diameter and up to 110 μm long, with walls that are 5 to 12 μm thick, and display near-circular cross-sections with negligible compaction-related deformation. We argue that the preserved alveolate microstructures represent silicified sheaths of filamentous cyanobacteria, with iron oxides/carbonate, silica or porespace replacing cellular trichomes. Interpreted cyanobacterial sheaths are preserved throughout the stromatolites investigated across outcrops several kilometres apart. Syn-depositional (biogenic) or earliest diagenetic (post-mortem silicification) mechanisms are required to silicify sheaths and mitigate the compaction and heterotrophic-related degradation/collapse of cellular structures. Secondary iron alteration, and perhaps authigenic quartz cementation, occurred subsequently but these are subordinate drivers of cell structure preservation. The syn-depositional to earliest diagenetic preservation style in a fluvio-lacustrine setting has significant ramifications for looking for environmental settings conducive to such preservation methods throughout the geological record.

Keywords: Microbialite; Cyanobacteria; Redox; Perth Basin; Silicification; sheath

1 Introduction

Microbial organisms represent the earliest physical evidence of life (Bosak et al., 2013; Djokic et al., 2017; Knoll, 2008), and were the dominant life-form for ~85% of Earth's biological history (Awramik, 1992; Awramik, Margulis, & Barghoorn, 1976; Awramik & Sprinkle, 1999; Bosak et al., 2013; Knoll, 2008; Suosaari et al., 2016), as well as being responsible for oxygenation of the early atmosphere. As such, microbial communities are important for understanding Earth's past environments, the evolution of life, and also how the biosphere has been modified by past catastrophic events (i.e. mass extinctions and associated biotic crises).

Some of the most distinctive microbial communities are stromatolites; colonies of cyanobacteria that self-lithify (Burne & Moore, 1987; Logan et al., 1964; Riding, 2011). Macroscopic stromatolite structures have a high preservation potential; however, their cellular microstructures are rarely preserved (Knoll, 2008; Rippka, Deruelles, Waterbury, Herdman, & Stanier, 1979; Schopf, 2006, 2012; Wacey et al., 2018). Even in modern occurrences, the preservation of cyanobacterial microstructures is usually limited to the top few millimetres of the stromatolites, with deeper portions destroyed by compaction and heterotrophic degradation (Jahnert & Collins, 2011; Playford, 1990; Playford et al., 2013; Playford et al., 1976; Reid et al., 2000). In the fossil record, preservation of cellular microstructures is predominantly found in secondary cherts and phosphates, broadly restricted to carbonate shelf environments during the Proterozoic and peritidal carbonate settings during the Palaeozoic and Mesozoic (Knoll, 2008; Manning-Berg, Wood, Williford, Czaja, & Kah, 2019; Manning-Berg & Kah, 2017; Martín-Algarra & Sánchez-Navas, 1995; Schopf, 2012). There is an apparent absence of cellular preservation in terrestrial settings during the Phanerozoic, with the exception of lakes with volcanic and/or hydrothermal influences (Kremer et al., 2012).

Mid-Phanerozoic stromatolites within a siliciclastic sequence in the Perth Basin, Western Australia, demonstrate exceptional preservation of filamentous microstructures that comprise pitted cavities enveloped by a mineralized mantle (Chen et al., 2014; Olden et al., In Review; Olden et al., 2019). Here, we refer to these microstructures as alveolate (meaning 'with cavities') to avoid presumptive assignment of biogenicity. These alveolate microstructures were originally described as cells, from a single locality, based on reported original organic material and carbonate still preserved (Chen et al., 2014). Recent mapping has shown that the stromatolitic sequence is developed beyond the original ~6 km^2, to at least 24 km^2, and possibly extends much further (Olden et al., In Review; Olden et al., 2019).

In this study, we use petrography, scanning electron microscopy (SEM), energy dispersive X-ray spectroscopy (EDS), electron backscattered diffraction (EBSD), and high-resolution X-ray computed tomography (HRXCT) to identify the composition and morphology of the alveolate microstructures, and their association with the stromatolitic laminae. The combination of all these techniques allow us to assess their origin, mechanism(s) responsible for their preservation and may aid in the search for other exceptionally preserved stromatolite occurrences throughout the geological record.

2 Perth Basin stromatolites

The Perth Basin stromatolite sequence (PBS) unconformably overlies the Mid-Palaeozoic Tumblagooda Sandstone and is disconformably succeeded by the Early Triassic (Olenekian) Kockatea Shale (Fig. 3.1; Mory et al., 2005; Olden et al., In Review; Olden et al., 2019). Chen et al. (2014) originally proposed an Early Triassic age for the stromatolitic sequence, interpreting a conformable relationship with the overlying Kockatea Shale and overall association with the Permian mass extinction. Based on revised interpretations of stratigraphic relationships, Olden et al. (In Review); (2019) considered that the age constraints on these stromatolites are, in the most conservative sense, Permian to earliest Triassic.

Stromatolites in the northern Perth Basin are intercalated with a thin sequence (~2–6 m) of coarse-grained terrigenous material (Olden et al., In Review). The stromatolites grow in ten different morphological forms that can be broadly grouped into columnar, domal and mini-columnar forms, which alternate vertically and laterally. The variations between the different stromatolite forms have been attributed to changes in environmental conditions (e.g., amount of detrital input, water level changes, etc.) and biogenic responses (e.g., lateral growth of stromatolites upon reaching photosynthetic zenith; Olden et al., In Review; Olden et al., 2019). Stromatolite-associated clastic lithologies comprise both matrix-supported conglomerates and coarse-grained sandstones that together have been interpreted as mass flow deposits, formed in a restricted aquatic setting (Olden et al., In Review; Olden et al., 2019). The PBS stromatolites are similar to those observed in the East African Rift Valley (Casanova, 1986, 1994), where mass flow deposition, sourced from the hinterland, alternated with periods of quiescence, allowing for microbial growth.

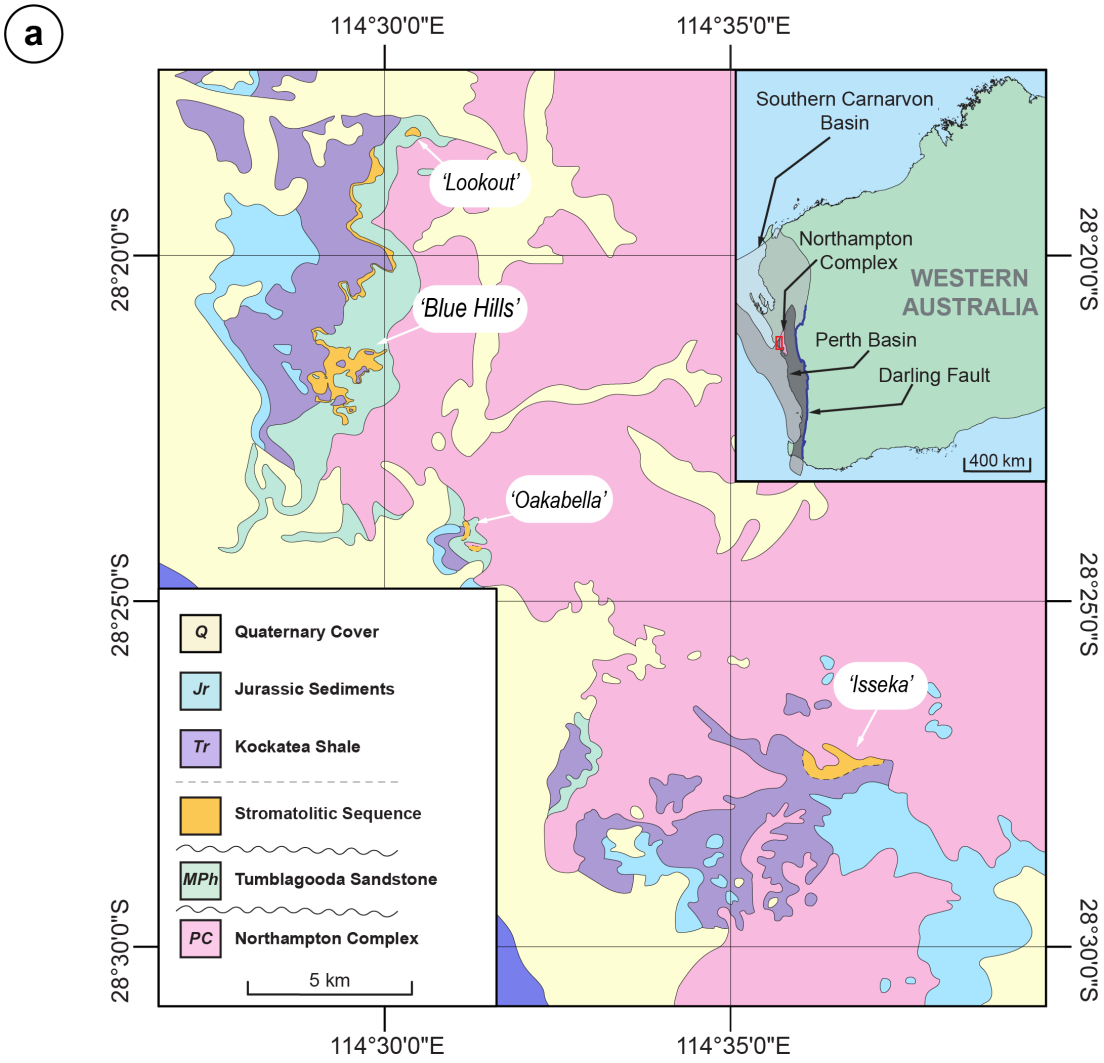

Fig. 3.1: a) Interpreted bedrock map of known outcrop localities of Western Australian Mid-Phanerozoic stromatolitic sequences, insert map shows location of site (red box) with regards to major

geological features of Western Australia, b) schematic stratigraphic-sections of each of the major field localities. Adapted from Olden et al. (In Review) and Olden et al. (2019).

3 Samples and methods

1.1 Sample descriptions

The PBS was extensively sampled over three of the four major outcrop regions: Blue Hills (the type locality), Oakabella and Isseka (Table 3.1, Fig. 3.1). Detailed descriptions are given in Olden et al. (2019) and Olden et al. (In Review), but the salient features are outlined briefly here.

Table 3.1: Samples used in this study and techniques applied.

Sample ID	Locality	Latitude[a]	Longitude[a]	Media	Advanced analytical techniques[b]
SG-1	Blue Hills	-28.358648000	114.490533000	Thin section	-
SG-2	Blue Hills	-28.359011000	114.491310000	Thin section	-
BH1-1	Blue Hills	-28.362077944	114.482382948	Thin section	HRXCT
BH1-2	Blue Hills	-28.365817139	114.484069418	Thin section	-
BH1-3	Blue Hills	-28.365817139	114.484069418	Thin section; Polished mount	-
BH1S	Blue Hills	-28.359070582	114.498385150	Thin section	-
OB1	Oakabella	-28.404429866	114.522859555	Thin section	-
OB2	Oakabella	-28.404280266	114.523067111	Thin section	FIB-SEM
OB3	Oakabella	-28.404330000	114.523045000	Polished mount; crushed material	EBSD, FIB-SEM
IS1	Isseka	-28.455002513	114.611324176	Polished mount	HRXCT
[a] Coordinates are in Geodetic WGS 1984					
[b] All samples have petrographic analyses, secondary electron imaging, backscatter electron imaging and Fiji image analysis					
All samples were collected by authors in 2018-19					

3.1.1 Blue Hills

The stromatolitic sequence sits unconformably atop the mid-Palaeozoic Tumblagooda Sandstone and is on-lapped by the Lower Triassic Kockatea Shale (Fig. 3.1b). Morphologically distinct forms of stromatolites are intercalated with coarse-grained, poorly sorted siliciclastics. Morphological forms at this site include stratiform, stubby columnar, domal, mini-branching [alpha ± beta] columnar and tepee stromatolites (Grey & Awramik, 2020). At Blue Hills, the PBS is ~2–6 m thick, with the thickest sections associated with palaeo-channels that incised into the Tumblagooda Sandstone. Twenty-six samples were

collected from this locality, with six samples chosen for microanalysis in this study (Table 1). These six samples capture the diversity of stromatolite forms and are representative of the lower and upper parts of the PBS.

3.1.2 Oakabella

The stromatolitic sequence sits unconformably atop the mid-Palaeozoic Tumblagooda Sandstone and is overlain by the Lower Triassic Kockatea Shale, although the contact is not evident (Fig. 3.1b). The Oakabella succession is lithologically similar to Blue Hills, with the exception of the presence of 'tear up' clasts of stromatolitic bioherms incorporated into the siliciclastic sedimentary rocks (Fig. 3.1b). Morphological forms at this site include stratiform, stubby columnar, slender columnar, domal, bulbous and mini-branching (Grey & Awramik, 2020). At Oakabella, the PBS is ~2–5 m thick. Six samples were collected from this locality, of which three representative samples were further characterized here for microanalysis (Table 1).

3.1.3 Isseka

The stromatolitic sequence sits nonconformably atop the Neoproterozoic Northampton Complex at the Isseka locality (Fig. 3.1b). The PBS is covered by the Lower Triassic Kockatea Shale, though the contact is not visible at this locality. Morphological forms at this site include mini-branching [beta ± gamma] columnar, lobate columns, slender columns (Grey & Awramik, 2020). At Isseka, the PBS is ~1.5–4.0 m thick, although mapping indicates that its full thickness is not captured in outcrop (Olden et al., In Review; Olden et al., 2019). Columnar stromatolites at Isseka are sporadically elongated with preferential alignment throughout the outcrops. Six samples were collected from this locality, with one representative sample further characterized in this study (Table 1).

3.2 Sample preparation

Eight of the ten representative samples selected for further detailed analysis were trimmed into thin section-sized billets and impregnated with clear epoxy resin to increase structural integrity (Table 1). Blocks were mounted on glass slides and polished to a thickness of 30 μm at the Smithsonian Museum of Natural History, Washington D.C., and Minerex Services, Esperance, Western Australia. Full thin sections were scanned on a motorized Zeiss Axio Imager 2 optical microscope in the School of Earth and Planetary Sciences (EPS) at Curtin University, Perth,

Australia, in both reflected and transmitted light to provide broad overviews of the samples and aid in navigation for subsequent microscopic analyses.

Two representative stromatolites from each locality were cored with a 1-inch diameter hollow drill, impregnated with resin and polished flat (Table 1). One of these samples is a duplicate of a thin sectioned region. The round mounts were also scanned in full on the Zeiss Axio Imager 2 but only in reflect light.

One additional stromatolite sample from Oakabella was crushed using a hydraulic press, with the resultant material sieved into size fractions < 125 µm, 125–212 µm, and >212 µm at EPS (Table 1). Fractions were placed in an ultrasonic bath to remove clay-sized particles and representative fragments were picked for SEM analysis.

Thin sections, round mounts and crushed fragments were carbon-coated for 2000 ms (~20 nm) to create a conductive surface for subsequent scanning electron microscopy (SEM) analysis.

One stromatolite mini-columnar sample from Isseka was sawn into a large rectangular block (~7 × 7 × 15 cm) and impregnated with epoxy resin. The block was then trimmed into a narrow (~2 × 2 × 10 cm) rectangular slab bounding a single, complete mini-columnar stromatolite, in preparation for HRXCT.

3.3 Scanning electron microscopy

Reconnaissance SEM was conducted using a HITACHI TM3030 tabletop microscope at EPS, Curtin University, on all thin sections, round mounts and crushed fragments. Thin sections were scanned and imaged in backscattered electron (BSE) and topographic modes to identify compositional and structural variations along the alveolate microstructures, respectively.

Detailed imaging and qualitative chemical analyses of selected regions in all thin sections, round mounts and stromatolite fragments was conducted using a Tescan Mira3 Field Emission Gun SEM (FEG-SEM) at the John de Laeter Centre (JdLC), Curtin University. Secondary electron (SE) and BSE imaging was conducted with a nominal working distance of 15 mm, a beam current of 935 pA, a spot size of 14 nm, and an accelerating voltage of 20 kV. EDS mapping of the thin sections, crushed material and cross-sections of alveolate microstructures was conducted using an Oxford Instruments X-Max^N detector in the same instrument and under the same operating conditions used for SE and BSE imaging, using the Oxford Instruments Aztec software package to process the data.

For one thin-sectioned sample from Oakabella, the alveolate microstructures were cross-sectioned using a Lyra3 Ga^+ Focused Ion Beam SEM (FIB-SEM, Table 1). A 2 × 30 μm strip of platinum was deposited to protect the region of interest prior to the ion milling. The ion beam was operated at 30 kV accelerating voltage, with coarse milling done at a current of 5 nA and polished with a current of 1 nA.

On two representative samples from Oakabella, electron backscatter diffraction (EBSD) analyses were conducted to identify grain boundaries and the size of siliceous components surrounding the alveolate microstructures (Table 1). Electron backscatter diffraction was undertaken within the JdLC using the Mira3 FEG-SEM mentioned above, equipped with a Symmetry CMOS electron backscatter pattern detector from Oxford Instruments. Data were collected at a step size of 0.1 μm with an accelerating voltage of 20 kV and a beam intensity of 16, at a working distance of 20 mm and a sample tilt of 70º. Data were subsequently processed using the AZtecCrystal data analysis software. Noise reduction was performed using the nearest-neighbour algorithm within AZtecCrystal to remove erroneous data points and systematic misindexing. Grain boundaries were defined based on a misorientation of >10º between crystallographic orientations of neighbouring pixels. A grain size map was subsequently generated and plotted as a function of grain area.

3.4 High-resolution X-ray computed tomography

A representative stromatolite column from Isseka was scanned in 3D using a Zeiss Versa XRM520 3D X-ray microscope fitted with a flat panel detector located at the Australian Resources Research Centre (CSIRO Mineral Resources, Perth). A series of scans were recorded along the long axis of the sample and were subsequently stitched to form a single 3D volume (3062 × 3062 × 4700 voxels in size). For each scan, the instrument was set-up to maximize phase contrast of the different constituents of the sample, with 1601 projections recorded over 360° rotation and a voxel size of 12 μm. Beam hardening was corrected during reconstruction and ring artefacts were minimized during acquisition using a dynamic ring removal algorithm. Image segmentation and quantification were performed using CSIRO workflows using Avizo 2019.2 and Matlab 2019b software.

3.5 Image analysis

Internal alveolate dimensions can be quantified in 2D to illustrate potential size differences in distinct parts of the stromatolite column. Backscattered electron maps of the alveolate microstructures were converted to 8-bit files and thresholded using Fiji freeware (Sezgin &

Sankur, 2004). Size analysis of alveolate microstructures was conducted on the thresholded maps with field of views of 2 mm using representative rounds from each major stromatolite locality (Table 1).

The alveolate microstructures in the 3D HRXCT dataset were segmented from the greyscale images and morphological parameters of individual alveolate microstructures (~3×10^6 across the sample) were calculated and used for shape and size characterization. Alveolate microstructures smaller than 3 voxels width were discarded to reduce errors resulting from partial volume effects. Shape analysis of the alveolate microstructures was conducted by plotting small/intermediate against intermediate/long axis following Oakey et al. (2005).

4 Results

4.1 Stromatolite alveolate morphology

Stromatolite alveolate microstructures were imaged both parallel and perpendicular to growth axis in thin sections, in fine-grained crushed particles, along cross-sectional micro-excavations (FIB-SEM) and in 3D (HRXCT). The stromatolite alveolate microstructures consist of prolate spheroids aligned with the stromatolitic laminae, with a defined outer rim, referred to herein as a sheath, and a core that is hollow or infilled by iron or silica (Fig. 3.2). In 2D view the alveolate microstructures have typical internal dimensions of 20–190 µm on the long axis and 8–30 µm on the short/intermediate axis, taken from the 'core' of the structure (Fig. 3.3). Enveloping mantles of the alveolate microstructures have average thicknesses of 5–12 µm. We note that in thin section, some non-perpendicular sectioning through the alveolate microstructures occurs, so the apparently smaller lengths may be an artefact. As revealed from the crushed particles in one Oakabella sample, in 3D the alveolate microstructures reveal elongate, vermiform morphologies with diameters of 10–14 µm and lengths of 90–110 µm (Fig. 3.4).

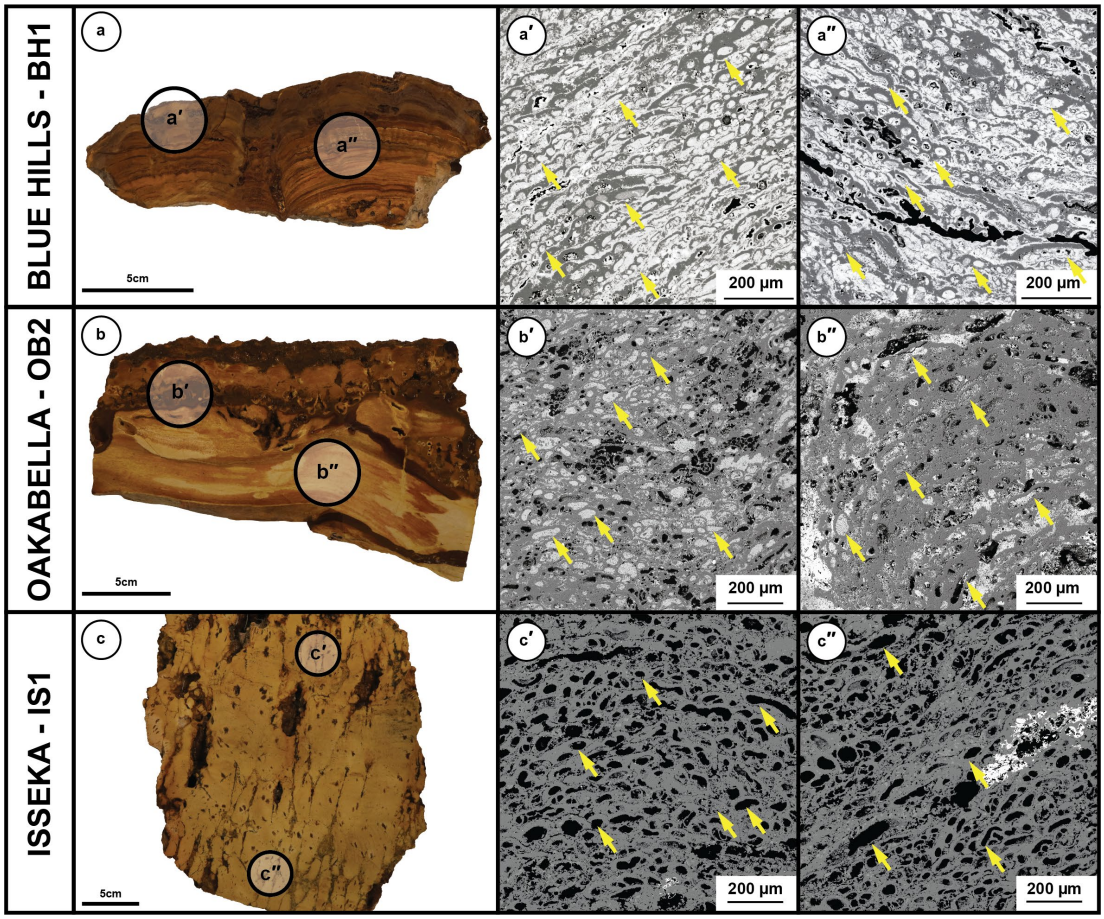

Fig. 3.2: Representative stromatolite samples and corresponding backscattered electron images of cellular microstructures (yellow arrows; a'–c"); a) BH1-1, b) OB2, c) IS1.

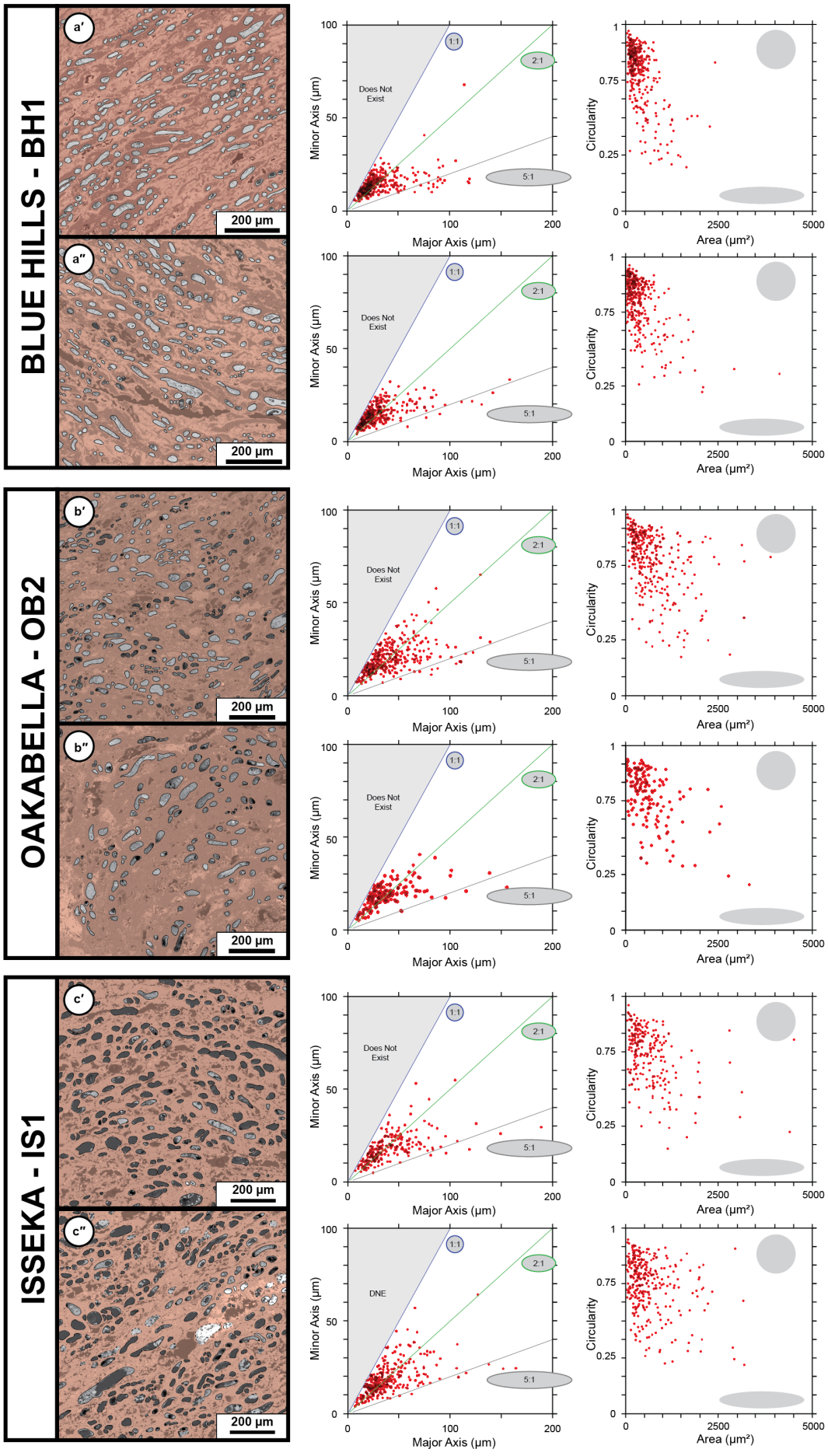
BLUE HILLS - BH1
OAKABELLA - OB2
ISSEKA - IS1
a′
a″
b′
b″
c′
c″
200 µm
Does Not Exist
DNE
1:1
2:1
5:1
Minor Axis (µm)
Major Axis (µm)
Circularity
Area (µm²)
0
50
100
200
0.25
0.75
1
2500
5000

Fig. 3.3: Dimensions of alveolate microstructures from representative stromatolites, where a'–c' and a''–c'' are from the top and bottom of stromatolitic samples, respectively (see Fig. 3.2). A semi-transparent red layer is overlain on the over the alveolate mantles and other interstitial cement, with the un-highlighted portions representing the alveolate cores. Major and minor axis, circularity and area were measured using best fit ellipsoids in Fiji freeware. Grey ellipses represent shapes based on measurements provided.

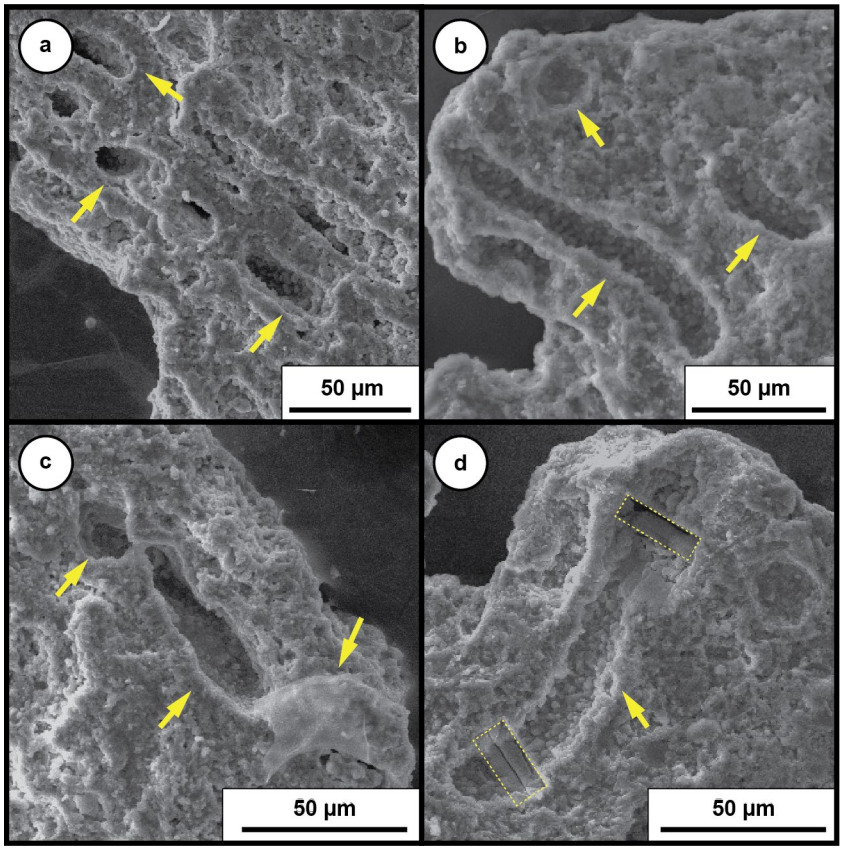

Fig. 3.4: Crushed stromatolite OB2, showing alveolate microstructures (yellow arrows) in 3 dimensions. Dotted yellow rectangles are FIB sections.

Thin sections oriented perpendicular to stromatolite growth axes across the top of stromatolite mini-columns show similar alveolate microstructures to those seen in vertical cross-sections, defining the laminae that characterises the stromatolite (Fig. 3.2). There is a subtle reduction in length of the long axis and the aspect ratio of the cells from top to base within a single stromatolite column (Fig. 3.3–Fig. 3.5). In stromatolite morphological lows (Fig. 3.5), this long-axis reduction is markedly smaller (~10–15%) than in stromatolite morphological highs (~30%). There is also a significant dichotomy between cell sizes in morphological lows (Fig. 3.5) and highs, with the lows being consistently smaller than those on morphological highs by

~15–30% (Fig. 3.5b). The mantles of the alveolate microstructures are proportionally thicker at the tops of the structures in comparison the bases (Fig. 3.2).

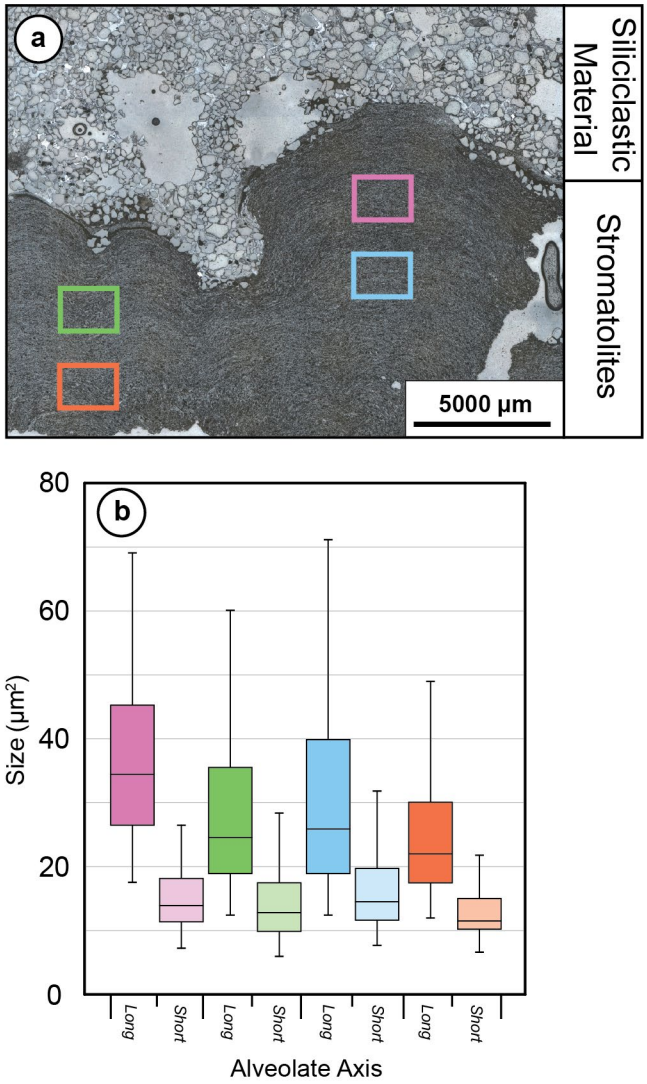

Fig. 3.5: Statistical morphological comparison between alveolate microstructures in morphological highs (pink and blue) and lows (green and red) in Oakabella sample OB2. a) photomicrograph of locations sampled for shape analysis (colours refer to respective box-and-whisker plots). b) Box-and-whisker plots of alveolate microstructure area via 2D particle analysis from different sections of stromatolite columns. Colours are from a, with the darker and lighter shades corresponding to the long and short axes, respectively.

Volume rendering of the segmented HRXCT data displays three main phases within the stromatolite sample, including siliceous alveolate mantles, interstitial porosity and interstitial haematite and siderite (Fig. 3.6). Siliceous mantles of the alveolate microstructures were

segmented from total porosity using the bounding stromatolite column, leaving interstitial porosity. To extract the porosity within the column we used a 3D filling algorithm to remove all the porosity within the column and then used that volume to mask the porosity which is in the column (the blue on Fig. 3.6) Porosity in the sample is primarily situated within the alveolate sheaths, with subordinate portions part of the interstitial matrix. The shape of the alveolate microstructures defined via CT are primarily vermiform/filamentous, as observed via other media (Fig. 3.2–Fig. 3.5), but distinct circular structures are also identified (circular; Fig. 3.7). The prolate, alveolate microstructures are aligned broadly parallel to the lamination of the stromatolite (Fig. 3.6).

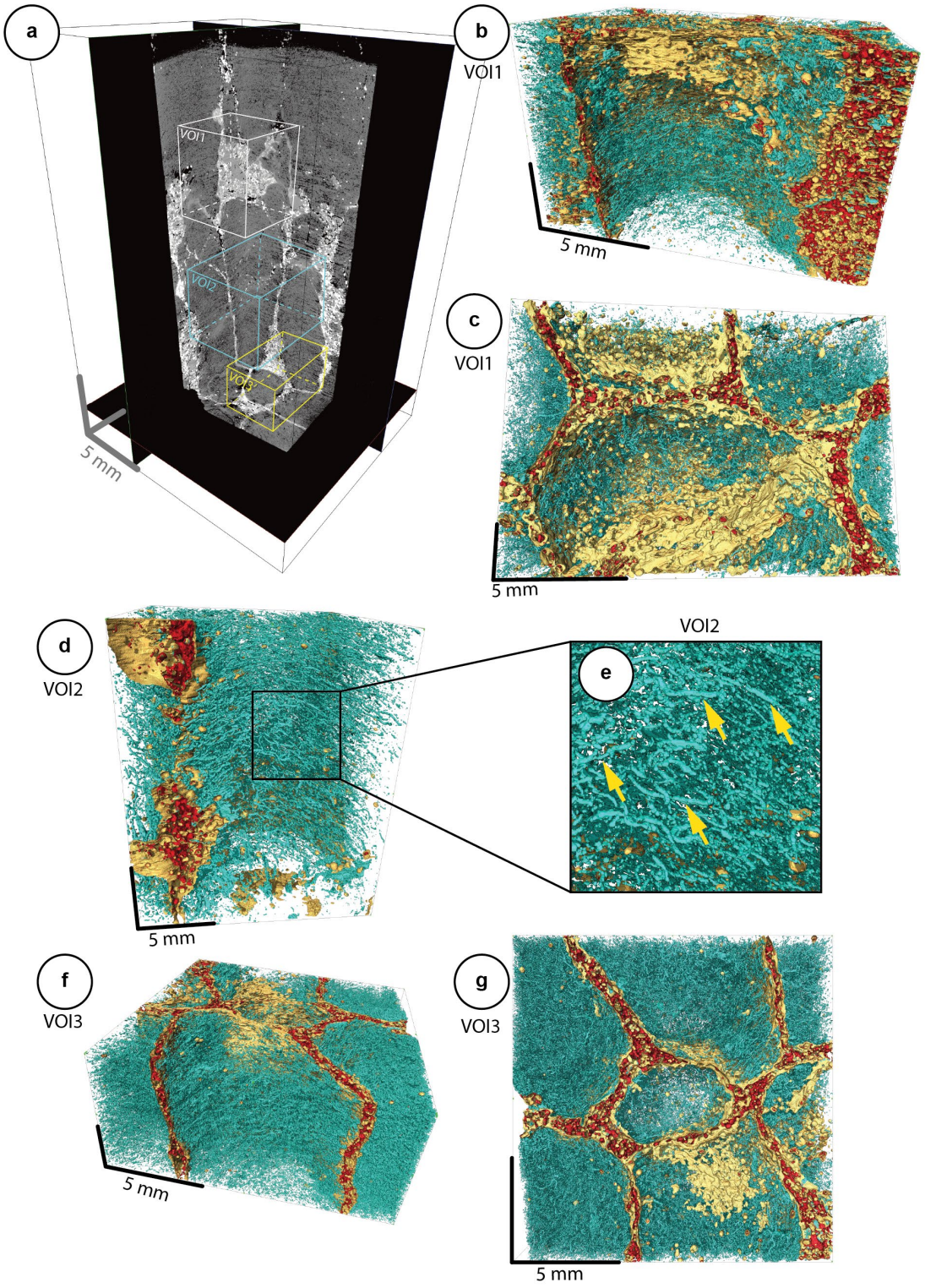

Fig. 3.6: HRXCT results for lobate columnar stromatolites from Isseka. a) Orthogonal slices virtually cut through the reconstructed greyscale volume, coloured VOI boxes represent various volume of interest highlighted in the subsequent pictures. b) Volume rendering showing the top of a lobate column in VOI1 where alveolate core pore space in blue, and interstitial pore space in in yellow and iron

(haematite and siderite) in red. c) Volume rendering of a lobate column in VOI1 looking from the top. d) Volume rendering of central portion of a lobate column in VOI2. e) Zoom of volume render VOI2 showing prolate nature of the alveolate microstructures (blue), marked by yellow arrows. f) Volume rendering of lobate columns in VOI3 from base. g) Top view of volume rendering VOI3.

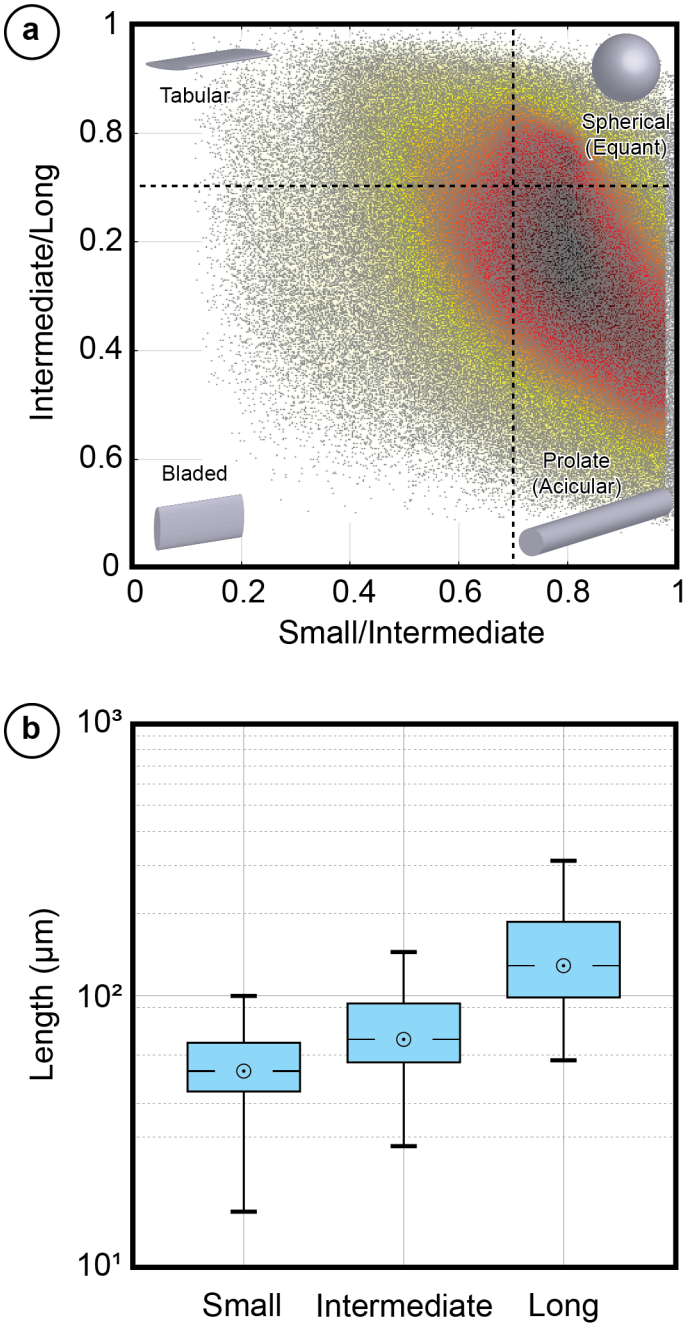

Fig. 3.7: Statistics on 3D shape and size of voids within the 'Isseka' sample: a) short, intermediate and long axes of best fitted ellipsoid (Feret distribution) for each alveolate microstructure where colour contours highlight the density of points within a given 0.01 ratio range (from shades of yellow to black), dashed lines show boundaries between shapes; b) statistical analysis of each axis of the best fit spheroids.

4.2 Stromatolite microstructure geochemistry

Energy-dispersive X-ray spectroscopic maps of the thin sections show that the alveolate microstructures are either hollow (e.g., from Isseka, Fig. 3.8), infilled by haematite and/or siderite (e.g., from Blue Hills, Fig. 3.8), or infilled by silica (e.g., from Oakabella, Fig. 3.8). The haematite is bladed and botryoidal in nature and most abundant in the northernmost stromatolites (Blue Hills).

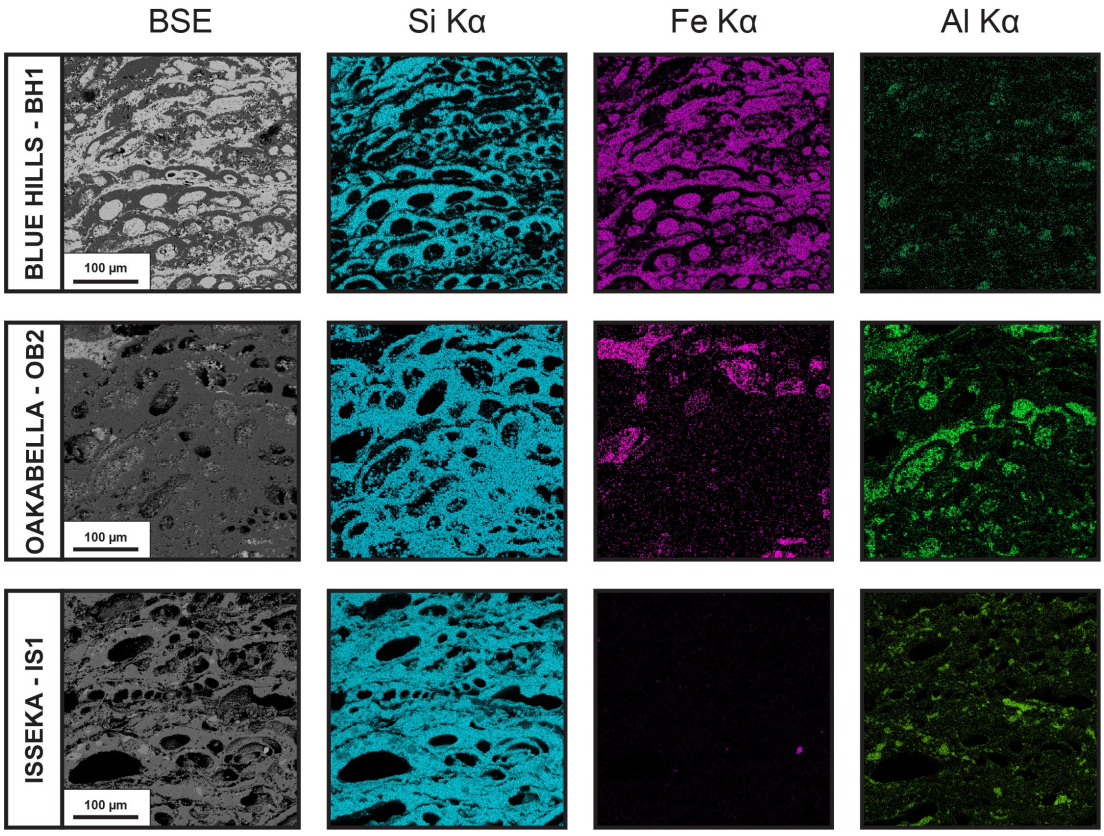

Fig. 3.8: Energy-dispersive X-ray spectroscopy of alveolate microstructures within the stromatolites. Si Kα, Fe Kα and Al Kα peaks highlight the presence of quartz, haematite/siderite and clay minerals, respectively.

Backscattered electron imaging combined with energy-dispersive X-ray spectroscopy (EDS) shows the alveolate sheaths are composed almost entirely of quartz (Fig. 3.8). Electron backscatter diffraction (EBSD) analysis of OB2 shows the sheaths have differing crystal sizes of micro-crystalline quartz. The 'tops' of the mantle, on average, have larger grain sizes than those on the 'bottom' of the sheaths (Fig. 3.9).

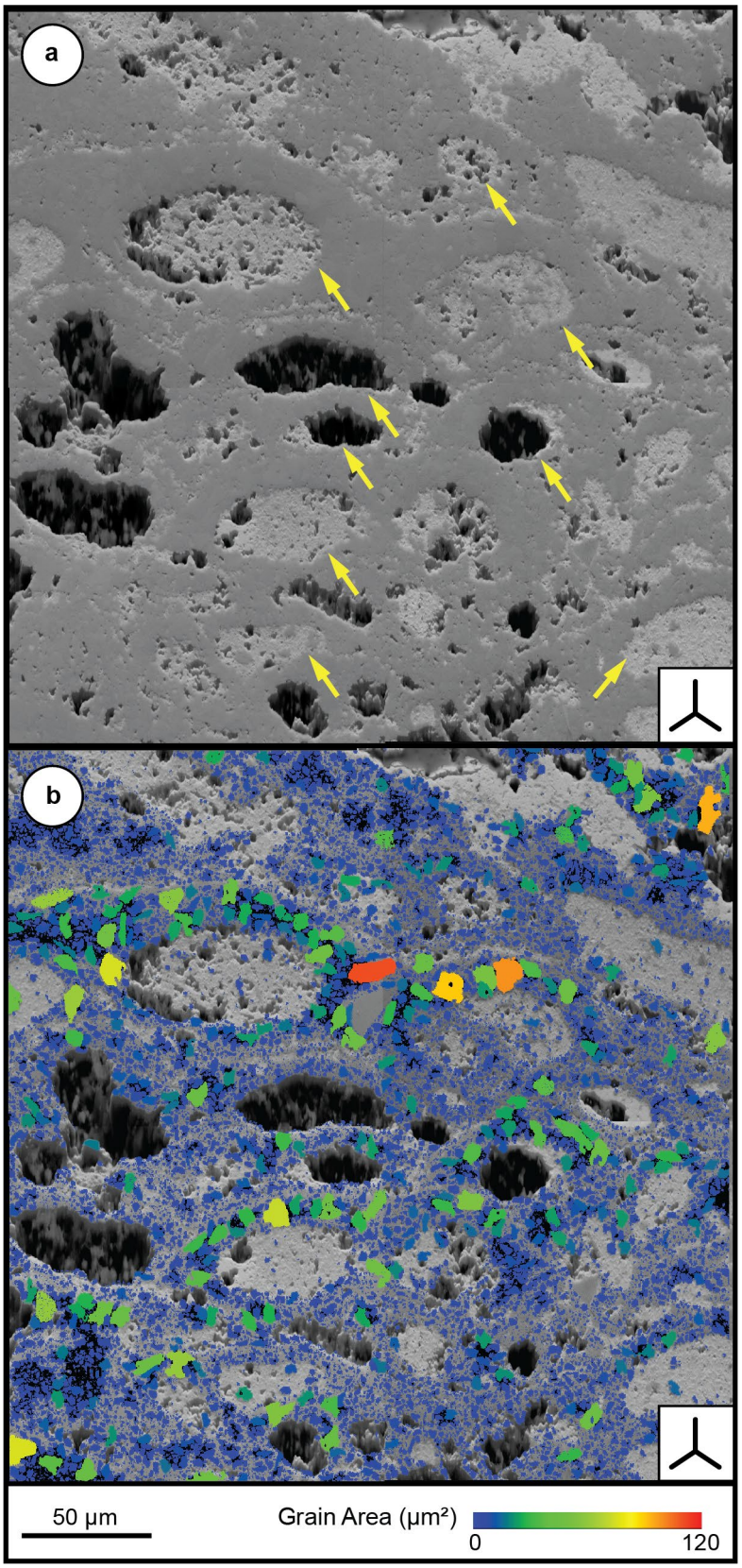

Fig. 3.9: EBSD analysis of stromatolite OB2; a) Forescatter Diode (FSD) image of target area yellow arrows indicate alveolate microstructures, b) silica grains coloured according to area (µm²).

Ion beam milling in OB2 demonstrates a cross-sectional view of the alveolate microstructures with elemental distributions similar to their longitudinal counterparts (Fig. 3.10).

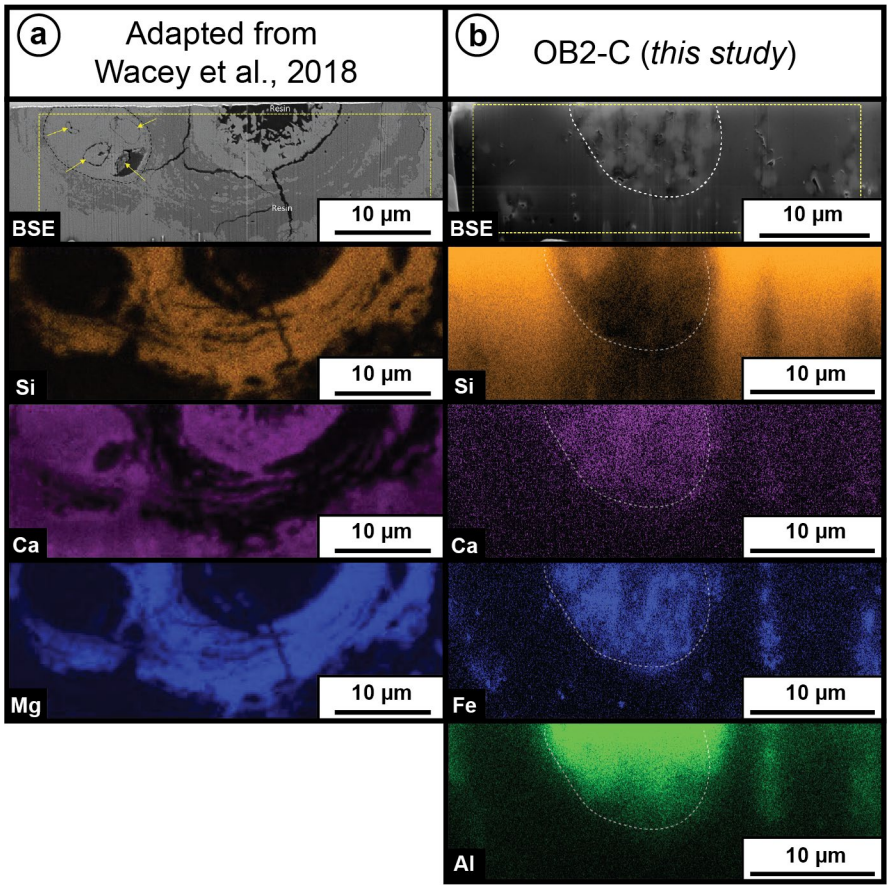

Fig. 3.10: : Comparison of EDS maps of cross-sections of modern cyanobacteria (a; Wacey et al., 2018), with that of this study (b). Both sets of cross-sections were made milled-out using a FIB-SEM. Dashed white line in b highlights the boundary between the alveolate core and mantle.

5 Discussion

5.1 Assessing biogenicity of alveolate microstructures

Typically, biogenicity is determined using isotopic signatures of Ca, N, O, C and S within the target (Javaux, 2019; Oehler et al., 2009; Schopf, 2006; Schopf, Kudryavtsev, Agresti, Czaja, & Wdowiak, 2005; Wacey, 2010; Wacey, Gleeson, & Kilburn, 2010). However, the Perth Basin stromatolites analysed have been subject to significant chemical alteration, in particular ferruginous and siliceous replacement (Fig. 3.8; Fig. 3.10). Thus, evaluating biogenicity of the alveolate microstructures requires alternative methods relating to chemistry, morphology and size. Following Grey and Williams (1990), alveolate microstructures in the Perth Basin

stromatolites have been morphologically and chemically compared against multiple biogenic and abiogenic microstructures to determine their origin (Table 3.2).

Table 3.2 Summary comparison with alveolate microstructures (this study) with similar known structures, following Grey and Williams (1990). Black, bolded and grey, italic text corresponds to features that are similar and dissimilar to the alveolate microstructures observed in this study, respectively.

Shape	Long Axis (µm)	Short Axis (µm)	Internal Structre	Chemistry		Origin	Climate/ Environment	Source
				Mantle/rim	Core			
Cylindrical	**20 — 190**	**8 — 30**	**Hollow/secondary infill (Fe)**	**SiO_2**	**Fe_2O_3, $FeCO_3$**	**Biological** [1]	**Restricted water body** [2]	**This Study**
Cylindrical	**up to 300**	**5 — 20**	**Hollow/secondary infill (Ca)**	**Si, Mg**	**Secondary Ca**	Biological	NA	Bertrand-Sarfati & Pentecost, 1992; Wacey et al., 2018; Defert et al., 1994; Schopf, 2004
Concentric Rings	NA	**10 — >10,000**	Solid, Chalcedonic	Si Undifferentiated		Chemical	NA	Butts & Briggs, 2011
Spheroidal	**100 — 1,000**	100 — 1,000	Massive micrite (no internal structures)	Ca	Detrital grains	Chemical± biological (fecal pellets)	NA	Flugel, 2013
Sub-Spheroidal	200 — 10,000	200 — 10,000	Non-biogenic nucleus, divergent and radial microfabrics in laminae	Ca	Nucleus dependent	Chemical	(Sub) Tropical	Flugel, 2013
Spheroidal	200-2000	200-2000	Non-biogenic nucleus, with concentric radial microfabrics in laminae.	Ca	Nucleus dependent	Chemical± biological	(Sub) Tropical, Marine and **non-marine**	Flugel, 2013
Sub-Spheroidal	1,000 — 200,000	1,000 — 200,000	Distinct nucleus (biogenic) with irregular, nonconcentric micritic laminae	Ca	Nucleus dependent (usually Ca)	Biological	(Sub) Tropical	Flugel, 2013
Hemispherical	**30 — 1,000**	30 — 1,000	Radiating filaments. Dark rings around the tussocks can develop. Can form concentric rings of alternating dark and light zones, historically interperted as variations in growth	NA	NA	Biological	NA	Bertrand-Sarfati & Pentecost, 1976; Fairchild, 1991; Bertrand-Sarfati et al., 1991
Cylindrical ; simple & complex branching	> 10,000	> 10,000	Sedimentary infills (primary or secondary)	NA	NA	Biological	Organic rich sediments	MacEachern et al., 2012
Laminoid	1000	200	**Hollow/ Secondary infill** of sillica with chalcedony or megaquartz	NA	NA	Mechanical/ Chemical	intertidal/supratidal carbonate settings	Blendiger, 1986; Allwood et al., 2009; Southgate, 1980; Hoffman et al., 1980
Irregular	20000	2000	**Hollow/ Secondary infill** of sillica with chalcedony or megaquartz	NA	NA	Mechanical/ Chemical	intertidal/supratidal carbonate settings	Allwood et al., 2009; Southgate, 1980; Hoffman et al., 1980
Tubular	NA	NA	**Hollow/ Secondary infill** of sillica with chalcedony or megaquartz	NA	NA	Mechanical/ Chemical	intertidal/supratidal carbonate settings	Allwood et al., 2009; Hoffman et al., 1980

ed in section 5.1

e by Olden et al (In review) and Olden (2020)

Filamentous cyanobacteria are the most likely origin for the alveolate microstructures in the Perth Basin. Morphologically, the alveolate microstructures in the Perth Basin closely match that of modern filamentous cyanobacteria, with diameters of 5–20 µm and lengths of up to 90 µm (Défarge, Trichet, & Coute, 1994; Wacey et al., 2018). The primary vermiform morphology of the alveolate microstructures measured is analogous to that of undifferentiated filamentous cyanobacteria (Fig. 3.11; Gong et al., 2019). Chemically, there are subtle differences between the alveolate microstructures and cyanobacterial structures found in modern stromatolites. In modern stromatolites, mineralised sheaths of filamentous bacteria are typically composed of silica and magnesium silicates (Gong et al., 2019; Kremer et al., 2012; Wacey et al., 2018), but the PBS alveolate microstructures mantles are instead almost exclusively composed of silica (Fig. 3.8; Fig. 3.10). The cores of modern cyanobacterial structures are hollow or infilled by secondary calcite (Kremer et al., 2012; Wacey et al., 2018), while the Perth Basin stromatolite alveolate microstructures are infilled with siderite (±ankerite) and secondary haematite or pore space (Fig. 8). Both of these apparent inconsistencies can be explained by Ca and Mg being highly mobile as 2^{+} ions in deuteric conditions (Fantle & Higgins, 2014; Schroeder, 1969; Walls, Ragland, & Crisp, 1977), and thus could conceivably be replaced by iron during diagenesis (see Section 5.2).

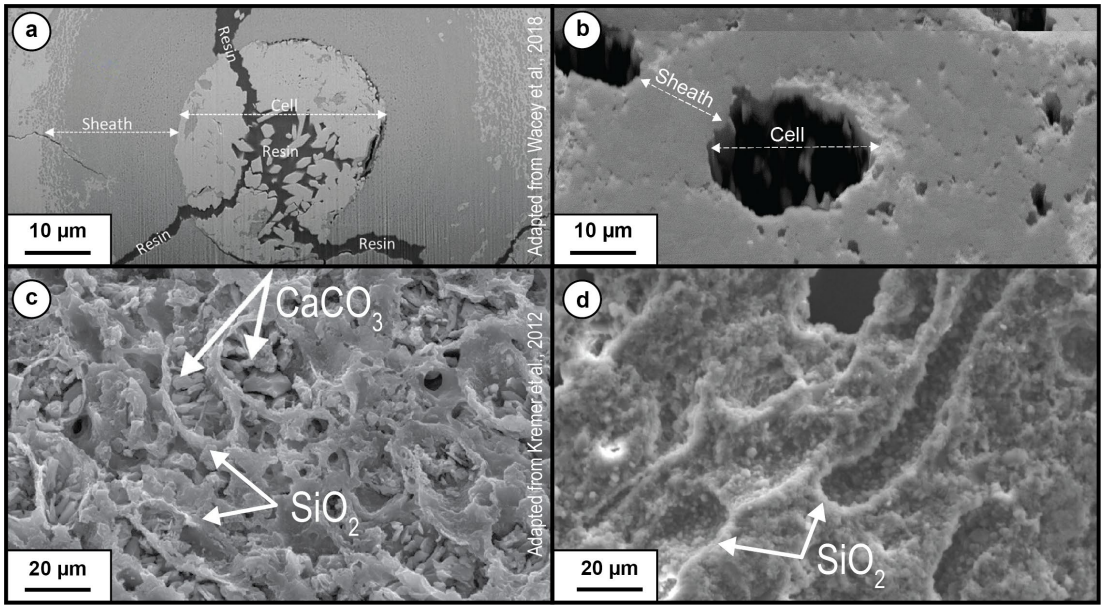

Fig. 3.11: Comparison of modern filamentous cyanobacteria preserved from Lake Thetis (a, type 2 filament, Wacey et al. (2018)) and Niuafo'ou's Caldera Lakes (c, type 1 filament, Kremer et al. (2012)) with fossilised cyanobacterial structures of the Western Australian Mid-Phanerozoic stromatolites (b, d). a was imaged in BSE, b is a FSD image, and c–d were imaged in SE.

The mantles of the alveolate microstructures are thicker at the tops of the mantle, in comparison to the base of the mantles (Fig. 3.9). This suggests that mantles grew larger at the surface as they were unrestricted in space, whereas the base of the mantle was restricted in space it could develop. Microcrystalline quartz in the mantles of the alveolate microstructures show crystals are larger in the tops of the mantle in comparison the bases (Fig. 3.9). This would be resultant of the tops of the mantles were at the fluid interface, therefore, having a greater access to silica allowing the growth of larger microcrystalline quartz. Therefore, the alveolate microstructures observed in Western Australia morphologically and chemically resemble preserved cyanobacteria, albeit without the internal cellular trichomes.

Other biological and chemical structures share some similarities with the observed alveolate microstructures, including carbonate grains (ooids, peloids, oncoids and pisoids), beekites, tussocks, burrows and fenestrae, but these structures are a poor match in other categories (Table 3.2). For the shape, only burrow structures, laminoid fenestrae and tubular fenestrae are similar to the alveolate microstructures. With respect to particle size and aspect ratios, most chemically- and mechanically-formed particles are significantly too large, except perhaps beekite structures, tussocks and peloids, but all of these have very large ranges in size. The alveolate microstructures of the PBS lack oscillatory zoning, precluding carbonate grains, tussocks and beekite structures (Bertrand-Sarfati, 1976; Bertrand-Sarfati, Freytet, & Plaziat, 1991; Butts & Briggs, 2011; Flügel, 2013). Alveolate microstructures are predominantly aligned parallel to the laminae of the PBS stromatolites (Fig. 3.2; Fig. 3.6), which are similar to that of laminoid fenestrae that form parallel to the depositional layering (Bertrand-Sarfati, 1976). In contrast, other forms of fenestrae, as well as tussock internal fabrics, and many dwelling and feeding traces, occur perpendicular to depositional surfaces (Bain & Kindler, 1994; Bertrand-Sarfati, 1976; Grey & Awramik, 2020; Logan, Hoffman, & Gebelein, 1974; Pemberton & Frey, 1982). Simple burrow networks are open in some directions whereas the PBS alveolate microstructures are enclosed (Fig. 3.6). Chemically, the alveolate microstructures are generally homogeneous in composition, with mantles composed of silica and cores that are either hollow or infilled by secondary silica, haematite or clay minerals. Peloids are micritic, which is absent in the PBS alveolate microstructures (though it could have been replaced/altered), and, more importantly, do not demonstrate differentiation into the core and sheath structures described herein. The PBS is thought to have developed between mid-Permian to Early Triassic (Olden et al., In Review; Olden et al., 2019), during which south-west Australia was at high southern latitudes (Blakey, 2008). Subsequently, conditions in the Perth Basin were likely too cool to produce abiogenic carbonate grains, which are formed in

warm shallow marine environments conducive to abiogenic and biogenic carbonate production (Flügel, 2013; Kershaw & Cundy, 2013).

5.2 Mechanisms of preservation

Preservation of cyanobacterial microstructures is important for understanding early life (Hofmann, 2000; Hofmann, Grey, Hickman, & Thorpe, 1999; Riding, 1991a, 2001, 2011). Thus, it is important to evaluate the mechanisms that have led to such preservation in the Mid-Phanerozoic stromatolites. Typically, cellular structures (trichomes) have low preservation potential, since trichomes comprise organic carbon and are typically infilled by calcite or aragonite following organism death, both of which are highly fluid-mobile (Bartley, 1996; Horodyski, Bauld, Lipps, & Mendelson, 1992; Knoll, 2008; Schopf, 2012). However, silica and phosphate (± carbonate) mineralisation can increase the preservation potential of cell walls and sheaths (Bartley, 1996; Knoll, 1985). Here, we propose three stages for preservation for the cyanobacteria in the Perth Basin stromatolites, in the order in which they occur: (i) syn-depositional biogenic mineralisation, (ii) early diagenetic post-mortem silicification, and (iii) diagenetic ferruginisation (Fig. 3.12). We suggest that biogenic and/or post-mortem silicification are critical for the preservation of cellular sheaths documented in the Western Australian Mid-Phanerozoic stromatolites, with later mechanisms playing second-order roles.

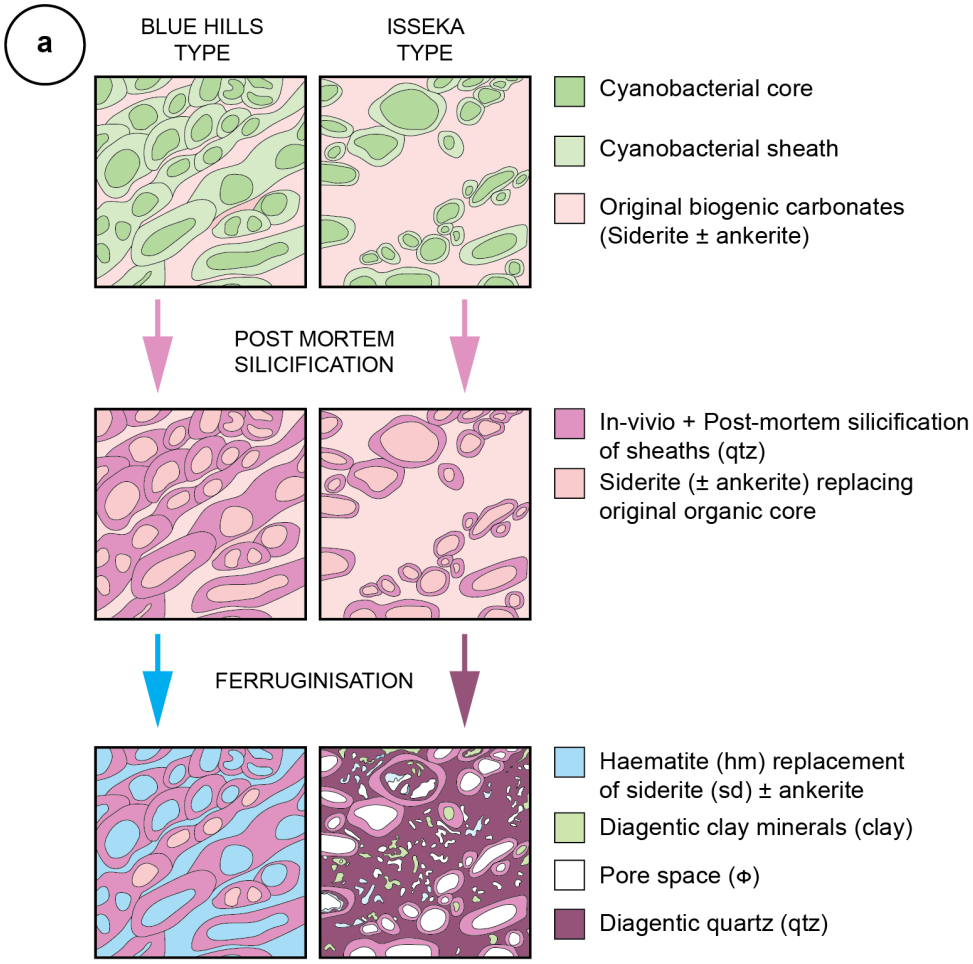
a
BLUE HILLS TYPE
ISSEKA TYPE
Cyanobacterial core
Cyanobacterial sheath
Original biogenic carbonates (Siderite ± ankerite)
POST MORTEM SILICIFICATION
In-vivio + Post-mortem silicification of sheaths (qtz)
Siderite (± ankerite) replacing original organic core
FERRUGINISATION
Haematite (hm) replacement of siderite (sd) ± ankerite
Diagentic clay minerals (clay)
Pore space (Φ)
Diagentic quartz (qtz)

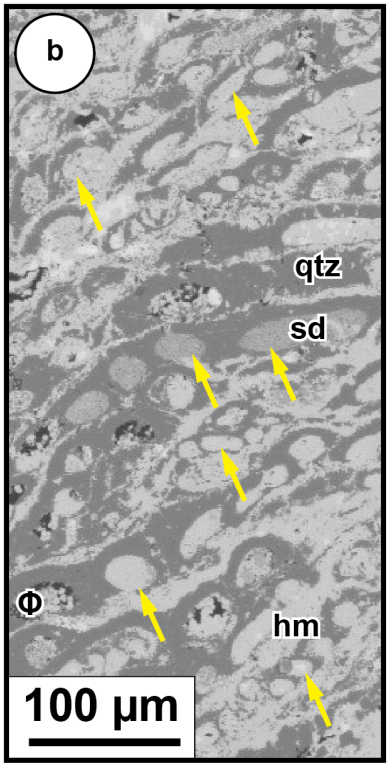
b
qtz
sd
Φ
hm
100 µm

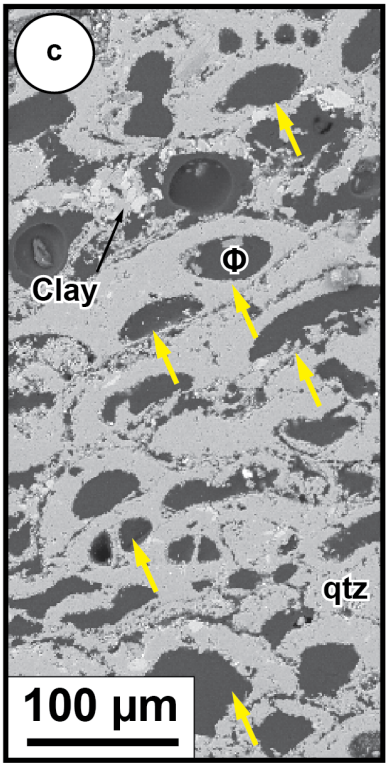
c
Clay
Φ
qtz
100 µm

Fig. 3.12: a) Genetic evolution of Mid-Phanerozoic stromatolites from Western Australia (discussed in the text), b) BSE image of stromatolite altered by post-mortem silicification followed by ferruginous alteration corresponding to Blue Hills Type preservation, c) BSE image of stromatolite altered by post-mortem silicification corresponding Isseka Type preservation. Yellow arrows point to filamentous cyanobacteria microstructure preserved in the stromatolites. Φ = porosity.

Near-circular vertical cross-sections of the filamentous cyanobacteria, irrespective of where they are situated in the stromatolite column (Fig. 3.3), indicates the microstructures rapidly became resistant to compaction. If compaction of the filamentous cyanobacterial sheaths had occurred, there would be no microstructures with a 1:1 short to intermediate axis ratio, instead yielding higher horizontal-to-vertical aspect ratios. Modern stromatolitic environments (e.g. Shark Bay, Western Australia) show compaction of their cellular microstructures during accretion of new layers with, at any given point in time, only the top few millimetres preserving circular aspect ratios (pers. comm., Erica Suosaari, 2018). Thus, the primary drivers for the preservation of the Western Australian cyanobacteria must have occurred in a geologically rapid timeframe.

Biogenic and abiogenic mechanisms that result in the silicification of cellular sheaths have been shown to enhance preservation before compaction can occur (Kremer et al., 2012). Two such rapid processes are considered: syn-depositional biogenic mineralisation, and early diagenetic post-mortem silicification. Modern filamentous cyanobacteria in stromatolites have been shown to form biogenic silica *in vivo* (Konhauser, Phoenix, Bottrell, Adams, & Head, 2001; Wacey et al., 2018). Biogenic precipitation of silica in cyanobacteria typically occurs in the cell walls, trichomes and mucilage sheaths (Konhauser et al., 2001; Kremer et al., 2012; Wacey et al., 2018). Immediately following the death of the bacteria, early diagenetic silicification can occur (Knoll, 1985; Kremer et al., 2012). This 'post-mortem' silicification commonly enhances primary *in vivo* biogenic silica in the cyanobacterial microstructures (muscilage sheaths, cell walls and trichomes; Konhauser et al., 2001; Kremer et al., 2012). The process typically occurs rapidly, as seen in the silicification of wood (Knoll, 1985). This rapidity increases preservation of original organic microstructures.

The PBS preserve the original biogenic structure, albeit without the cellular trichomes. This is similar to observations in modern Tongan stromatolites in lacustrine settings (Fig. 3.11; Kremer et al., 2012). The interpreted filamentous cyanobacteria sheaths are composed of relatively pure silica, with little other minor elements detected using EDS (Fig. 3.5b). A possible explanation for the high silica content in these stromatolites is that they grew in a restricted lacustrine setting (as proposed by Olden et al., in review; Olden, 2019), which is

more susceptible to fluctuations in pH than buffered marine environments (Casanova, 1994). Carbonate buffering in seawater keeps the system at pH levels inconsistent with precipitation of silica (Garrels, 1965; Kershaw & Cundy, 2013). For the PBS, the likely hinterland (Tumblagooda Sandstone and Northampton Complex) comprises > 95% quartz (Ksienzyk et al., 2012; Trewin, 1993), providing an abundant source for dissolved silica in the water. Such a silica-rich system might allow for an increase in precipitation of silica. Differences in the size of microcrystalline quartz in the cyanobacterial sheaths further attest to silicification prior to burial, with the 'tops' of the cell interacting with more of the water than the 'bottoms' (Fig. 3.9). Although it is uncertain whether specifically syn-depositional and/or post-mortem silicification was responsible for the silicification of the PBS, it is clear that at least one of these early processes was necessary to preserve the cyanobacterial structures at the PBS.

Following syn-depositional and/or early diagenetic silicification, other processes may have served to modify the preserved cyanobacterial sheaths. Ferruginous alteration of the stromatolites offers a viable mechanism for preservation of original cellular sheaths and could have been a secondary mechanism for facilitating enhanced silica precipitation. Stromatolites in lacustrine settings are able to form siderite ($FeCO_3$; as observed in Fig. 3.8), rather than calcite or aragonite ($CaCO_3$) or ankerite ($Ca(Fe,Mg)(CO_3)_2$), which could provide an internal source for iron in the system (Kremer et al., 2012). Diagenesis of the siderite can result in the formation of haematite (Roh & Moon, 2001; Roh et al., 2003), which has been preserved in the northernmost Perth Basin stromatolites (Blue Hills to Lookout; Olden et al., In Review). This reaction can be summarised as:

$$2FeCO_3 + H_2O \overset{Ox}{\rightarrow} Fe_2O_3 + H^+ + 2CO_2$$

In oxygenating conditions and in the presence of water, siderite forms haematite and carbonic acid, resulting in a decrease in pH of the system. As pH drops, the solubility of silica decreases resulting in precipitation, while the solubility of carbonate increases, leading to its dissolution (Scholle & Ulmer-Scholle, 2003; Schulz & White, 1999). Precipitation of silica in the cyanobacterial sheaths and intragranular space would likely increase the preservation potential of the filamentous cyanobacteria. The oxidation and subsequent drop in pH of the system would also impede the preservation of organic material within the system. As such, the ferruginous alteration and silicification of the stromatolites would have destroyed organic material of the cyanobacteria. As the whole stromatolitic sequence is not completely ferruginised, many settings still preserve silica-rich compositions and original pore spaces (e.g., at Isseka, Fig. 3.5). This makes it unlikely that diagenetic alteration of siderite into

haematite is the primary driver for the preservation of the cyanobacterial sheaths. However, stromatolites subjected to ferruginous alteration have a higher structural contrast than those without Fe infills (Fig. 3.2). The Fe oxides (along with original siderite) completely encompass the cyanobacterial sheaths and internal framework. Pervasive iron alteration would have negated secondary silicification associated with diagenesis, damaging the cyanobacterial microstructures.

Clay minerals within the PBS form post silicification, with most being euhedral in nature. The clay minerals seem to have no effect on the preservation of the cyanobacterial microstructures within the PBS.

5.3 Implications for stromatolite cellular preservation

Evidence for preservation of bacterial filaments have been found throughout the rock record, with the oldest sulphur-reducing variety dating back as far as 3.43 Ga (Riding, 1991a; 1991b; 2001; Wacey et al., 2011; Wacey et al., 2012). The first conclusive cyanobacteria within the fossil record dates back to 2450–2320 Ma (Brocks, Buick, Logan, & Summons, 2003; Brocks, Buick, Summons, & Logan, 2003; Brocks, Logan, Buick, & Summons, 1999; Hofmann, 1976b). Cyanobacterial biomarkers in the Gun Flint Chert, Western Australia, at ~2.7 Ga suggest that possibly even older cyanobacteria existed (Rasmussen, Fletcher, Brocks, & Kilburn, 2008). The cyanobacterial fossil record is known to be biased, as preservation favours those with large extracellular sheaths, which can be easily mineralised. In the Precambrian the most common style of preservation is via early diagenetic silicification, where silica mobilised during diagenesis forms thin chert bands and nodules in carbonate platforms (Knoll, 2008; Manning-Berg et al., 2019; Manning-Berg & Kah, 2017). During the Palaeozoic, and subsequently Mesozoic, early diagenetic silicification expanded to peritidal settings following the diversification of siliceous organisms (Manning-Berg & Kah, 2017). Although early diagenetic silicification is present throughout the fossil record, the preservation of individual cellular structures within filamentous sheaths is rare (Schirrmeister, Sanchez-Baracaldo, & Wacey, 2016). The Mid-Phanerozoic stromatolites from the northern Perth Basin lack thin chert bands and nodules, instead occurring as part of a siliciclastic sequence. The proposed model for preservation of the Perth Basin filamentous cyanobacterial sheaths (see section 5.2) follows a different model to what has been observed in Precambrian occurrences. The different mode of preservation of these Western Australian stromatolites to Precambrian examples opens up the possibility of looking in depositional environments (e.g., lacustrine) that were previously not thought to preserve cellular micro-structures (Wacey et al., 2018).

6 Conclusions

Detailed microanalysis of alveolate microstructures within the Perth Basin stromatolites from Western Australia has revealed that these likely represent fossilised remnants of filamentous cyanobacterial sheaths. These cyanobacterial sheaths are present throughout the whole stromatolite column and are conceivably the first recorded occurrence of such extensive fossilisation of cyanobacteria within a Mid-Phanerozoic stromatolitic community. The mechanisms behind this exceptional preservation are suggested to be twofold, with syn-depositional biogenic silicification and early diagenetic post-mortem preserving the cyanobacterial sheaths, and a secondary component of ferruginous alteration filling the internal framework, impeding secondary silicification that might otherwise have destroyed evidence of filamentous cyanobacteria. This compound method of preservation in fluvio-lacustrine settings has significant ramifications for bridging the gap between modern filamentous cyanobacteria and the Precambrian cellular fossil record. Mechanisms that induced the exceptional preservation of cyanobacterial sheaths could be used as a marker to search for cell microstructures in similar depositional settings under similar environmental conditions.

ACKNOWLEDGEMENTS

The authors would like to thank the Smithsonian National Museum of Natural History for preparation of thin sections. This research was undertaken using the Tescan Mira3 VP-FESEM at the John de Laeter Centre, Curtin University (ARC LE130100053) and the Tescan Lyra3 FIBSEM housed at the Advanced Resource Characterization Facility (ARCF). The ARCF is being developed under the auspices of the National Resource Sciences Precinct (NRSP) – a collaboration between CSIRO, Curtin University and The University of Western Australia – and is supported by the Science and Industry Endowment Fund (SIEF RI13-01). Special thanks is given to K. Grey for advice on stromatolite microstructures and edits of draft works. L.J.O. acknowledges the support of the Australian Government Research Training Program (RTP) Scholarship, GSA bursaries, and the Curtin University small grant scheme. D.F. acknowledges ARC funding DE190101307. The authors would like to thank L. Kah and two anonymous reviewers for constructive comments, and the editorial handling of K. Konhauser on an earlier draft.

REFERENCES

Awramik, S. M. (1992). The history and significance of stromatolites. In *Early Organic Evolution* (pp. 435-449): Springer.

Awramik, S. M., Margulis, L., & Barghoorn, E. S. (1976). .4 Evolutionary Processes in the Formation of Stromatolites. In *Developments in Sedimentology* (Vol. 20, pp. 149-162): Elsevier.

Awramik, S. M., & Sprinkle, J. (1999). Proterozoic stromatolites: the first marine evolutionary biota. *Historical Biology, 13*(4), 241-253.

Bain, R. J., & Kindler, P. (1994). Irregular fenestrae in Bahamian eolianites; a rainstorm-induced origin. *Journal of Sedimentary Research, 64*(1a), 140-146.

Bartley, J. K. (1996). Actualistic taphonomy of cyanobacteria: implications for the Precambrian fossil record. *Palaios*, 571-586.

Bertrand-Sarfati, J. (1976). .2 An Attempt to Classify Late Precambrian Stromatolite Microstructures. In *Developments in Sedimentology* (Vol. 20, pp. 251-259): Elsevier.

Bertrand-Sarfati, J., Freytet, P., & Plaziat, J. C. (1991). Microstructure and biogenic remains in non-marine stromatolites (Tertiary, France). Comparison with some Proterozoic stromatolites. *Phanerozoic Stromatolites II. Springer, Berlin*.

Blakey, R. C. (2008). Gondwana paleogeography from assembly to breakup—A 500 my odyssey. *Geological Society of America Special Papers, 441*, 1-28.

Bosak, T., Knoll, A. H., & Petroff, A. P. (2013). The meaning of stromatolites. *Annual Review of Earth and Planetary Sciences, 41*, 21-44.

Brocks, J. J., Buick, R., Logan, G. A., & Summons, R. E. (2003). Composition and syngeneity of molecular fossils from the 2.78 to 2.45 billion-year-old Mount Bruce Supergroup, Pilbara Craton, Western Australia. *Geochimica et Cosmochimica Acta, 67*(22), 4289-4319.

Brocks, J. J., Buick, R., Summons, R. E., & Logan, G. A. (2003). A reconstruction of Archean biological diversity based on molecular fossils from the 2.78 to 2.45 billion-year-old Mount Bruce Supergroup, Hamersley Basin, Western Australia. *Geochimica et Cosmochimica Acta, 67*(22), 4321-4335.

Brocks, J. J., Logan, G. A., Buick, R., & Summons, R. E. (1999). Archean molecular fossils and the early rise of eukaryotes. *Science, 285*(5430), 1033-1036.

Burne, R. V., & Moore, L. S. (1987). Microbialites: organosedimentary deposits of benthic microbial communities. *Palaios*, 241-254.

Butts, S. H., & Briggs, D. E. G. (2011). Silicification through time. In *Taphonomy* (pp. 411-434): Springer.

Casanova, J. (1986). East African rift stromatolites. *Geological Society, London, Special Publications, 25*(1), 201-210.

Casanova, J. (1994). Stromatolites from the East African Rift: a synopsis. In *Phanerozoic stromatolites II* (pp. 193-226): Springer.

Chen, Z.-Q., Wang, Y., Kershaw, S., Luo, M., Yang, H., Zhao, L., . . . Zhang, L. (2014). Early Triassic stromatolites in a siliciclastic nearshore setting in northern Perth Basin, Western Australia: Geobiologic features and implications for post-extinction microbial proliferation. *Global and Planetary Change, 121*, 89-100. doi:https://doi.org/10.1016/j.gloplacha.2014.07.004

Défarge, C., Trichet, J., & Coute, A. (1994). On the appearance of cyanobacterial calcification in modern stromatolites. *Sedimentary Geology, 94*(1-2), 11-19.

Djokic, T., Van Kranendonk, M. J., Campbell, K. A., Walter, M. R., & Ward, C. R. (2017). Earliest signs of life on land preserved in ca. 3.5 Ga hot spring deposits. *Nature communications, 8*, 15263.

Fantle, M. S., & Higgins, J. (2014). The effects of diagenesis and dolomitization on Ca and Mg isotopes in marine platform carbonates: implications for the geochemical cycles of Ca and Mg. *Geochimica et Cosmochimica Acta, 142*, 458-481.

Flügel, E. (2013). *Microfacies of carbonate rocks: analysis, interpretation and application*: Springer Science & Business Media.

Garrels, R. M. (1965). Silica: role in the buffering of natural waters. *Science, 148*(3666), 69-69.

Gong, J., Myers, K. D., Munoz-Saez, C., Homann, M., Rouillard, J., Wirth, R., . . . van Zuilen, M. A. (2019). Formation and Preservation of Microbial Palisade Fabric in Silica Deposits from El Tatio, Chile. *Astrobiology*.

Grey, K., & Awramik, S. M. (2020). *Handbook for the study and description of microbialites*: Geological Survey of Western Australia.

Grey, K., & Williams, I. R. (1990). Problematic bedding-plane markings from the Middle Proterozoic manganese subgroup, Bangemall Basin, Western Australia. *Precambrian Research, 46*(4), 307-327.

Hofmann, H. J. (1976). Precambrian microflora, Belcher Islands, Canada: significance and systematics. *Journal of Paleontology*, 1040-1073.

Hofmann, H. J. (2000). Archean stromatolites as microbial archives. In *Microbial sediments* (pp. 315-327): Springer.

Hofmann, H. J., Grey, K., Hickman, A. H., & Thorpe, R. I. (1999). Origin of 3.45 Ga coniform stromatolites in Warrawoona Group, Western Australia. *GSA*

Bulletin, 111(8), 1256-1262. doi:10.1130/0016-7606(1999)111<1256:OOGCSI>2.3.CO;2

Horodyski, R. J., Bauld, J., Lipps, J. H., & Mendelson, C. V. (1992). Preservation of prokaryotes and organic-walled and calcareous and siliceous protists. *The proterozoic biosphere*, 185-192.

Jahnert, R. J., & Collins, L. B. (2011). Significance of subtidal microbial deposits in Shark Bay, Australia. *Marine Geology, 286*(1-4), 106-111.

Javaux, E. J. (2019). Challenges in evidencing the earliest traces of life. *Nature, 572*(7770), 451-460.

Kershaw, S., & Cundy, A. (2013). *Oceanography: An earth science perspective*: Routledge.

Knoll, A. H. (1985). Exceptional preservation of photosynthetic organisms in silicified carbonates and silicified peats. *Philosophical Transactions of the Royal Society of London. B, Biological Sciences, 311*(1148), 111-122.

Knoll, A. H. (2008). Cyanobacteria and earth history. *The Cyanobacteria: Molecular Biology, Genomics, and Evolution, 484*.

Konhauser, K. O., Phoenix, V. R., Bottrell, S. H., Adams, D. G., & Head, I. M. (2001). Microbial–silica interactions in Icelandic hot spring sinter: possible analogues for some Precambrian siliceous stromatolites. *Sedimentology, 48*(2), 415-433.

Kremer, B., Kazmierczak, J., Łukomska-Kowalczyk, M., & Kempe, S. (2012). Calcification and silicification: fossilization potential of cyanobacteria from stromatolites of Niuafo ‘ou's Caldera Lakes (Tonga) and implications for the early fossil record. *Astrobiology, 12*(6), 535-548.

Ksienzyk, A. K., Jacobs, J., Boger, S. D., Košler, J., Sircombe, K. N., & Whitehouse, M. J. (2012). U–Pb ages of metamorphic monazite and detrital zircon from the Northampton Complex: evidence of two orogenic cycles in Western Australia. *Precambrian Research, 198*, 37-50.

Logan, B. W., Hoffman, P., & Gebelein, C. D. (1974). Algal mats, cryptalgal fabrics, and structures, Hamelin Pool, Western Australia.

Logan, B. W., Rezak, R., & Ginsburg, R. N. (1964). Classification and Environmental Significance of Algal Stromatolites. *The Journal of Geology, 72*(1), 68-83. doi:10.1086/626965

Manning-Berg, A. R., Wood, R. S., Williford, K. H., Czaja, A. D., & Kah, L. C. (2019). The taphonomy of proterozoic microbial mats and implications for early diagenetic silicification. *Geosciences, 9*(1), 40.

Manning-Berg, A. R., & Kah, L. C. (2017). Proterozoic microbial mats and their constraints on environments of silicification. *Geobiology, 15*(4), 469-483.

Martín-Algarra, A., & Sánchez-Navas, A. (1995). Phosphate stromatolites from condensed cephalopod limestones, Upper Jurassic, Southern Spain. *Sedimentology, 42*(6), 893-919.

Mory, A. J., Haig, D. W., McLoughlin, S., & Hocking, R. M. (2005). Geology of the Northern Perth Basin, Western Australia - A Field Guide. *Geological Society of Western Australia Record, 2005/09*, 1-58.

Oakey, R. J., Green, M., Carling, P. A., Lee, M. W. E., Sear, D. A., & Warburton, J. (2005). Grain-shape analysis—A new method for determining representative particle shapes for populations of natural grains. *Journal of Sedimentary Research, 75*(6), 1065-1073.

Oehler, D. Z., Robert, F., Walter, M. R., Sugitani, K., Allwood, A., Meibom, A., . . . Gibson, E. K. (2009). NanoSIMS: insights to biogenicity and syngeneity of Archaean carbonaceous structures. *Precambrian Research, 173*(1-4), 70-78.

Olden, L. J., Barham, M., Cunneen, J., Olierook, H. K. H., Suosaari, E., & Smith, G. (In Review). Microbialite forms and facies controls on stromatolite occurrences in the Perth Basin, Western Australia and their relationship to the end Permian mass extinction. *Australian Journal of Earth Sciences*.

Olden, L. J., Cunneen, J., Barham, M., Olierook, H. K. H., Smith, G., & Suosaari, E. (2019). Are stromatolites in the northern Perth Basin following the End Permian mass extinction? *ASEG Extended Abstracts, 2019*(1), 1-4.

Pemberton, S. G., & Frey, R. W. (1982). Trace fossil nomenclature and the Planolites-Palaeophycus dilemma. *Journal of Paleontology*, 843-881.

Playford, P. E. (1990). Geology of the Shark Bay area, Western Australia. *Research in Shark Bay: Report of the France-Australe Bicentenary Expedition Committee'.(Eds PF Berry, SD Bradshaw and BR Wilson.) pp*, 13-31.

Playford, P. E., Cockbain, A. E., Berry, P. F., Roberts, A. P., Haines, P. W., & Brooke, B. P. (2013). The Geology of Shark Bay. *Geological Survey of Western Australia Bulletin, 146*, 176-246.

Playford, P. E., Cockbain, A. E., & Low, G. H. (1976). Geology of the Perth Basin Western Australia. *Geological Survey of Western Australia Bulletin, 124*.

Rasmussen, B., Fletcher, I. R., Brocks, J. J., & Kilburn, M. R. (2008). Reassessing the first appearance of eukaryotes and cyanobacteria. *Nature, 455*(7216), 1101-1104.

Reid, R. P., Visscher, P. T., Decho, A. W., Stolz, J. F., Bebout, B. M., Dupraz, C., . . . DesMarais, D. J. (2000). The role of microbes in accretion, lamination and early lithification of modern marine stromatolites. *Nature, 406*, 989. doi:10.1038/35023158

Riding, R. (1991a). Calcified cyanobacteria. In *Calcareous algae and stromatolites* (pp. 55-87): Springer.

Riding, R. (1991b). Classification of microbial carbonates. In *Calcareous algae and stromatolites* (pp. 21-51): Springer.

Riding, R. (2001). Calcified algae and bacteria. *Ecology of the Cambrian Radiation. Columbia University Press, New York*, 445-473.

Riding, R. (2011). Microbialites, stromatolites, and thrombolites. *Encyclopedia of geobiology*, 635-654.

Rippka, R., Deruelles, J., Waterbury, J. B., Herdman, M., & Stanier, R. Y. (1979). Generic assignments, strain histories and properties of pure cultures of cyanobacteria. *Microbiology, 111*(1), 1-61.

Roh, Y., & Moon, H.-S. (2001). Iron reduction by a psychrotolerant Fe (III)-reducing bacterium isolated from ocean sediment. *Geosciences Journal, 5*(3), 183-190.

Roh, Y., Zhang, C. L., Vali, H., Lauf, R. J., Zhou, J., & Phelps, T. J. (2003). Biogeochemical and environmental factors in Fe biomineralization: magnetite and siderite formation. *Clays and Clay Minerals, 51*(1), 83-95.

Schirrmeister, B. E., Sanchez-Baracaldo, P., & Wacey, D. (2016). Cyanobacterial evolution during the Precambrian. *International Journal of Astrobiology, 15*(3), 187-204.

Scholle, P. A., & Ulmer-Scholle, D. (2003). Cements and cementation. In G. V. Middleton, M. J. Church, M. Coniglio, L. A. Hardie, & F. J. Longstaffe (Eds.), *Encyclopedia of Sediments and Sedimentary Rocks* (pp. 110-119). Dordrecht: Springer Netherlands.

Schopf, J. W. (2006). Fossil evidence of Archaean life. *Philosophical Transactions of the Royal Society B: Biological Sciences, 361*(1470), 869-885.

Schopf, J. W. (2012). The Fossil Record of Cyanobacteria. In B. A. Whitton (Ed.), *Ecology of Cyanobacteria II: Their Diversity in Space and Time* (pp. 15-36). Dordrecht: Springer Netherlands.

Schopf, J. W., Kudryavtsev, A. B., Agresti, D. G., Czaja, A. D., & Wdowiak, T. J. (2005). Raman imagery: a new approach to assess the geochemical maturity and biogenicity of permineralized Precambrian fossils. *Astrobiology, 5*(3), 333-371.

Schroeder, J. H. (1969). Experimental dissolution of calcium, magnesium, and strontium from recent biogenic carbonates: a model of diagenesis. *Journal of Sedimentary Research, 39*(3).

Schulz, M. S., & White, A. F. (1999). Chemical weathering in a tropical watershed, Luquillo Mountains, Puerto Rico III: quartz dissolution rates. *Geochimica et Cosmochimica Acta, 63*(3-4), 337-350.

Sezgin, M., & Sankur, B. (2004). Survey over image thresholding techniques and quantitative performance evaluation. *Journal of Electronic imaging, 13*(1), 146-166.

Suosaari, E. P., Reid, R. P., Playford, P. E., Foster, J. S., Stolz, J. F., Casaburi, G., . . . Eberli, G. P. (2016). New multi-scale perspectives on the stromatolites of Shark Bay, Western Australia. *Scientific Reports, 6*, 20557. doi:10.1038/srep20557

Trewin, N. H. (1993). Controls on fluvial deposition in mixed fluvial and aeolian facies within the Tumblagooda Sandstone (Late Silurian) of Western Australia. *Sedimentary Geology, 85*(1-4), 387-400.

Wacey, D. (2010). Stromatolites in the~ 3400 Ma Strelley Pool Formation, Western Australia: examining biogenicity from the macro-to the nano-scale. *Astrobiology, 10*(4), 381-395.

Wacey, D., Gleeson, D., & Kilburn, M. R. (2010). Microbialite taphonomy and biogenicity: new insights from NanoSIMS. *Geobiology, 8*(5), 403-416.

Wacey, D., Kilburn, M. R., Saunders, M., Cliff, J., & Brasier, M. D. (2011). Microfossils of sulphur-metabolizing cells in 3.4-billion-year-old rocks of Western Australia. *Nature Geoscience, 4*(10), 698.

Wacey, D., Menon, S., Green, L., Gerstmann, D., Kong, C., McLoughlin, N., . . . Brasier, M. (2012). Taphonomy of very ancient microfossils from the~ 3400 Ma Strelley Pool Formation and~ 1900 Ma Gunflint Formation: New insights using a focused ion beam. *Precambrian Research, 220*, 234-250.

Wacey, D., Urosevic, L., Saunders, M., & George, A. D. (2018). Mineralisation of filamentous cyanobacteria in Lake Thetis stromatolites, Western Australia. *Geobiology, 16*(2), 203-215.

Walls, R. A., Ragland, P. C., & Crisp, E. L. (1977). Experimental and natural early diagenetic mobility of Sr and Mg in biogenic carbonates. *Geochimica et Cosmochimica Acta, 41*(12), 1731-1737.

Chapter 4 THESIS CONCLUSIONS

Stromatolites from the northern Perth Basin, Western Australia, crop out over an area of 24 km^2, with several new major localities identified. Ten discrete morphological forms of stromatolite have been identified and described in detail. Stromatolite morphologies are shown to vary laterally and vertically throughout the field area. The intercalated nature of the stromatolites is interpreted to represent periods of depositional quiescence with contrasting periods of high energy resulting in the coarse grained siliciclastics and rip-up clasts of stromatolitic layers. Observed variation in stromatolite morphology is interpreted to result from fluctuating environmental conditions. It is suggested that the PBS formed in a restricted non-marine aquatic setting, rather than the previously suggested wave cut platform. The Early Triassic Kockatea shale onlaps directly onto the Perth Basin stromatolitic sequence, with a depositional hiatus at the boundary, decoupling the stromatolites from the biostratigraphical age constraints of the overlying shales. This thesis suggests that the PBS could tentatively be Guadalupian to Lopingian (Permian) in age. Despite the current ambiguity in age, the PBS is ultimately unlikely to be associated with the End Permian Mass Extinction event (EPME), rather forming due to favourable environmental conditions as is seen with modern microbialites.

The PBS stromatolites were found to preserve alveolate – cell like – microstructures throughout the field area. The alveolate microstructures are composed of a quartz mantle with a core preserving porosity or filled with primary siderite replaced by haematite. Due to extensive alteration and lack of original organic material in the PBS, typical methods of defining biogenicity were impractical. Biogenicity of the alveolate microstructures was assessed using chemical, morphological and size relationships to known biogenic and abiogenic microstructures. Alveolate microstructures are inferred to represent preserved skeletal filamentous cyanobacterial sheaths, with the cellular trichromes long since absent. Preservation of the cyanobacterial sheaths is primarily due to biogenic (*in vivo*) mineralisation and/or post-mortem silicification, following what is observed in modern microbialites from silica springs and caldera lakes. Historically, lithological units with little alteration have exhibited the highest preservation potential. This research suggests that units that have been heavily altered can still preserve biogenic structures, albeit without organic carbon. Proposed mechanisms of preservation can be used to identify palaeo-environmental settings that would be favourable for the preservation of cellular material and soft tissue, both of which are important for understanding the evolution of life.

Chapter 5 BIBLIOGRAPHY

Adachi, N., Asada, Y., Ezaki, Y., & Liu, J. (2017). Stromatolites near the Permian–Triassic boundary in Chongyang, Hubei Province, South China: A geobiological window into palaeo-oceanic fluctuations following the end-Permian extinction. *Palaeogeography, Palaeoclimatology, Palaeoecology, 475*, 55-69. doi:https://doi.org/10.1016/j.palaeo.2017.01.030

Allen, H., & Trinajstic, K. (2017). *An Early Devonian fish fauna from an unnamed sandstone in petroleum exploration well Wendy 1, northern Perth Basin*.

Angiolini, L., Carabelli, L., Nicora, A., Crasquin-Soleau, S., Marcoux, J., & Rettori, R. (2007). Brachiopods and other fossils from the Permo–Triassic boundary beds of the Antalya Nappes (SW Taurus, Turkey). *Geobios, 40*(6), 715-729.

Angiolini, L., Checconi, A., Gaetani, M., & Rettori, R. (2010). The latest Permian mass extinction in the Alborz Mountains (north Iran). *Geological Journal, 45*(2-3), 216-229.

Arenas-Abad, C., Vázquez-Urbez, M., Pardo-Tirapu, G., & Sancho-Marcén, C. (2010). Fluvial and associated carbonate deposits. *Developments in Sedimentology, 61*, 133-175.

Arp, G., Bielert, F., Hoffmann, V.-E., & Löffler, T. (2005). Palaeoenvironmental significance of lacustrine stromatolites of the Arnstadt Formation ("Steinmergelkeuper", Upper Triassic, N-Germany). *Facies, 51*(1-4), 419-441.

Australia, G. S. o. W. (Cartographer). (1971). 1:250 000 geological map - GERALDTON - HOUTMAN ABROLHOS (SH50-01 and part SH49-04), first edition

Awramik, S. M. (1992). The history and significance of stromatolites. In *Early Organic Evolution* (pp. 435-449): Springer.

Awramik, S. M., & Buchheim, H. P. (2015). Giant stromatolites of the Eocene Green River Formation (Colorado, USA). *Geology, 43*(8), 691-694.

Awramik, S. M., Margulis, L., & Barghoorn, E. S. (1976). .4 Evolutionary Processes in the Formation of Stromatolites. In *Developments in Sedimentology* (Vol. 20, pp. 149-162): Elsevier.

Awramik, S. M., & Sprinkle, J. (1999). Proterozoic stromatolites: the first marine evolutionary biota. *Historical Biology, 13*(4), 241-253.

Bain, R. J., & Kindler, P. (1994). Irregular fenestrae in Bahamian eolianites; a rainstorm-induced origin. *Journal of Sedimentary Research, 64*(1a), 140-146.

Bartley, J. K. (1996). Actualistic taphonomy of cyanobacteria: implications for the Precambrian fossil record. *Palaios*, 571-586.

Baud, A., Béchennec, F., Krystyn, L., Le Métour, J., Marcoux, J., Maury, R., & Richoz, S. (2001, 2001). *Permo-Triassic Deposits: from the Platform to the Basin and Seamounts. Conference on the Geology of Oman, Field guidebook, Excursion A01*.

Baud, A., & Bernecker, M. (2010, 2010). *The Permian-Triassic transition in the Oman mountains.* Paper presented at the IGCP.

Baud, A., Cirilli, S., & Marcoux, J. (1997). Biotic response to mass extinction: the lowermost Triassic microbialites. *Facies, 36*, 238-242.

Baud, A., Richoz, S., & Marcoux, J. (2005). Calcimicrobial cap rocks from the basal Triassic units: western Taurus occurrences (SW Turkey). *Comptes Rendus Palevol, 4*(6-7), 569-582.

Benvenuti, M. (2003). Facies analysis and tectonic significance of lacustrine fan-deltaic successions in the Pliocene–Pleistocene Mugello Basin, Central Italy. *Sedimentary Geology, 157*(3-4), 197-234.

Bertrand-Sarfati, J. (1976). .2 An Attempt to Classify Late Precambrian Stromatolite Microstructures. In *Developments in Sedimentology* (Vol. 20, pp. 251-259): Elsevier.

Bertrand-Sarfati, J., Freytet, P., & Plaziat, J. C. (1991). Microstructure and biogenic remains in non-marine stromatolites (Tertiary, France). Comparison with some Proterozoic stromatolites. *Phanerozoic Stromatolites II. Springer, Berlin*.

Blair, T. C., & McPherson, J. G. (1994). Alluvial fan processes and forms. In *Geomorphology of desert environments* (pp. 354-402): Springer.

Blakey, R. C. (2008). Gondwana paleogeography from assembly to breakup—A 500 my odyssey. *Geological Society of America Special Papers, 441*, 1-28.

Bosak, T., Knoll, A. H., & Petroff, A. P. (2013). The meaning of stromatolites. *Annual Review of Earth and Planetary Sciences, 41*, 21-44.

Brocks, J. J., Buick, R., Logan, G. A., & Summons, R. E. (2003). Composition and syngeneity of molecular fossils from the 2.78 to 2.45 billion-year-old Mount Bruce Supergroup, Pilbara Craton, Western Australia. *Geochimica et Cosmochimica Acta, 67*(22), 4289-4319.

Brocks, J. J., Buick, R., Summons, R. E., & Logan, G. A. (2003). A reconstruction of Archean biological diversity based on molecular fossils from the 2.78 to 2.45 billion-year-old Mount Bruce Supergroup, Hamersley Basin, Western Australia. *Geochimica et Cosmochimica Acta, 67*(22), 4321-4335.

Brocks, J. J., Logan, G. A., Buick, R., & Summons, R. E. (1999). Archean molecular fossils and the early rise of eukaryotes. *Science, 285*(5430), 1033-1036.

Buick, R. (1992). The antiquity of oxygenic photosynthesis: evidence from stromatolites in sulphate-deficient Archaean lakes. *Science, 255*(5040), 74-77.

Burgess, S. D., Bowring, S., & Shen, S.-z. (2014). High-precision timeline for Earth's most severe extinction. *Proceedings of the National Academy of Sciences, 111*(9), 3316-3321.

Burne, R. V., & Moore, L. S. (1987). Microbialites: organosedimentary deposits of benthic microbial communities. *Palaios*, 241-254.

Buser, S., Ramovš, A., & Turnšek, D. (1982). Triassic reefs in Slovenia. *Facies, 6*(1), 15-23.

Butts, S. H., & Briggs, D. E. G. (2011). Silicification through time. In *Taphonomy* (pp. 411-434): Springer.

Casanova, J. (1986). East African rift stromatolites. *Geological Society, London, Special Publications, 25*(1), 201-210.

Casanova, J. (1994). Stromatolites from the East African Rift: a synopsis. In *Phanerozoic stromatolites II* (pp. 193-226): Springer.

Cawood, P. A., & Nemchin, A. A. (2000). Provenance record of a rift basin: U/Pb ages of detrital zircons from the Perth Basin, Western Australia. *Sedimentary Geology, 134*(3-4), 209-234.

Chen, Z.-Q., & Benton, M. J. (2012). The timing and pattern of biotic recovery following the end-Permian mass extinction. *Nature Geoscience, 5*, 375. doi:10.1038/ngeo1475

https://www.nature.com/articles/ngeo1475#supplementary-information

Chen, Z.-Q., Fraiser, M. L., & Bolton, C. (2012). Early Triassic trace fossils from Gondwana Interior Sea: Implication for ecosystem recovery following the end-Permian mass extinction in south high-latitude region. *Gondwana Research, 22*(1), 238-255. doi:https://doi.org/10.1016/j.gr.2011.08.015

Chen, Z.-Q., Wang, Y., Kershaw, S., Luo, M., Yang, H., Zhao, L., . . . Zhang, L. (2014). Early Triassic stromatolites in a siliciclastic nearshore setting in northern Perth Basin, Western Australia: Geobiologic features and implications for post-extinction microbial proliferation. *Global and Planetary Change, 121*, 89-100. doi:https://doi.org/10.1016/j.gloplacha.2014.07.004

Chuvashov, B. I. (1983). Permian reefs of the Urals. *Facies, 8*(1), 191.

Clemmensen, L. B. (1978). Lacustrine facies and stromatolites from the Middle Triassic of East Greenland. *Journal of Sedimentary Research, 48*(4), 1111-1127.

Clemmensen, L. B., & Andreasen, F. (1977). Sedimentological observations in middle and late Triassic rocks, Jameson Land Basin, central East Greenland. In *Rapp. Grønlands Geol. Unders* (pp. 106-110).

Cloud, P. E., & Semikhatov, M. A. (1969). Proterozoic stromatolite zonation. *American Journal of Science, 267*(9), 1017-1061.

Courtillot, V., Jaupart, C., Manighetti, I., Tapponnier, P., & Besse, J. (1999). On causal links between flood basalts and continental breakup. *Earth and Planetary Science Letters, 166*(3), 177-195. doi:https://doi.org/10.1016/S0012-821X(98)00282-9

Cross, T. A., & Klosterman, M. J. (1981a). Autecology and development of a stromatolitic-bound phylloid algal bioherm, Laborcita Formation (Lower Permian), Sacramento Mountains, New Mexico, USA. In *Phanerozoic Stromatolites* (pp. 45-59): Springer.

Cross, T. A., & Klosterman, M. J. (1981b). Primary submarine cements and neomorphic spar in a stromatolitic-bound phylloid algal bioherm, Laborcita Formation (Wolfcampian), Sacramento Mountains, New Mexico, USA. In *Phanerozoic stromatolites* (pp. 60-73): Springer.

Défarge, C., Trichet, J., & Coute, A. (1994). On the appearance of cyanobacterial calcification in modern stromatolites. *Sedimentary Geology, 94*(1-2), 11-19.

Djokic, T., Van Kranendonk, M. J., Campbell, K. A., Walter, M. R., & Ward, C. R. (2017). Earliest signs of life on land preserved in ca. 3.5 Ga hot spring deposits. *Nature communications, 8*, 15263.

Elmore, R. D. (1983). Precambrian non-marine stromatolites in alluvial fan deposits, the Copper Harbor Conglomerate, upper Michigan. *Sedimentology, 30*(6), 829-842.

Erwin, D. H. (1994). The Permo-Triassic extinction. *Nature, 367*(6460), 231.

Escher, A., & Watt, W. S. (1976). *Geology of Greenland*: Geological Survey of Greenland.

Eyles, N., Mory, A. J., & Eyles, C. H. (2006). 50-Million-year-long record of glacial to postglacial marine environments preserved in a Carboniferous–Lower Permian graben, Northern Perth Basin, Western Australia. *Journal of Sedimentary Research, 76*(3), 618-632.

Ezaki, Y., Liu, J., & Adachi, N. (2003). Earliest Triassic microbialite micro-to megastructures in the Huaying area of Sichuan Province, South China:

implications for the nature of oceanic conditions after the end-Permian extinction. *Palaios, 18*(4-5), 388-402.

Ezaki, Y., Liu, J., Nagano, T., & Adachi, N. (2008). Geobiological aspects of the earliest Triassic microbialites along the southern periphery of the tropical Yangtze Platform: initiation and cessation of a microbial regime. *Palaios, 23*(6), 356-369.

Ezaki, Y., Liu, J. B., & Adachi, N. (2012). Lower Triassic stromatolites in Luodian County, Guizhou Province, South China: evidence for the protracted devastation of the marine environments. *Geobiology., 10*(1), 48-59.

Fang, Y., Chen, Z.-Q., Kershaw, S., Li, Y., & Luo, M. (2017a). An Early Triassic (Smithian) stromatolite associated with giant ooid banks from Lichuan (Hubei Province), South China: Environment and controls on its formation. *Palaeogeography, Palaeoclimatology, Palaeoecology, 486*, 108-122. doi:https://doi.org/10.1016/j.palaeo.2017.02.006

Fang, Y., Chen, Z.-Q., Kershaw, S., Yang, H., & Luo, M. (2017b). Permian–Triassic boundary microbialites at Zuodeng Section, Guangxi Province, South China: Geobiology and palaeoceanographic implications. *Global and Planetary Change, 152*, 115-128. doi:https://doi.org/10.1016/j.gloplacha.2017.02.011

Fannin, N. G. T. (1969). Stromatolites from the middle Old Red Sandstone of western Orkney. *Geological Magazine, 106*(1), 77-88.

Fantle, M. S., & Higgins, J. (2014). The effects of diagenesis and dolomitization on Ca and Mg isotopes in marine platform carbonates: implications for the geochemical cycles of Ca and Mg. *Geochimica et Cosmochimica Acta, 142*, 458-481.

Flügel, E. (2013). *Microfacies of carbonate rocks: analysis, interpretation and application*: Springer Science & Business Media.

Freytet, P., Kerp, H., & Broutin, J. (1996). Permian freshwater stromatolites associated with the conifer shoots Cassinisia orobica Kerp et al.—a very peculiar type of fossilization. *Review of Palaeobotany and Palynology, 91*(1-4), 85-105.

Freytet, P., Lebreton, M.-L., & Paquette, Y. (1992). The carbonates of the Permian lakes of North Massif Central, France. *Carbonates and Evaporites, 7*(2), 122.

Gaetani, M., Angiolini, L., Ueno, K., Nicora, A., Stephenson, M. H., Sciunnach, D., . . . Sabouri, J. (2009). Pennsylvanian–Early Triassic stratigraphy in the Alborz Mountains (Iran). *Geological Society, London, Special Publications, 312*(1), 79-128.

Garrels, R. M. (1965). Silica: role in the buffering of natural waters. *Science, 148*(3666), 69-69.

Garrett, P. (1970). Phanerozoic stromatolites: noncompetitive ecologic restriction by grazing and burrowing animals. *Science, 169*(3941), 171-173.

Gawthorpe, R. L., & Leeder, M. R. (2000). Tectono-sedimentary evolution of active extensional basins. *Basin Research, 12*(3-4), 195-218.

Gibbons, A. D., Whittaker, J. M., & Müller, R. D. (2013). The breakup of East Gondwana: Assimilating constraints from Cretaceous ocean basins around India into a best-fit tectonic model. *Journal of geophysical research: solid earth, 118*(3), 808-822.

Golubic, S. (1976). .2 Taxonomy of Extant Stromatolite-Building Cyanophytes. In *Developments in Sedimentology* (Vol. 20, pp. 127-140): Elsevier.

Gong, J., Myers, K. D., Munoz-Saez, C., Homann, M., Rouillard, J., Wirth, R., . . . van Zuilen, M. A. (2019). Formation and Preservation of Microbial Palisade Fabric in Silica Deposits from El Tatio, Chile. *Astrobiology*.

Gore, P. J. W. (1988). Paleoecology and sedimentology of a Late Triassic lake, Culpeper basin, Virginia, USA. *Palaeogeography, Palaeoclimatology, Palaeoecology, 62*(1-4), 593-608.

Gorter, J. D., Hearty, D. J., & Bond, A. J. (2004). Jurassic petroleum systems in the Houtman Sub-Basin, northwestern offshore Perth Basin, Western Australia: A frontier petroleum province on the doorstep? *The APPEA Journals*, 13-58. doi:https://doi.org/10.1071/AJ03001

Grasmück, K., & Trümpy, R. (1969). Triassic stratigraphy and general geology of the country around Fleming Fjord (East Greenland). *Meddelelser om Grønland, 168*(2), 3-76.

Grey, K., & Awramik, S. M. (2020). *Handbook for the study and description of microbialites*: Geological Survey of Western Australia.

Grey, K., & Williams, I. R. (1990). Problematic bedding-plane markings from the Middle Proterozoic manganese subgroup, Bangemall Basin, Western Australia. *Precambrian Research, 46*(4), 307-327.

Groves, J. R., & Calner, M. (2004, 2004). *Lower Triassic oolites in Tethys: a sedimentologic response to the end-Permian mass extinction*.

Groves, J. R., Rettori, R., Payne, J. L., Boyce, M. D., & Altiner, D. (2007). End-Permian mass extinction of lagenide foraminifers in the southern Alps (northern Italy). *Journal of Paleontology, 81*(3), 415-434.

Haig, D. W., Martin, S. K., Mory, A. J., McLoughlin, S., Backhouse, J., Berrell, R. W., . . . Bevan, J. C. (2015). Early Triassic (early Olenekian) life in the interior of East Gondwana: mixed marine–terrestrial biota from the Kockatea Shale, Western Australia. *Palaeogeography, Palaeoclimatology, Palaeoecology, 417*, 511-533. doi:https://doi.org/10.1016/j.palaeo.2014.10.015

Hallam, A., & Wignall, P. B. (1997). *Mass extinctions and their aftermath*: Oxford University Press, UK.

Hamilton, D. (1961). Algal growths in the Rhaetic Cotham Marble of southern England. *Palaeontology, 4*(3), 324-333.

Harries, P. J., Kauffman, E. G., & Hansen, T. A. (1996). Models for biotic survival following mass extinction. *Geological Society, London, Special Publications, 102*(1), 41-60.

Heydari, E., Hassandzadeh, J., & Wade, W. J. (2000). Geochemistry of central Tethyan upper Permian and lower Triassic strata, Abadeh region, Iran. *Sedimentary Geology, 137*(1-2), 85-99.

Hips, K., & Haas, J. (2006). Calcimicrobial stromatolites at the Permian–Triassic boundary in a western Tethyan section, Bükk Mountains, Hungary. *Sedimentary Geology, 185*(3-4), 239-253.

Hocking, R. M. (1991). *The Silurian Tumblagooda Sandstone, Western Australia* (Vol. 27): Geological Survey of Western Australia.

Hofmann, H. J. (1969). *Stromatolites from the Proterozoic Animikie and Sibley Groups, Ontario* (Vol. 68): Department of Energy, Mines and Resources.

Hofmann, H. J. (1976a). .2 Graphic Representation of Fossil Stromatoids; New Method with Improved Precision. In *Developments in Sedimentology* (Vol. 20, pp. 15-20): Elsevier.

Hofmann, H. J. (1976b). Precambrian microflora, Belcher Islands, Canada: significance and systematics. *Journal of Paleontology*, 1040-1073.

Hofmann, H. J. (2000). Archean stromatolites as microbial archives. In *Microbial sediments* (pp. 315-327): Springer.

Hofmann, H. J., Grey, K., Hickman, A. H., & Thorpe, R. I. (1999). Origin of 3.45 Ga coniform stromatolites in Warrawoona Group, Western Australia. *GSA Bulletin, 111*(8), 1256-1262. doi:10.1130/0016-7606(1999)111<1256:OOGCSI>2.3.CO;2

Horodyski, R. J. (1977). Environmental influences on columnar stromatolite branching patterns: examples from the Middle Proterozoic Belt Supergroup, Glacier National Park, Montana. *Journal of Paleontology*, 661-671.

Horodyski, R. J., Bauld, J., Lipps, J. H., & Mendelson, C. V. (1992). Preservation of prokaryotes and organic-walled and calcareous and siliceous protists. *The proterozoic biosphere*, 185-192.

Huang, Y., Tong, J., & Fraiser, M. L. (2018). A Griesbachian (Early Triassic) Mollusc Fauna from the Sidazhai Section, Southwest China, with Paleoecological

Insights on the Proliferation of Genus Claraia (Bivalvia). *Journal of Earth Science, 29*(4), 794-805.

Insalaco, E., Virgone, A., Courme, B., Gaillot, J., Kamali, M., Moallemi, A., . . . Monibi, S. (2006). Upper Dalan Member and Kangan Formation between the Zagros Mountains and offshore Fars, Iran: depositional system, biostratigraphy and stratigraphic architecture. *GeoArabia, 11*(2), 75-176.

Jahnert, R. J., & Collins, L. B. (2011). Significance of subtidal microbial deposits in Shark Bay, Australia. *Marine Geology, 286*(1-4), 106-111.

Javaux, E. J. (2019). Challenges in evidencing the earliest traces of life. *Nature, 572*(7770), 451-460.

Kalkowsky, E. (1908). Oolith und Stromatolith im norddeutschen Buntsandstein. *Zeitschrift der deutschen geologischen Gesellschaft*, 68-125.

Keller, G. (2005). Impacts, volcanism and mass extinction: random coincidence or cause and effect? *Australian Journal of Earth Sciences, 52*(4-5), 725-757. doi:10.1080/08120090500170393

Kerp, H., Penati, F., Brambilla, G., Clement-Westerhof, J. A., & van Bergen, P. F. (1996). Aspects of Permian palaeobotany and palynology. XVI. Three-dimensionally preserved stromatolite-incrusted conifers from the Permian of the western Orobic Alps (northern Italy). *Review of Palaeobotany and Palynology, 91*(1-4), 63-84.

Kershaw, S., Crasquin, S., Collin, P.-Y., Li, Y., Feng, Q., & Forel, M. B. (2009). Microbialites as disaster forms in anachronistic facies following the end-Permian mass extinction: a discussion. *Australian Journal of Earth Sciences, 56*(6), 809-813.

Kershaw, S., Crasquin, S., Forel, M. B., Randon, C., Collin, P. Y., Kosun, E., . . . Baud, A. (2011). Earliest Triassic microbialites in Çürük Dag, southern Turkey: composition, sequences and controls on formation. *Sedimentology, 58*(3), 739-755.

Kershaw, S., Crasquin, S., Li, Y., Collin, P. Y., Forel, M. B., Mu, X., . . . Guo, L. (2012). Microbialites and global environmental change across the Permian-Triassic boundary: a synthesis. *Geobiology., 10*(1), 25-47.

Kershaw, S., & Cundy, A. (2013). *Oceanography: An earth science perspective*: Routledge.

Kershaw, S., Guo, L., Swift, A., & Fan, J. (2002). ? Microbialites in the Permian-Triassic boundary interval in central China: Structure, age and distribution. *Facies, 47*(1), 83-89.

Kershaw, S., Li, Y., Crasquin-Soleau, S., Feng, Q., Mu, X., Collin, P.-Y., . . . Guo, L. (2007). Earliest Triassic microbialites in the South China block and other areas: controls on their growth and distribution. *Facies, 53*(3), 409-425.

Kershaw, S., Zhang, T., & Lan, G. (1999). A? microbialite carbonate crust at the Permian–Triassic boundary in South China, and its palaeoenvironmental significance. *Palaeogeography, Palaeoclimatology, Palaeoecology, 146*(1-4), 1-18.

Knoll, A. H. (1985). Exceptional preservation of photosynthetic organisms in silicified carbonates and silicified peats. *Philosophical Transactions of the Royal Society of London. B, Biological Sciences, 311*(1148), 111-122.

Knoll, A. H. (2008). Cyanobacteria and earth history. *The Cyanobacteria: Molecular Biology, Genomics, and Evolution, 484*.

Konhauser, K. O., Phoenix, V. R., Bottrell, S. H., Adams, D. G., & Head, I. M. (2001). Microbial–silica interactions in Icelandic hot spring sinter: possible analogues for some Precambrian siliceous stromatolites. *Sedimentology, 48*(2), 415-433.

Kremer, B., Kazmierczak, J., Łukomska-Kowalczyk, M., & Kempe, S. (2012). Calcification and silicification: fossilization potential of cyanobacteria from stromatolites of Niuafo ‘ou's Caldera Lakes (Tonga) and implications for the early fossil record. *Astrobiology, 12*(6), 535-548.

Ksienzyk, A. K., Jacobs, J., Boger, S. D., Košler, J., Sircombe, K. N., & Whitehouse, M. J. (2012). U–Pb ages of metamorphic monazite and detrital zircon from the Northampton Complex: evidence of two orogenic cycles in Western Australia. *Precambrian Research, 198*, 37-50.

Lehrmann, D. J. (1999). Early Triassic calcimicrobial mounds and biostromes of the Nanpanjiang basin, south China. *Geology, 27*(4), 359-362.

Lehrmann, D. J., Payne, J. L., Felix, S. V., Dillett, P. M., Wang, H., Yu, Y., & Wei, J. (2003). Permian–Triassic boundary sections from shallow-marine carbonate platforms of the Nanpanjiang Basin, South China: implications for oceanic conditions associated with the end-Permian extinction and its aftermath. *Palaios, 18*(2), 138-152.

Link, M. H., & Osborne, R. H. (1978). Lacustrine facies in the Pliocene Ridge Basin Group: Ridge Basin, California. *Modern and Ancient Lake Sediments, Spec. Publ, 2*, 169-187.

Link, M. H., Osborne, R. H., & Awramik, S. M. (1978). Lacustrine stromatolites and associated sediments of the Pliocene ridge Route Formation, Ridge Basin, California. *Journal of Sedimentary Research, 48*(1), 143-157.

Logan, B. W., Hoffman, P., & Gebelein, C. D. (1974). Algal mats, cryptalgal fabrics, and structures, Hamelin Pool, Western Australia.

Logan, B. W., Rezak, R., & Ginsburg, R. N. (1964). Classification and Environmental Significance of Algal Stromatolites. *The Journal of Geology, 72*(1), 68-83. doi:10.1086/626965

Luo, M., Chen, Z.-Q., Shi, G. R., Fang, Y., Song, H., Jia, Z., . . . Yang, H. (2016). Upper Lower Triassic stromatolite from Anhui, South China: Geobiologic features and paleoenvironmental implications. *Palaeogeography, Palaeoclimatology, Palaeoecology, 452*, 40-54. doi:https://doi.org/10.1016/j.palaeo.2016.04.008

Luo, M., Chen, Z.-Q., Shi, G. R., Feng, X., Yang, H., Fang, Y., & Li, Y. (2019). Microbially induced sedimentary structures (MISSs) from the Lower Triassic Kockatea Formation, northern Perth Basin, Western Australia: Palaeoenvironmental implications. *Palaeogeography, Palaeoclimatology, Palaeoecology, 519*, 236-247.

Luo, M., Chen, Z.-Q., Zhao, L., Kershaw, S., Huang, J., Wu, L., . . . Jia, Z. (2014). Early Middle Triassic stromatolites from the Luoping area, Yunnan Province, Southwest China: Geobiologic features and environmental implications. *Palaeogeography, Palaeoclimatology, Palaeoecology, 412*, 124-140. doi:https://doi.org/10.1016/j.palaeo.2014.07.028

Manning-Berg, A. R., Wood, R. S., Williford, K. H., Czaja, A. D., & Kah, L. C. (2019). The taphonomy of proterozoic microbial mats and implications for early diagenetic silicification. *Geosciences, 9*(1), 40.

Manning-Berg, A. R., & Kah, L. C. (2017). Proterozoic microbial mats and their constraints on environments of silicification. *Geobiology, 15*(4), 469-483.

Marenco, P. J., Griffin, J. M., Fraiser, M. L., & Clapham, M. E. (2012). Paleoecology and geochemistry of Early Triassic (Spathian) microbial mounds and implications for anoxia following the end-Permian mass extinction. *Geology, 40*(8), 715-718.

Markwitz, V., Kirkland, C. L., Wyrwoll, K. H., Hancock, E. A., Evans, N. J., & Lu, Y. (2017). Variations in zircon provenance constrain age and geometry of an Early Paleozoic rift in the Pinjarra Orogen, East Gondwana. *Tectonics, 36*(11), 2477-2496.

Martín-Algarra, A., & Sánchez-Navas, A. (1995). Phosphate stromatolites from condensed cephalopod limestones, Upper Jurassic, Southern Spain. *Sedimentology, 42*(6), 893-919.

Mary, M., & Woods, A. D. (2008). Stromatolites of the Lower Triassic Union Wash Formation, CA: evidence for continued post-extinction environmental stress in western North America through the Spathian. *Palaeogeography, Palaeoclimatology, Palaeoecology, 261*(1-2), 78-86.

Mastandrea, A., Perri, E., Russo, F., Spadafora, A., & Tucker, M. (2006). Microbial primary dolomite from a Norian carbonate platform: northern Calabria, southern Italy. *Sedimentology, 53*(3), 465-480.

Maurer, F., Martini, R., Rettori, R., Hillgärtner, H., & Cirilli, S. (2009). The geology of Khuff outcrop analogues in the Musandam Peninsula, United Arab Emirates and Oman. *GeoArabia, 14*(3), 125-158.

Mayall, M. J., & Wright, V. P. (1981). Algal tuft structures in stromatolites from the Upper Triassic of south-west England. *Palaeontology, 24*(3), 655-660.

Metcalfe, I., Nicoll, R. S., & Willink, R. J. (2008). Conodonts from the Permian–Triassic transition in Australia and position of the Permian–Triassic boundary. *Australian Journal of Earth Sciences, 55*(3), 365-377. doi:10.1080/08120090701769480

Miall, A. D., & Postma, G. (1997). The Geology of Fluvial Deposits, Sedimentary Facies, Basin Analysis and Petroleum Geology. *Sedimentary Geology, 110*(1), 149.

Monty, C. L. V. (1976). .1 The Origin and Development of Cryptalgal Fabrics. In *Developments in Sedimentology* (Vol. 20, pp. 193-249): Elsevier.

Mory, A., & Iasky, R. (1994). *Structural evolution of the onshore northern Perth Basin, Western Australia*.

Mory, A. J., Haig, D. W., McLoughlin, S., & Hocking, R. M. (2005). Geology of the Northern Perth Basin, Western Australia - A Field Guide. *Geological Society of Western Australia Record, 2005/09*, 1-58.

Mory, A. J., & Iasky, R. P. (1996). Stratigraphic and structure of the onshore Northern Perth Basin, Western Australia. *46*, 1-101.

Mory, A. J., Iasky, R. P., & Ghori, K. A. R. (2003). A summary of the geological evolution and petroleum potential of the Southern Carnarvon Basin, Western Australia. *Geological Survey of Western Australia Report, 86*, 1-26.

Mory, A. J., Redfern, J., & Martin, J. R. (2008). A review of Permian–Carboniferous glacial deposits in Western Australia. *Geological Society of America Special Papers, 441*, 29-40.

Newell, N. D. (1955). Depositional fabric in Permian reef limestones. *The Journal of Geology, 63*(4), 301-309.

Noffke, N., Gerdes, G., Klenke, T., & Krumbein, W. E. (2001). Microbially induced sedimentary structures: a new category within the classification of primary sedimentary structures. *Journal of Sedimentary Research, 71*(5), 649-656.

Norvick, M. S. (2004). Tectonic and Stratigraphic History of the Perth Basin. Record 2004/16. *Geoscience Australia Record, 2004/16*, 1-18.

Nutman, A. P., Bennett, V. C., Friend, C. R. L., Van Kranendonk, M. J., & Chivas, A. R. (2016). Rapid emergence of life shown by discovery of 3,700-million-year-old microbial structures. *Nature, 537*(7621), 535.

Oakey, R. J., Green, M., Carling, P. A., Lee, M. W. E., Sear, D. A., & Warburton, J. (2005). Grain-shape analysis—A new method for determining representative particle shapes for populations of natural grains. *Journal of Sedimentary Research, 75*(6), 1065-1073.

Oehler, D. Z., Robert, F., Walter, M. R., Sugitani, K., Allwood, A., Meibom, A., . . . Gibson, E. K. (2009). NanoSIMS: insights to biogenicity and syngeneity of Archaean carbonaceous structures. *Precambrian Research, 173*(1-4), 70-78.

Olden, L. J., Barham, M., Cunneen, J., Olierook, H. K. H., Suosaari, E., & Smith, G. (In Review). Microbialite forms and facies controls on stromatolite occurrences in the Perth Basin, Western Australia and their relationship to the end Permian mass extinction. *Australian Journal of Earth Sciences*.

Olden, L. J., Cunneen, J., Barham, M., Olierook, H. K. H., Smith, G., & Suosaari, E. (2019). Are stromatolites in the northern Perth Basin following the End Permian mass extinction? *ASEG Extended Abstracts, 2019*(1), 1-4.

Olierook, H. K. H., Barham, M., Fitzsimons, I. C. W., Timms, N. E., Jiang, Q., Evans, N. J., & McDonald, B. J. (2019a). Tectonic controls on sediment provenance evolution in rift basins: Detrital zircon U–Pb and Hf isotope analysis from the Perth Basin, Western Australia. *Gondwana Research, 66*, 126-142.

Olierook, H. K. H., Jiang, Q., Jourdan, F., & Chiaradia, M. (2019b). Greater Kerguelen large igneous province reveals no role for Kerguelen mantle plume in the continental breakup of eastern Gondwana. *Earth and Planetary Science Letters, 511*, 244-255.

Olierook, H. K. H., Jourdan, F., Merle, R. E., Timms, N. E., Kusznir, N., & Muhling, J. R. (2016). Bunbury Basalt: Gondwana breakup products or earliest vestiges of the Kerguelen mantle plume? *Earth and Planetary Science Letters, 440*, 20-32. doi:https://doi.org/10.1016/j.epsl.2016.02.008

Olierook, H. K. H., Timms, N. E., Wellmann, J. F., Corbel, S., & Wilkes, P. G. (2015). 3D structural and stratigraphic model of the Perth Basin, Western Australia: Implications for sub-basin evolution. *Australian Journal of Earth Sciences, 62*(4), 447-467.

Paul, J., & Peryt, T. M. (2000). Kalkowsky's stromatolites revisited (Lower Triassic Buntsandstein, Harz Mountains, Germany). *Palaeogeography, Palaeoclimatology, Palaeoecology, 161*(3-4), 435-458.

Pemberton, S. G., & Frey, R. W. (1982). Trace fossil nomenclature and the Planolites-Palaeophycus dilemma. *Journal of Paleontology*, 843-881.

Perch-Nielsen, K., Birkenmajer, K., Birkelund, T., & Aellen, M. (1974). Revision of Triassic stratigraphy of the Scoresby Land an d Jameson Land region, east Greenland. *Meddelelser om Gronland*.

Perch-Nielsen, K., Bromley, R. G., Birkenmajer, K., & Aellen, M. (1972). Field observations in Palaeozoic and Mesozoic sediments of Scoresby Land and northern Jameson Land. *Danmarks Og Grønlands Geologiske Undersøgelse, Rapport*(48), 39-59.

Perri, E., Mastandrea, A., Neri, C., & Russo, F. (2003). A micrite-dominated Norian carbonate platform from Northern Calabria (Southern Italy). *Facies, 49*(1), 101-118.

Perri, E., & Tucker, M. (2007). Bacterial fossils and microbial dolomite in Triassic stromatolites. *Geology, 35*(3), 207-210.

Peryt, T. M. (1975). Significance of stromatolites for the environmental interpretation of the Buntsandstein (Lower Triassic) rocks. *Geologische Rundschau, 64*(1), 143-158.

Peryt, T. M., & Piatkowski, T. S. (1977). Stromatolites from the Zechstein Limestone (Upper Permian) of Poland. In *Fossil Algae* (pp. 124-135): Springer.

Playford, P. E. (1990). Geology of the Shark Bay area, Western Australia. *Research in Shark Bay: Report of the France-Australe Bicentenary Expedition Committee'.(Eds PF Berry, SD Bradshaw and BR Wilson.) pp*, 13-31.

Playford, P. E., Cockbain, A. E., Berry, P. F., Roberts, A. P., Haines, P. W., & Brooke, B. P. (2013). The Geology of Shark Bay. *Geological Survey of Western Australia Bulletin, 146*, 176-246.

Playford, P. E., Cockbain, A. E., & Low, G. H. (1976). Geology of the Perth Basin Western Australia. *Geological Survey of Western Australia Bulletin, 124*.

Pollard, J. E., Steel, R. J., & Undersrud, E. (1982). Facies sequences and trace fossils in lacustrine/fan delta deposits, Hornelen Basin (M. Devonian), western Norway. *Sedimentary Geology, 32*(1-2), 63-87.

Preiss, W. V. (1976). .1 Basic Field and Laboratory Methods for the Study of Stromatolites. In *Developments in Sedimentology* (Vol. 20, pp. 5-13): Elsevier.

Pruss, S. B., & Bottjer, D. J. (2004). Late Early Triassic microbial reefs of the western United States: a description and model for their deposition in the aftermath of the end-Permian mass extinction. *Palaeogeography, Palaeoclimatology, Palaeoecology, 211*(1-2), 127-137.

Pruss, S. B., Bottjer, D. J., Corsetti, F. A., & Baud, A. (2006). A global marine sedimentary response to the end-Permian mass extinction: examples from southern Turkey and the western United States. *Earth-Science Reviews, 78*(3-4), 193-206.

Rasmussen, B., Fletcher, I. R., Brocks, J. J., & Kilburn, M. R. (2008). Reassessing the first appearance of eukaryotes and cyanobacteria. *Nature, 455*(7216), 1101-1104.

Reid, R. P., Visscher, P. T., Decho, A. W., Stolz, J. F., Bebout, B. M., Dupraz, C., . . . DesMarais, D. J. (2000). The role of microbes in accretion, lamination and early lithification of modern marine stromatolites. *Nature, 406*, 989. doi:10.1038/35023158

Richoz, S., Baud, A., Krystyn, L., Twitchett, R., & Marcoux, J. (2005). Permo-Triassic deposits of the Oman Mountains: from basin and slope to the shallow platform.

Richoz, S., Krystyn, L., Baud, A., Brandner, R., Horacek, M., & Mohtat-Aghai, P. (2010). Permian–Triassic boundary interval in the Middle East (Iran and N. Oman): Progressive environmental change from detailed carbonate carbon isotope marine curve and sedimentary evolution. *Journal of Asian Earth Sciences, 39*(4), 236-253.

Riding, R. (1991a). Calcified cyanobacteria. In *Calcareous algae and stromatolites* (pp. 55-87): Springer.

Riding, R. (1991b). Classification of microbial carbonates. In *Calcareous algae and stromatolites* (pp. 21-51): Springer.

Riding, R. (2000). Microbial carbonates: the geological record of calcified bacterial–algal mats and biofilms. *Sedimentology, 47*, 179-214.

Riding, R. (2001). Calcified algae and bacteria. *Ecology of the Cambrian Radiation. Columbia University Press, New York*, 445-473.

Riding, R. (2011). Microbialites, stromatolites, and thrombolites. *Encyclopedia of geobiology*, 635-654.

Rippka, R., Deruelles, J., Waterbury, J. B., Herdman, M., & Stanier, R. Y. (1979). Generic assignments, strain histories and properties of pure cultures of cyanobacteria. *Microbiology, 111*(1), 1-61.

Roh, Y., & Moon, H.-S. (2001). Iron reduction by a psychrotolerant Fe (III)-reducing bacterium isolated from ocean sediment. *Geosciences Journal, 5*(3), 183-190.

Roh, Y., Zhang, C. L., Vali, H., Lauf, R. J., Zhou, J., & Phelps, T. J. (2003). Biogeochemical and environmental factors in Fe biomineralization: magnetite and siderite formation. *Clays and Clay Minerals, 51*(1), 83-95.

Ross, C. A., & Ross, J. R. P. (1987). Late Paleozoic sea levels and depositional sequences. *Cushman Foundation for Foraminiferal Research*, 137.

Sano, H., & Nakashima, K. (1997). Lowermost Triassic (Griesbachian) microbial bindstone-cementstone facies, southwest Japan. *Facies, 36*(1), 1-24.

Schäfer, A., & Stapf, K. R. G. (1978). Permian Saar-Nahe Basin and recent Lake Constance (Germany): two environments of lacustrine algal carbonates. *Modern and ancient lake sediments*, 83-107.

Schirrmeister, B. E., Sanchez-Baracaldo, P., & Wacey, D. (2016). Cyanobacterial evolution during the Precambrian. *International Journal of Astrobiology, 15*(3), 187-204.

Scholle, P. A., & Ulmer-Scholle, D. (2003). Cements and cementation. In G. V. Middleton, M. J. Church, M. Coniglio, L. A. Hardie, & F. J. Longstaffe (Eds.), *Encyclopedia of Sediments and Sedimentary Rocks* (pp. 110-119). Dordrecht: Springer Netherlands.

Schopf, J. W. (2006). Fossil evidence of Archaean life. *Philosophical Transactions of the Royal Society B: Biological Sciences, 361*(1470), 869-885.

Schopf, J. W. (2012). The Fossil Record of Cyanobacteria. In B. A. Whitton (Ed.), *Ecology of Cyanobacteria II: Their Diversity in Space and Time* (pp. 15-36). Dordrecht: Springer Netherlands.

Schopf, J. W., Kudryavtsev, A. B., Agresti, D. G., Czaja, A. D., & Wdowiak, T. J. (2005). Raman imagery: a new approach to assess the geochemical maturity and biogenicity of permineralized Precambrian fossils. *Astrobiology, 5*(3), 333-371.

Schroeder, J. H. (1969). Experimental dissolution of calcium, magnesium, and strontium from recent biogenic carbonates: a model of diagenesis. *Journal of Sedimentary Research, 39*(3).

Schubert, J. K., & Bottjer, D. J. (1992). Early Triassic stromatolites as post-mass extinction disaster forms. *Geology, 20*(10), 883-886. doi:10.1130/0091-7613(1992)020<0883:ETSAPM>2.3.CO;2

Schulz, M. S., & White, A. F. (1999). Chemical weathering in a tropical watershed, Luquillo Mountains, Puerto Rico III: quartz dissolution rates. *Geochimica et Cosmochimica Acta, 63*(3-4), 337-350.

Sezgin, M., & Sankur, B. (2004). Survey over image thresholding techniques and quantitative performance evaluation. *Journal of Electronic imaging, 13*(1), 146-166.

Shapiro, R. S., & West, R. R. (1999). Late Paleozoic stromatolites: new insights from the Lower Permian of Kansas. *Lethaia, 32*(2), 131-139.

Shen, J., Algeo, T. J., Zhou, L., Feng, Q., Yu, J., & Ellwood, B. (2012). Volcanic perturbations of the marine environment in South China preceding the latest Permian mass extinction and their biotic effects. *Geobiology., 10*(1), 82-103.

Smith, A., Cooper, A., Misra, S., Bharuth, V., Guastella, L., & Botes, R. (2018). The extant shore platform stromatolite (SPS) facies association: a glimpse into the Archean? *Biogeosciences, 15*(7), 2189-2203.

Smith, A. M., Andrews, J. E., Uken, R., Thackeray, Z., Perissinotto, R., Leuci, R., & Marca-Bell, A. (2011). Rock pool tufa stromatolites on a modern South African wave-cut platform: partial analogues for Archaean stromatolites? *Terra Nova, 23*(6), 375-381.

Song, T., & Cawood, P. A. (2000). Structural styles in the Perth Basin associated with the Mesozoic break-up of Greater India and Australia. *Tectonophysics, 317*(1), 55 - 72. doi:https://doi.org/10.1016/S0040-1951(99)00273-5

Suosaari, E. P., Reid, R. P., Oehlert, A. M., Playford, P. E., Steffensen, C. K., Andres, M. S., . . . Eberli, G. P. (2019). Stromatolite Provinces of Hamelin Pool: Physiographic Controls On Stromatolites and Associated Lithofacies. *Journal of Sedimentary Research, 89*(3), 207-226.

Suosaari, E. P., Reid, R. P., Playford, P. E., Foster, J. S., Stolz, J. F., Casaburi, G., . . . Eberli, G. P. (2016). New multi-scale perspectives on the stromatolites of Shark Bay, Western Australia. *Scientific Reports, 6*, 20557. doi:10.1038/srep20557

Surdam, R. C., & Wray, J. L. (1976). .3 Lacustrine Stromatolites, Eocene Green River Formation, Wyoming. In *Developments in Sedimentology* (Vol. 20, pp. 535-541): Elsevier.

Szulc, J., & Cwizewicz, M. (1989). The Lower Permian freshwater carbonates of the Slawkow graben, southern Poland: Sedimentary facies context and stable isotope study. *Palaeogeography, Palaeoclimatology, Palaeoecology, 70*(1-3), 107-120.

Tałanda, M., Bajdek, P., Niedźwiedzki, G., & Sulej, T. (2017). Upper Triassic freshwater oncoids from Silesia (southern Poland) and their microfossil biota. *Neues Jahrbuch für Geologie und Paläontologie-Abhandlungen, 284*(1), 43-56.

Taraz, H., Golshani, F., Nakazawa, K., Shimizu, D., Bando, Y., Ishii, K.-i., . . . Nakamura, K. (1981). The Permian and the Lower Triassic systems in Abadeh region, central Iran.

Thomas, B. M., & Barber, C. J. (2004). A re-evaluation of the hydrocarbon habitat of the Northern Perth Basin. *The APPEA Journals, 44*(1), 59-92. doi:https://doi.org/10.1071/AJ03002

Thomas, B. M., Willink, R. J., Grice, K., Twitchett, R. J., Purcell, R. R., Archbold, N. W., . . . Barber, C. J. (2004). Unique marine Permian-Triassic boundary section from Western Australia. *Australian Journal of Earth Sciences, 51*(3), 423-430.

Thomas, C. M. (2014). The Tectonic Framework of the Perth Basin: Current understanding. *14*, 1-36.

Trewin, N. H. (1993). Controls on fluvial deposition in mixed fluvial and aeolian facies within the Tumblagooda Sandstone (Late Silurian) of Western Australia. *Sedimentary Geology, 85*(1-4), 387-400.

Trewin, N. H., & McNamara, K. J. (1994). Arthropods invade the land: trace fossils and palaeoenvironments of the Tumblagooda Sandstone (? late Silurian) of Kalbarri, Western Australia. *Earth and Environmental Science Transactions of The Royal Society of Edinburgh, 85*(3), 177-210.

Tucker, M. E. (1978). Triassic Lacustrine Sediments from South Wales: Shore-Zone, Evaporites and Carbonates. *Modern and ancient lake sediments*, 205-224.

Von der Borch, C. C., Bolton, B., & Warren, J. K. (1977). Environmental setting and microstructure of subfossil lithified stromatolites associated with evaporites, Marion Lake, South Australia. *Sedimentology, 24*(5), 693-708.

Wacey, D. (2010). Stromatolites in the~ 3400 Ma Strelley Pool Formation, Western Australia: examining biogenicity from the macro-to the nano-scale. *Astrobiology, 10*(4), 381-395.

Wacey, D., Gleeson, D., & Kilburn, M. R. (2010). Microbialite taphonomy and biogenicity: new insights from NanoSIMS. *Geobiology, 8*(5), 403-416.

Wacey, D., Kilburn, M. R., Saunders, M., Cliff, J., & Brasier, M. D. (2011). Microfossils of sulphur-metabolizing cells in 3.4-billion-year-old rocks of Western Australia. *Nature Geoscience, 4*(10), 698.

Wacey, D., Menon, S., Green, L., Gerstmann, D., Kong, C., McLoughlin, N., . . . Brasier, M. (2012). Taphonomy of very ancient microfossils from the~ 3400 Ma Strelley Pool Formation and~ 1900 Ma Gunflint Formation: New insights using a focused ion beam. *Precambrian Research, 220*, 234-250.

Wacey, D., Urosevic, L., Saunders, M., & George, A. D. (2018). Mineralisation of filamentous cyanobacteria in Lake Thetis stromatolites, Western Australia. *Geobiology, 16*(2), 203-215.

Walls, R. A., Ragland, P. C., & Crisp, E. L. (1977). Experimental and natural early diagenetic mobility of Sr and Mg in biogenic carbonates. *Geochimica et Cosmochimica Acta, 41*(12), 1731-1737.

Walter, M. R. (1977). Interpreting stromatolites: these fossils can tell us much about past organisms and environments if we can learn to decode their message. *American Scientist, 65*(5), 563-571.

Wang, Y., Tong, J., Wang, J., & Zhou, X. (2005). Calcimicrobialite after end-Permian mass extinction in South China and its palaeoenvironmental significance. *Chinese Science Bulletin, 50*(7), 665-671.

Wescott, W. A. (1988). A late Permian fan-delta system in the southern Morondava Basin, Madagascar. *Fan deltas: sedimentology and tectonic settings. Blackie, London*, 226-238.

Wescott, W. A., & Diggens, J. N. (1998). Depositional history and stratigraphical evolution of the Sakamena Group (Middle Karoo Supergroup) in the southern Morondava Basin, Madagascar. *Journal of African Earth Sciences, 27*(3-4), 461-479.

Wignall, P. B. (2007). The End-Permian mass extinction–how bad did it get? *Geobiology, 5*(4), 303-309.

Wignall, P. B., & Hallam, A. (1992). Anoxia as a cause of the Permian/Triassic mass extinction: facies evidence from northern Italy and the western United States. *Palaeogeography, Palaeoclimatology, Palaeoecology, 93*(1-2), 21-46.

Wignall, P. B., & Twitchett, R. J. (2002). Permian–Triassic sedimentology of Jameson Land, East Greenland: incised submarine channels in an anoxic basin. *Journal of the Geological Society, 159*(6), 691-703. doi:10.1144/0016-764900-120

Wright, V. P., & Mayall, M. (1981). Organism-sediment interactions in stromatolites: an example from the Upper Triassic of South West Britain. In *Phanerozoic Stromatolites* (pp. 74-84): Springer.

Wu, S., Chen, Z.-Q., Fang, Y., Pei, Y., Yang, H., & Ogg, J. (2017). A Permian-Triassic boundary microbialite deposit from the eastern Yangtze Platform (Jiangxi Province, South China): Geobiologic features, ecosystem composition and redox conditions. *Palaeogeography, Palaeoclimatology, Palaeoecology, 486*, 58-73. doi:https://doi.org/10.1016/j.palaeo.2017.05.015

Yang, H., Chen, Z. Q., Wang, Y., Tong, J., Song, H., & Chen, J. (2011). Composition and structure of microbialite ecosystems following the end-Permian mass extinction in South China. *Palaeogeography, Palaeoclimatology, Palaeoecology, 308*(1), 111-128. doi:https://doi.org/10.1016/j.palaeo.2010.05.029

Young, A., Flament, N., Maloney, K., Williams, S., Matthews, K., Zahirovic, S., & Müller, R. D. (2018). Global kinematics of tectonic plates and subduction zones since the late Paleozoic Era. *Geoscience Frontiers*.

Every reasonable effort has been made to acknowledge the owners of copyright material. I would be pleased to hear from any copyright owner who has been omitted or incorrectly acknowledged.

Chapter 6 APPENDICES

Appendix A

PUBLICATIONS INCLUDED WITHIN THIS THESIS

The following statement of authorships pertain to chapters two and three, papers that currently under peer review with journals.

15/11/2020

Statement of Authorship

Title of Paper	Microbialite forms and facies controls on stromatolite occurrences in the Perth Basin, Western Australia and their relationship to the end Permian mass extinction
Publication Status	Published ○ Accepted for Publication ● Submitted for Publication ○ Publication Style
Publication Details	Olden, L. J., Barham, M., Cunneen, J., Olierook, H. K. H., Suosaari, E., & Smith, G. (In Review). Microbialite forms and facies controls on stromatolite occurrences in the Perth Basin, Western Australia and their relationship to the end Permian mass extinction. *Australian Journal of Earth Sciences*.

Author Contributions

By signing the Statement of Authorship, each author certifies that their stated contribution to the publication is accurate and that permission is granted for the publication to be included in the candidate's thesis.

Name of Principal Author (Candidate)	Liam J. Olden		
Contribution to the Paper	Liam led most aspects of the research and drafted the manuscript.		
Overall percentage (%)	60		
Signature		Date	13/11/2020

Name of Co-Author	Milo Barham		
Contribution to the Paper	Milo assisted in sample collection and field mapping of stromatolitic succession as well as writing and editing of the manuscript.		
Overall percentage (%)	10		
Signature		Date	13/11/2020

Name of Co-Author	Jane Cunneen		
Contribution to the Paper	Jane assisted in sample collection and field mapping of stromatolitic succession as well as writing and editing of the manuscript.		
Overall percentage (%)	10		
Signature		Date	15/11/2020

Type here

Name of Co-Author	Hugo K.H. Olierook		
Contribution to the Paper	Hugo assisted in sample collection, field mapping of stromatolitic succession, as well as writing and editing of the manuscript.		
Overall percentage (%)	10		
Signature		Date	13/11/2020

Name of Co-Author	Erica Suosaari		
Contribution to the Paper	Erica assisted in sample collection and field mapping of stromatolitic succession as well as editing of the manuscript.		
Overall percentage (%)	5		
Signature		Date	11/13/2020

Name of Co-Author	Gregory Smith		
Contribution to the Paper	Greg assisted in sample collection and editing of the manuscript.		
Overall percentage (%)	5		
Signature		Date	13.11.2020

Statement of Authorship

Title of Paper	The cell in the stone: exceptional preservation of cellular microstructures in Mid-Phanerozoic stromatolites from Western Australia
Publication Status	Published Accepted for Publication Submitted for Publication Publication Style
Publication Details	Olden, L. J., Barham, M., Olierook, H. K. H., Fougerouse, D., Belinda, G., Cunneen, J., & Forman, L. (In Review). The cell in the stone: exceptional preservation of cellular microstructures in Mid-Phanerozoic stromatolites from Western Australia. *Geobiology*.

Author Contributions

By signing the Statement of Authorship, each author certifies that their stated contribution to the publication is accurate and that permission is granted for the publication to be included in the candidate's thesis.

Name of Principal Author (Candidate)	Liam J. Olden		
Contribution to the Paper	Liam led most aspects of the research and drafted the manuscript.		
Overall percentage (%)	60		
Signature		Date	13/11/2020

Name of Co-Author	Milo Barham		
Contribution to the Paper	Milo assisted in writing and editing of the manuscript.		
Overall percentage (%)	10		
Signature	c	Date	13/11/2020

Name of Co-Author	Hugo K.H. Olierook		
Contribution to the Paper	Hugo assisted in sample preparation as well as writing and editing of the manuscript.		
Overall percentage (%)	10		
Signature		Date	13/11/2020

Name of Co-Author	Belinda Godel		
Contribution to the Paper	Belinda ran the Micro CT, volume rendering of stromatolites and editing of the manuscript		
Overall percentage (%)	5		
Signature		Date	13/11/2020

Name of Co-Author	Denis Fougerouse		
Contribution to the Paper	Denis ran the FIB analysis and editing of the manuscript.		
Overall percentage (%)	5		
Signature		Date	13/11/20

Name of Co-Author	Jane Cunneen		
Contribution to the Paper	Jane assisted in sample collection and editing of the manuscript.		
Overall percentage (%)	5		
Signature		Date	15/11/2020

Name of Co-Author	Lucy Forman		
Contribution to the Paper	Lucy conducted EBSD analysis and editing of the manuscript..		
Overall percentage (%)	5		
Signature		Date	13/11/2020